FEM Based Advanced Torsion Analysis of Curved Steel Box Girder Bridges

By

Wubie Enyew Fenta

A Thesis submitted to

The School of Civil and Environmental Engineering

Presented in partial fulfillment of the Requirements for the Degree of Master of Science in Structural Engineering

Addis Ababa University

Addis Ababa, Ethiopia

January, 2014

Addis Ababa University

School of graduate studies

This is to certify that the thesis prepared by Wubie Enyew, entitled: A FEM Based Advanced Torsion Analysis of a Curved Steel Box Girder Bridge and submitted in partial fulfillment of the requirements for the Degree of Master of Science complies with the regulations of the University and meets the accepted standards with respect to originality and quality.

Approved by Board of Examiners:

Dr.-Ing. Girma Z/yohannes	_____	_____
(Advisor)	Signature	Date
Dr.-Ing. Adil Zekaria	_____	_____
(Internal Examiner)	Signature	Date
Dr.-Ing. Bedilu Habte	_____	_____
(External Examiner)	Signature	Date
Dr. Bikila Teklu	_____	_____
(Chairman)	Signature	Date

ABSTRACT

A FEM Based Advanced Torsion Analysis of a Curved Steel Box Girder Bridge
Wubie Enyew
Addis Ababa University, 2013

Due to efficient dissemination of congested traffic, economic considerations, and aesthetic desirability, horizontally curved steel box girder bridges are usually best preferred structural unites irrespective of their production costs, in modern highway systems, including urban interchanges. The most important advantage of the steel box girder bridge is, however, its torsion resistance. Torsion effects in those complicated structural unites, are usually none considerable and causes a fatal effect.

Although a significant number of researches have been made on a manual based and advanced analysis for many years to better understand the behavior of all types of steel box girder bridges, however, an interactive Finite Element Modeling to analyze the integral system of the curved steel box girder bridges haven't been formalized, yet. Hence, an advanced, clear and more accurate analysis procedure is required to better understand curved steel box girder bridges. The non-composite steel section must support both the fresh concrete and the entire construction loads hence steel box girders are at their critical stage during construction.

Although the degree of fatality varies based on the structural integrity of the bracing, stiffening and box girder unites any eccentric loads such as centrifugal, vehicular and gravity loads induce torsion and distortional effects. Handling of the seventh Degree of freedom associated with the distortional stresses is highly desired in this paper. All mechanics of the analysis procedure and techniques of the FEM modeling have all been addressed so as to have a convenient result.

In the current study, non composite curved steel boxes are analyzed with shell elements using the three dimensional finite element analysis and their behavior is investigated. The general purpose program, the ANSYS software, is centrally used to model and analyze the integral system. Temperature effects and all realistic load combinations haven't been addressed in this research. Principles of applications of all the fundamental bridge loadings and reaction behavior of the integral structural system have generally been dealt. Further, the basics of the

finite element formulations with alternative and more consistent approaches are presented to verify program results.

An additional curved box girder (structural long spanning unite) with a rectangular (less stiff) section and higher radius of curvature is modeled and analyzed to further investigate and verify warping effects for the fact that the main subject doesn't clearly signify its fatality. The loading orientation is arranged in such a way that it creates the worst warp.

Regardless of its lesser economic desirability as to the current trend, curved steel box girder bridges are best recommended for long span ground requirements where torsion resistance is highly demanded. The reason why it is less important in bridge structures and of less construction culture is, because structural steel elements are generally cost incurring to manufacture, process and mobilize. Less fire resistance is also the drawback of steel structures unless treated carefully.

Acknowledgements

I am indebted to my advisor, Dr.-Ing Girma Z/yohannes, for his direction and support throughout my graduate studies at the University. His interest in my work and appreciation of my efforts provided me with the constant motivation needed to achieve my goal.

Contents

Table of figures

Chapter 1

1.0 Introduction

1.1 General back Ground

Bridge structures, apart from its general purpose, now a day, produces a deep look into the beauties of nature that the human kind can turn into, and reflects the whole entities of the humane aspiration. It also defines the cumulative conceptual status of the present day engineering. It also plays a role as an indignity and national proud, when as a droplet of knowledge is converted to a very huge mega structure. The newly constructed Gottera interchange in Addis Ababa, for instance, so named as the Nations and Nationalities Square, proves the whole scale growth needs of nations and brings an alternative construction cultures; and the Dalace High Five interchange, in US proves the same.

The most important parameter that structural engineers need first to deal with in designing and implementing structures is the type of material going to be used. Steel, concrete and steel concrete composite structures are commonly used structural materials in today's construction culture. The type of the physical structure, governs the type of material to select; and most important of all its availability.

Concrete structures are less torsion resistant by their nature unless carefully provided with torsion intensive reinforcements. In complicated structural unites, however, where all reaction behaviors are required such as tensile, flexural and torsional reactions, it is generally impossible to recommend it. It is because concrete structures are less tension and torsion resistant. Concrete structures, in general, in those long spanning curved box girder bridge complexes is usually in considerable for its fatal failure in torsional and distortional shear stresses. The way and mood of failure, and pattern and extent of the shear that needs an intensive study to handle, for reinforcement provisions, makes concrete structures difficult to recommend in those curved but long spanning situations.

Horizontally curved box girders, applicable for both simple and continuous spans, are used for grade-separation and elevated bridges where the structure must coincide with the curved roadway alignment. This condition occurs frequently at urban crossings and interchanges and

also at rural intersections where the structure must conform to the geometric requirements of the highway.

1.2 Advantage of Box Girder Sections over I-Sections

The most important advantage of the steel box girder bridge is its torsion resistance. Stiffening requirements of the closed (box) sections is quite better than the comparative open sections. Box girders are often selected over I-girders because of their pleasing appearance offering a smooth, uninterrupted, cross section. Bracing, web stiffeners, utilities, and other structural and nonstructural components are typically hidden from view within the steel box girder, leading to a clean, uncluttered appearance. Additionally, steel box girder bridges offer advantages over other superstructure types in terms of span range, stiffness, durability, and future maintenance.

Steel box girders can potentially be more economical than steel plate I-girders in long span applications due to the increased bending strength offered by their wide bottom flanges, and because they require less field work due to handling fewer pieces. Steel tub girders can also be suitable in short span ranges as well, especially when aesthetic preferences or constructability considerations preclude the use of other structure types.

Box girders, as closed-section structures, provide a more efficient cross section for resisting torsion than I-girders. The increased torsional resistance of a closed composite steel box girder also results in an improved lateral distribution of live loads. For curved bridges, warping, or flange lateral bending, stresses are lower in box girders, when compared to I-girders, since box girder carry torsion primarily by means of St. Venant torsional shear flow around the perimeter of their closed sections, whereas I-girders have very low St. Venant torsional stiffness and carry torsion primarily by means of warping.

The exterior surfaces of box girders are less susceptible to corrosion since there are fewer details for debris to accumulate, in comparison to an I-girder structure. For box girders, stiffeners and most diaphragms are located within the box girder, protected from the environment. Additionally, the interior surface of the box girder is protected from the environment, further reducing the likelihood of deterioration. Box girder bridges tend to be easy to inspect and maintain since much of the inspection can occur from inside the box girder, with the box serving as a protected walkway.

Erection costs for box girders may be lower than that of I-girders because the erection of a single box girder, in a single lift, is equivalent to the placement and connection of two I-girders. Box girders are also inherently more stable during erection, due to the presence of lateral bracing between the top flanges. Overall, the erection of a tub girder bridge may be completed in less time than that of an I-girder counterpart because there are fewer pieces to erect, a fewer number of external diaphragms to be placed in the field, and subsequently fewer field connections to be made. This is a significant factor to consider when available time for bridge erection is limited by schedule or site access.

Currently, curved girders have replaced straight segments because in urban areas where elevated highways and multi-level structures are necessary, modern highway bridges are often subjected to severe geometric restrictions; therefore they must be built in curved alignment. Even though the cost of the superstructure for the curved girder is higher, the total cost of the curved girder system is reduced considerably since the number of intermediate supports, expansion joints and bearing details are reduced. The continuous curved girder also provides more aesthetically pleasing structures.

Despite all the advantages mentioned above, horizontally curved girders are generally more complex than straight girders. Curved girders are subjected to vertical bending plus torsion caused by the girder curvature. The centrifugal force effects and the additional bending couples induced due to bridge curvature are areas of typical concern in this paper.

1.3 Objectives and Scope

The objective of this paper is to investigate the torsional and distorsional stress behaviors of steel box girder bridges. The FEM approach modeling and analysis of the integral system with bracing and stiffening member, and its requirements and configurations are the central objectives of the study in general. The objective and scope for the study can be summarized as,

1. Literature review of the analytical methods, previous experimental and theoretical research work, on the general behavior of box girder bridges.
2. To introduce the interactive general purpose program applications on a complex structural unit i.e in meaning so the integral concept of the area under investigation will be extended to all possible alternatives.

3. Investigate warping just by accounting it as through an added seventh DOFs for curved box girders using the commercially available finite element Computer program "ANSYS" and verify an alternate finite element approach analysis techniques.

4. Perform investigations utilizing the FEM model of the curved box to determine the effect and spacing of bracings and stiffeners on the stresses. To address the statically indeterminate complex jointed brace lay outs using the general purpose program, the ANSYS. To compare and interpret computer simulated results with the theoretical preliminaries.

1.4 Outline of the Thesis

This thesis is organized into seven chapters. Chapter 1 is an introduction to the topic followed by the objectives and scope of the study. A literature review of the earlier analytical and experimental work on box girder bridges is presented in Chapter 2. Chapter three is about the general behavior of curved bridge structures. Its behavior from the perspectives of its geometrical implications and different loading combinations and orientations is assessed in detail. Chapter 4, is about the stress analysis. Stress contour, shear pattern and distributions along the quasi closed section and the bracing and stiffening members stress contribution, along with its physical interpretations has been dealt. Fundamentals of the finite element analysis including finite element formulations are briefly described in Chapter 5. In chapter 6, local and general buckling resistance contributions of the stiffening and bracing members, has been issued. The last chapter is the computer output and is physical interpretation.

Chapter 2

2.0 Literature Review

2.1 Introduction

From the perspectives of analysis and design, all high scale Bridge structures are supposed to be complex in general and box girder composite bridges are worse too, to investigate its reaction and resistance behavior, in particular. To deal with such complexities, several approximate analysis methods were developed starting from the sixties. In the past, curved girders were generally composed of a series of straight segments that were used as chords in forming a curved alignment. Literatures proved that the first work on the static analysis of horizontally curved beams was published by De Saint Venant during the first half of the 19th century.

Many of the recent researchers of the subject matter had developed their cumulative skills from the comprehensive and systematic research efforts made from 1969 to 1976 by The Consortium of University Research team (CURT) which were organized by the US Federal Highway Administration (FHWA) and participating States Departments of Transportation to undertake and produce an extensive knowledge on the static and dynamic behavior of curved bridges. According to many references, the CURT research efforts resulted in the publication of the first edition of the Guide Specification, a working stress design guide for Horizontally Curved Bridges by the American Association of State Highway and Transportation Officials (AASHTO) in1976. Since then, there has little or no research efforts have been recorded for the following 10-20 years.

The current design methods, which are primarily based on the research conducted prior to early 1980th, have a number of deficiencies. Although significant research has been underway on advanced analysis for many years to better understand the behavior of all types of box-girder bridges, however, the results of these various research works are scattered and unevaluated. Hence, a clear understanding of more recent work on curved box-girder bridges is highly desired. There is no clearly set design guidelines and codes developed in any countries regarding to the subject matter.

2.2 Related Topics and Researches

Calculating warping related stresses is not a straightforward process. A number of literatures compiled in this research proved that the AASHTO curved box bridge specification insists that the effects of non uniform torsion must be considered in design, but does not provide any assistance or guidance on how to do so. The only guidance given to determine when warping stresses could be important falls under a section in the commentary dealing with top bracing. According to many literatures, this guidance is adapted from the work of Nakai and Heins (1977), who investigated a variety of curved bridge types and proposed criteria based on cross-section properties, bridge length, and subtended angle that would allow engineers to determine when warping is significant. The work of Nakai and Heins has the following limitations.

- Idealized loading and boundary conditions were assumed;
- Although, normal stresses due to warping were considered, shear stresses due to warping were ignored; and
- The effects of centrifugal forces were not accounted for.

As referenced by Zakia Begum, who first made the comparison between beam model and shell model analysis; other researchers such as Trukstra and Fam (1978) and Waldron (1988), have conducted their own research typically to investigate significance of warping on curved box girders. The former researchers have tried to investigate the effect of diaghrams on the behavior of curved box girder bridges. They have conducted a parametric study to investigate the ratio between stresses obtained from idealized beam models for simple load cases. The two researchers agreed that their investigative results showed, diaghrams improve load distribution and positively influence stress ratios.

Waldron (1988), on the other hand has carried an investigation on the effect of warping on normal stresses in single box girder. Forces were calculated by deriving closed form solutions of the fundamental equation governing torsion and warping for special loading cases. Using concrete box for examples, it was shown that warping could increase normal stresses by as much as 29%. This high stress ratio corresponds to a theoretical loading condition where a single concentrated load acts on one of the webs at mid span. For truck loads (following the British code), stress ratios drop to around 5%. Based on the study, it was concluded that the width to- depth ratio significantly impacts the normal warping stress ratio.

All the studies summarized above, suffer from a number of common drawbacks. They did not address warping shear stresses and were based on idealized loading and boundary conditions. They haven't also made a detailed investigation of effect of even gravity loads for warping and distortional stresses, the pattern or configurations of bracing members associated with local and global buckling problem.

According to many literatures, the development of the curved beam theory by Saint-Venant (1843) and later the thin-walled beam theory by Vlasov (1965) marked the birth of all research efforts published to date on the analysis and design of straight and curved box-girder bridges. Many technical papers, reports, and books have been published in the literature concerning various applications of, and even modifications to, the two theories. Recent literature on straight and curved box girder bridges has dealt with analytical formulations to better understand their complex behavior of and few authors have undertaken experimental studies to investigate the accuracy of the existing methods. This chapter summarizes all research efforts made so far to investigate the general static behavior of curved steel girder bridges under the following typical categories:

1. Literature pertaining to the elastic analysis methods
2. Experimental studies on elastic response of box girder bridges
3. Behavior of curved girder bridges

2.3 Analytical Methods for Box Girder Bridges

There are several methods available for the analysis of box girder bridges. In each analysis method, the three-dimensional bridge structure is usually simplified by means of assumptions in the geometry, materials and the relationship between its components. The accuracy of the structural analysis is dependent upon the choice of particular method and its assumptions. Theoretical highlights of the references pertaining to elastic analysis methods of straight and curved box girder bridges through which a review of different analytical methods for box girder bridges has been presented and the theoretical aspects of some of the methods has been derived in early 2000s. A brief review of the analytical methods of box girder bridges is presented in the following sections.

2.3.1 Grillage Analogy Method

Most of the analysis records, regarding to the subject matter were noticed between 1970s and 1980s. Very little number of researches has also been made after 2000s. Many researchers in

the 2000s, that followed a more practical approaches including the FEM approach to investigate the role of structural components other than the main girder, had referred the works of the former researchers such as Hambly and Pennells (1975), Kissane and Beal (1975). Accordingly, they have showed their respective researches regarding to the application of Grillage analysis on multiple cell boxes with vertical and sloping webs and voided slabs. In this method, the bridge deck was idealized as a grid assembly. Some of them have applied this idealization to the multi cellular superstructure and others to curved multi spine box-girder bridges. The continuous curved bridge is modeled as a system of discrete curved longitudinal members intersecting orthogonally with transverse grillage members. As a result of the fall-off in stress at points remote from webs due to shear lag, the slab width is replaced by a reduced effective width over which the stress is assumed to be uniform.

The equivalent stiffness of the continuum is lumped orthogonally along the grillage members. Begum quoted the works of Cheung (1982) that he had dealt with the calculations of the longitudinal bending moment and transverse shear in multi spine box-girder bridges using the grillage analogy method. The results from this method were compared favorably to the results obtained from 3D analysis using the finite-strip method. The main problems which arises by using the grillage analogy method was in determining the effective width of the slab to include the shear lag effects and faces difficulty in estimating the torsional stiffness of closed cells.

2.3.2 Orthotropic Plate Theory Method

The orthotropic plate theory method considers the interaction between the concrete deck and the curved girder of a box girder bridge. In this method the stiffness of the diaphragms is distributed over the girder length and the stiffness of the flanges and girders are lumped into an orthotropic plate of equivalent stiffness. However, the estimation of the flexural and torsional stiffness is considered to be one major problem in this method. Also, the evaluation of the stresses in the slab and girder presents another difficulty in adopting this approach. Many researchers provided the various methods of calculating the equivalent plate parameters, which are necessary for 2D analysis of curved cellular and voided slab bridges; and others applied the orthotropic plate method to calculate the longitudinal moments and transverse shear in multispine box-girder bridges. To establish the limits of validity of the orthotropic plate method, the results were compared to those obtained from 3D analysis using the finite-strip method. It was concluded that the orthotropic plate method gives accurate

results provided that the number of spines is not less than three. This method is suggested mainly for multiple-girder curved bridges with high torsional rigidity.

2.3.3 Folded Plate Method

This method produces solutions for linear elastic analysis of a box girder bridge, within the scope of the assumptions of the elasticity theory. In this method a box girder bridge can be modeled as a folded system which consists of an assembly of longitudinal plate elements interconnected at joints along their longitudinal edges and simply-supported at both ends by diaphragms. These diaphragms are infinitely stiff in their own planes but perfectly flexible perpendicular to their own plane. This method produces solution of simply supported straight or curved box-girder bridges for any arbitrary longitudinal load function by using direct stiffness harmonic analysis where any arbitrary longitudinal joint loading can be resolved into harmonic component of the loading using Fourier series and then, a direct stiffness analysis can be performed for each component. The first formal analytical procedure developed to determine longitudinal stresses, transverse moments and vertical deflections in folded plate structures by utilizing matrix algebra, is referenced to first be made by Scordelis (1960).

Others developed a method that incorporates a classical folded plate analysis of an assemblage of the orthotropic or isotropic plates to form box girders. One of the major drawbacks of the folded plate method is that it is tedious and complicated.

2.3.4 Finite Strip Method

The finite strip method can be regarded as a special form of displacement formulation of finite element. Using a strain-displacement relationship, the strain energy of the structure and the potential energy of external loads can be expressed by displacement parameters. It employs the minimum potential energy theorem where at equilibrium; the values of the displacement parameters should make the total potential energy of the structure become minimal. In this method, the box girders section is discretized into annular finite strips running from one end support to the other. The strips are connected transversely along their edges by longitudinal nodal lines. Then the stiffness matrix is calculated for each strip based upon a displacement function in terms of Fourier series. Similar to the folded plate method, in the finite strip method the direct stiffness harmonic analysis is performed. The finite strip method is considered as a transition between the folded plate method and the finite element method. The finite element method is basically different from the strip method in terms of the assumed

displacement interpolation functions. Unlike the finite element method, the displacement functions for the corresponding finite strip are assumed as combination of harmonics varying longitudinally and polynomials varying in the transverse direction.

The first introductory research on the finite strip method was first made as early as 1968 and was applied to analyze curved box girders after 1970th [Cheung, Y.K]. It has been reviewed in the Begum's work that following this introduction other researchers programmed this method and used a program to solve the numerical examples of curved bridges as well as straight bridges by making the radius of curvature very large and the subtended angle very small.

This method was used later to determine the effective width of the compression flange of straight multi-spine and multi-cell box-girder bridges. Cheung (1984) used a numerical technique based on the finite-strip method and the force method for the analysis of continuous curved multi cell box-girder bridges. Begum has discussed in his review that Branco and Green (1984) used this method to investigate the effect of the cross bracing system, as well as the transverse web stiffeners, in resisting distortion and twist of straight composite twin spine box girder bridges during service.

Others such as Bradford and Wong (1992) used the finite strip method with one harmonic to study the local buckling of the straight composite concrete deck-steel box section in negative bending region. Design graphs of the elastic buckling coefficients were produced. These graphs can be used to obtain accurate values of the web depth-thickness ratio that separates the boundary between slender and semi compact sections. Using the finite strip method, Cheung and Foo (1995) presented the results of a parametric study on the relative behavior of curved and straight box girder bridges using the finite strip method.
All the past analysis procedures of the finite strip method proved that it had an advantage over the finite element method because it required shorter computer time and smaller computer storage. This is because the amount of data input required in the analysis can be reduced drastically because of strip idealization. Although the finite strip method has broader applicability as compared to folded plate method, however the drawback is that the available design codes restrict its applicability to simply supported prismatic structures with simple line support.

Similar to all other approaches, it plays an important role to the introduction of a more formal FEM approach, though the fact that it lacks an authentic generality in handling structural components of the girder system such as the roles of stiffening members (brace and

diaphragms). It doesn't also address and investigate the warping behavior of the box section that the integral system produced.

2.3.5 Finite Element Method

The finite element method of analysis is generally the most powerful, versatile and more accurate method of all the available methods and has rapidly become a very popular technique for the computer solution of complex problems in engineering. It is very effective in the analysis of complicated structures such as that of a box girder bridge with complex geometry, material properties and support conditions and subjected to a variety of loading conditions. This method can be regarded as an extension of analysis techniques mentioned earlier in which a structure is represented as an assemblage of discrete elements interconnected at a finite number of nodal points.

A large number of elements have been developed for use in the finite element technique that includes one-dimensional beam-type elements, two dimensional plate or shell elements or even three-dimensional solid elements. Since the structure is composed of several finite elements interconnected at nodal points, the individual element stiffness matrix, which approximates the behavior in the continuum, is assembled based on assumed displacement or stress patterns. Then, the nodal displacements and hence the internal stresses in the finite element are obtained by the overall equilibrium equations. By using adequate mesh refinement, results obtained from finite element model usually satisfy compatibility and equilibrium

The only and best introductory formulation in finite element analysis using an interactive soft ware to investigate its general behavior of a single celled double trapezoidal box girder bridge was made by Zakia Begum in his master's thesis at Meryland University, 2010. He had centrally dealt the comparative behavior of beam and shell model of two identical single celled trapezoidal boxes Girder Bridge. He best reviewed almost all the formerly made researches, on straight and curved steel box girder bridges.

Begum in his reference described that prior to his works, (Zienkeiwicz, 1977), Sisodiya, Cheung and Ghali (1970) separately presented finite element analyses of single box girder skew bridges that were curved in plan. The bridge that could be analyzed by this method may be of varying width, curved in any shape, not just a circular shape and with any support conditions. They used rectangular elements for the webs and parallelogram or triangular

elements for top and bottom flanges. This approximation would require a large number of elements to achieve a satisfactory solution. Such an approach is impractical, especially for highly curved box bridges.

They pointed out that even symmetrical load components, induce distortional stresses in curved steel boxes, and showed that the use of sloping webs resulted in an increase in distortional stresses.

They haven't; however, issued a number of controlling parameters such as the effect of the intermediate diagrams, and cross versus diagonal frames to investigate the warping and distortional stresses, in general.

Chu and Pinjarkar (1971) developed a finite element approach for analyzing curved box girder bridges. The top and bottom flanges were modeled as horizontal sector plates while the web was idealized as vertical cylindrical shell elements. The sloped web elements were not considered as they require conical shell elements. Membrane and bending actions were both considered for the plate and shell elements, but no interaction between them was assumed. The method can be applied only to simply supported bridges without intermediate diaphragms.

William and Scordelis (1972) analyzed cellular structures of constant depth with arbitrary geometry in plan using quadrilateral elements in the finite element analysis. Bazant and El Nimeiri (1974) attributed the problems associated with the neglect of curvilinear boundaries in the elements used to model curved box beams by the loss of continuity at the end cross-section of two adjacent elements meeting at an angle.

Instead of developing curvilinear element boundaries, they developed the skew-ended finite element with shear deformation using straight elements and adopted a more accurate theory that allows for transverse shear deformations. Fam and Turkstra (1975) developed a finite element scheme for static and free vibration analysis of box girders with orthogonal boundaries and arbitrary combination of straight and horizontally curved sections. Four-node plate bending annular elements with two straight radial boundaries, for the top and bottom flanges, and conical elements for the inclined web members were used. The importance of warping and distortional stresses in single-cell curved bridges was established in relation to the longitudinal normal bending stresses, using the finite element method, by Truksta and Fam (1978).

Moffat and Lim (1976) demonstrated a finite-element technique to analyze straight composite box-girder bridges will complete or incomplete interaction with respect to the distribution of the shear connectors. Sargious et al. (1979) investigated the effect of providing end diaphragm with opening in single-cell concrete box-girder bridges supported by a central pier. At the same time, Daniels et al. (1979) studied the effect of spacing of the rigid interior diaphragms on the fatigue strength of curved steel box girders.

The results showed that reducing the interior diaphragms spacing effectively controls the distortional normal and bending stresses and increases the fatigue strength of curved steel box girders. Dezi (1985) examined the influence of some parameters including transverse and longitudinal locations of external loads, span-to-radius ratio, width-to-depth of the cell, and number of cross diaphragms on the deformation of the cross section in curved single cell box beams over those in straight single-cell box beams. Ishac and Smith (1985) presented approximations for determining the transverse moments in single-span single-cell concrete box-girder bridges. Dilger et al. (1988) studied the effect of presence and orientation of diaphragms on the reaction, internal forces, and the behavior of skew, single cell, concrete box-girder bridges.

Galuta and Cheung (1995) developed a hybrid analytical solution that combines the boundary element method with the finite-element method to analyze box-girder bridges. The finite-element method was used to model the webs and bottom flange of the bridge, while the boundary element method was employed to model the deck. The bending moments and vertical deflection were found to be in good agreement when compared with the finite strip solution. Abdelfattah (1997) used the 3D finite-element method to study the efficiency of different systems for stiffening steel box girders against shear lag. Sennah and Kennedy (1998) conducted an extensive parametric study on composite multi-cell box girder bridges using the finite element analysis. The results obtained from the finite element method were in good agreement with the experimental findings.

2.3.6 Thin-Walled Beam Theory Method

Saint-Venant (1843) established the curved beam theory for the case of a solid curved bar loaded in a direction normal to the plane of curvature. In general, curved beam theory cannot be applied to curved box girders bridges, because it cannot account for warping, distortion, and bending deformations of the individual wall elements of the box. Curved beam theory can

only provide the designer with an accurate distribution of the resultant bending moments, torque, and shear at any section of a curved beam if the axial, torsional and bending rigidities of the section are accurately known. The thin-walled beam theory was established by Vlasov (1965) for axisymmetric sections, and then extended by Dabrowski (1968) for asymmetric section who derived the fundamental equations that account for warping deformations caused by the gradient of normal stresses in individual box element. The theory assumes non-distortional cross section and, hence, does not account for all warping or bending stresses. The predication of shear lag or the response of deck slabs to local wheel load cannot be obtained using the theory. Oleinik and Heins (1975), and Heins and Oleinik (1976) analyzed the curved box girders in two parts. In the first part of the analysis, the box sections were assumed to retain their shape under the load. The load-deformation response of such a curved box that considers bending, torsion and warping deformations was developed by Vlasov. Vlasov's differential equations were solved using a finite difference approach to calculate the normal bending and normal warping stresses. In the second part of the analysis, the effect of cross sectional deformations was considered.

These cross sectional deformations were calculated using a differential equation developed by Dabrowski. This equation was also solved using the finite difference approach and the normal stresses that resulting from cross-sectional deformations were calculated. The effects of both parts were summed to give the total normal stress distribution. The above-mentioned formulations and the final solutions of these basic differential equations were programmed by Heins and Sheu (1982). A single straight or curved box girder with prismatic or section can be analyzed using this program. The box girder may have internal transverse diaphragms spaced along the box and top lateral bracing. A parametric study was conducted using this program to investigate the effect of internal diaphragms on the induced normal stresses in curved box girder bridges due to dead and live loads.

Chapter Three

3.0 General Behavior of Curved Box Girders

Horizontally curved box girders with both simple and continuous spans are used for grade-separation and elevated bridges where the structure must coincide with the curved roadway alignment. This condition occurs frequently at urban crossings and interchanges and also at rural intersections where the structure must conform to the geometric requirements of the highway. The objective of this section of the material is to present the overview of the general behavior of the box girder bridges. Horizontally curved bridges will undergo bending and associated shear stresses as well as torsional stresses because of the horizontal curvature even if they are only subjected to their own gravitational load.

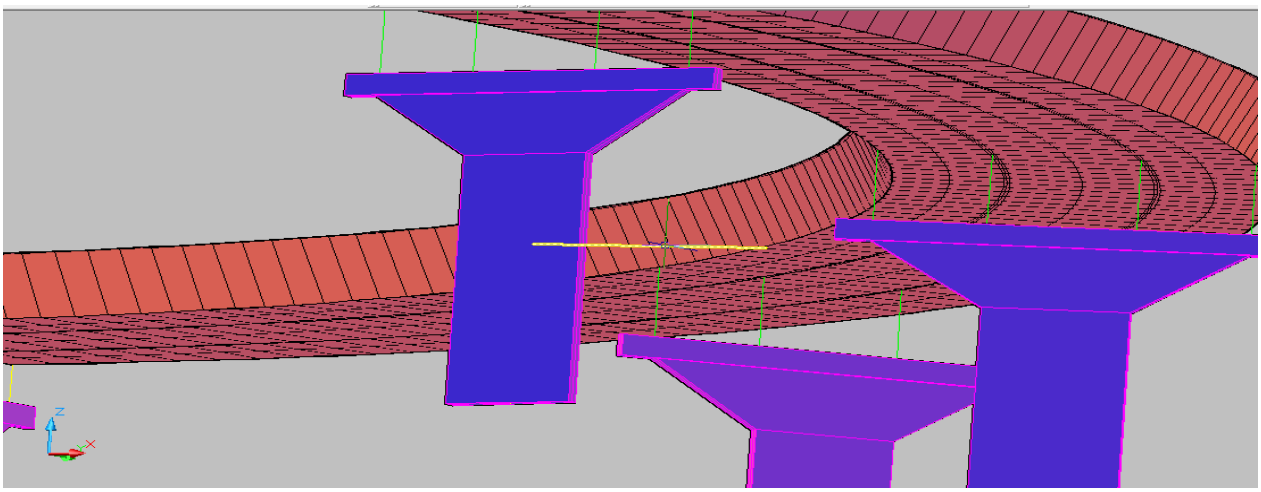

Fig.3.0 Curved Box Girder Bridge

Box Girder Sections in Bridge Structures generally meant the under deck structure that provides support to the whole of the super structure. The general load bearing principle is that it allows the shear to flow or circulate within the wall of the section and or simply to counter balance/cancel the shear potential at a point. If the role of the box geometry is compared with a solid beam of similar service, the solid beam may probably need as deep as the depth of the box section. It is with this general argument that thin walled structures are recommended with some or no flexural or bending effects as of shell structures.

It has been noted, however, that steel box girder bridges are primarily needed for torsion resistance. In this research, box girder bridge systems with different cross sections, radius of curvature and subtended angles are modeled to investigate their respective reactive behaviors. Triple celled, (bottom flange closed), continuous support with constant radius of curvature is typically concerned. Architectural, structural priorities and economic considerations are also governing parameters to select bridge geometry. Further, a rectangular (single unite) cross section (naturally less stiffened) bridge system is modeled and analyzed to further investigate warping effects. The loading matrix in this typical case is oriented in such a way that the integral system is subjected to the worst warping.

The twisting and distorting behavior of the box girder is generally resulted from either of any of the following factors or the other.

- Due to curvature of the bridge
- Due to the transverse position of the vertical load (eccentric)
- Due to the centrifugal load

3.1 Curvature effect of the bridge

3.1.1 Bending effect

The box girders have large span/depth ratio and due to that transverse load causes significant bending stresses in the girder. Different published evidences produced based on a series of experiments and surveys, proved that the average span to depth ratio of box girder bridges varies between 20 and 28. Similarly, according to a survey conducted by the task committee on horizontally curved steel box girder bridges (ASCE), Heins (1978) described that; box girders typically have an average span to depth ratio of 23 for single spans and 25 for continuous girder spans.

The bending causes the section to,

1. Deflect rigidly (longitudinal bending), and
2. Deform (bending distortion)

3.1.1.1 Longitudinal bending

Horizontally curved bridges will undergo bending and associated shear stresses as well as torsional stresses because of the horizontal curvature even if they are only subjected to their own gravitational load.

Consider a differential element of a horizontally curved girder flange of width, db, length, ds, thickness, t, and radius, R, under bending normal stress.

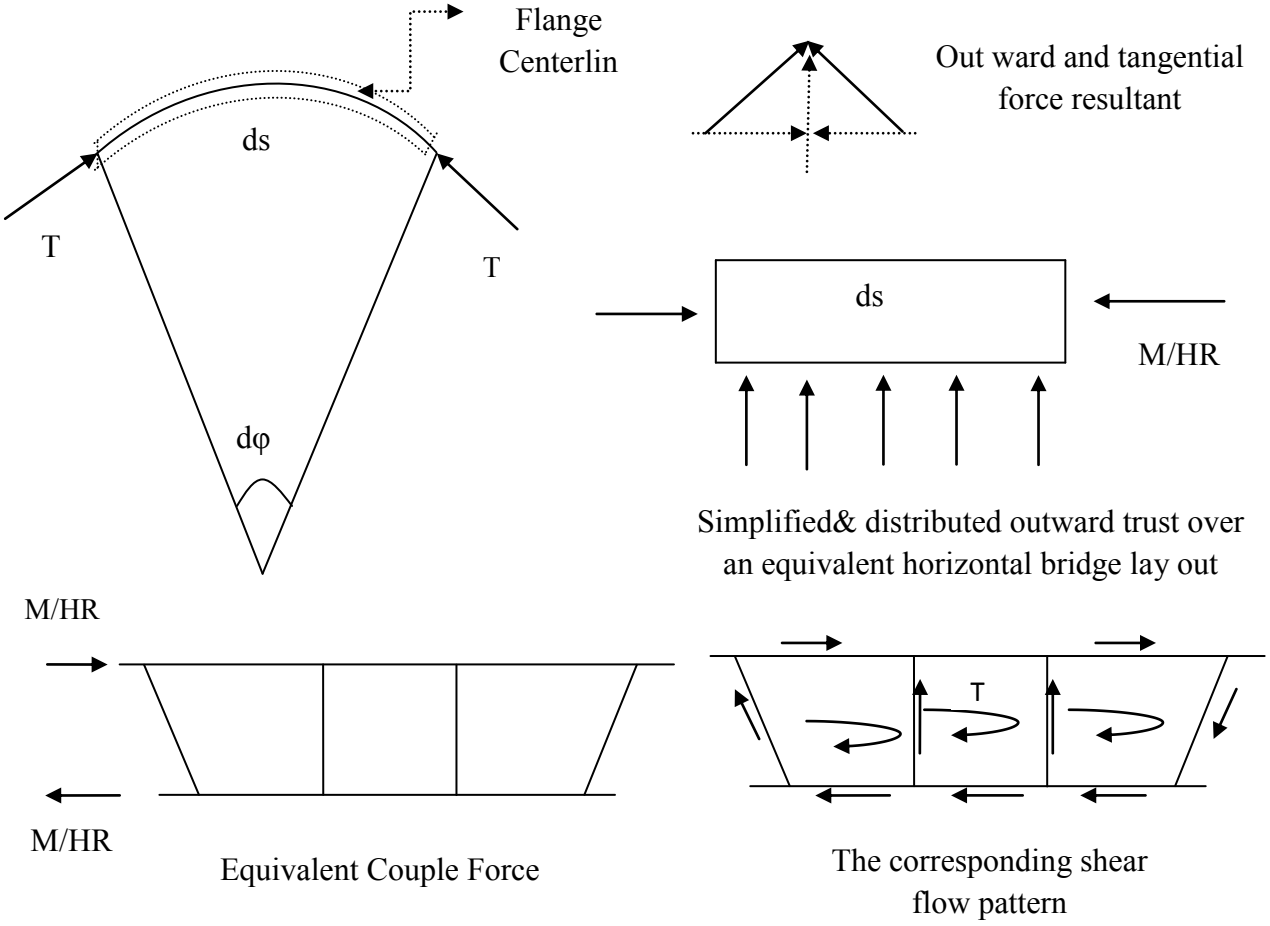

Fig.3.1 Distortional force due bridge geometry

Considering separately the bottom and top flange of the girder system, the bending σ_b, distortional σ_d and torsional warping $\sigma_{t\omega}$ stresses are given below. h_f is depth of the flange.

The bottom and top flanges experience stresses differently (either tensile or compressive in an opposite sense). It is this resultant stress that produces either the tensile or compressive stresses in the respective section. For the bending stress, for example, the top flange is under compression while the bottom flange is under tension at mid span of the bridge.

Bending stress+ Distortional stress+ Tortional warping stress=Resultant stress

$$\sigma_{RES} = \sigma_b + \sigma_d + \sigma_{t\omega}$$

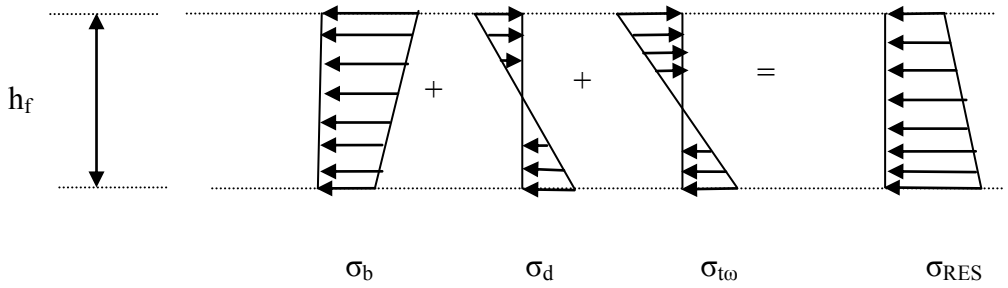

Fig.3.2a Normal stress component of bottom flange

The force can then be resolved into radial and tangential components as shown in fig3.2a, producing an outward trust on the top flange (under compression). The counter balancing force is induced in the bottom flange and hence produces a horizontal couple.

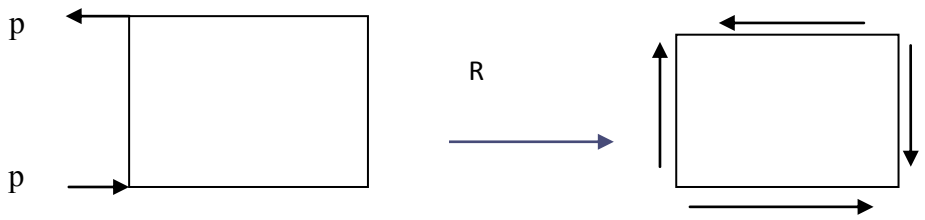

Fig.3.2b Negative moment region

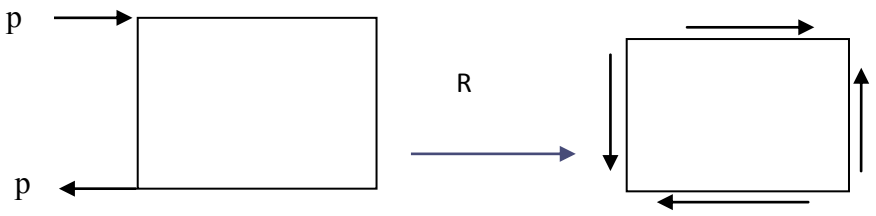

Fig.3.2c Positive moment region

3.1.1.2 Bending Distortion

Bending distortion occurs when transverse loads are applied to the open box. If the box girder does not have a full width steel top flange, the girder must be treated as an open section. In open box girders, this distortion causes outward bending of the webs, upward bending of the bottom flange and in-plane bending of the top flange (Figure 3.5). The out of plane bending of the plates forming the girder also causes the cross section to change shape. Therefore, to

prevent bending distortion the top bracing (ties and struts) are usually placed between top flanges as detailed in unit 6.

3.2 Eccentric (transverse position) vertical load

An arbitrary line load on one of the end flange of the triple celled continuous span box girder (Figure (3.4a)) produces component wise reaction coupled load with different action effects.

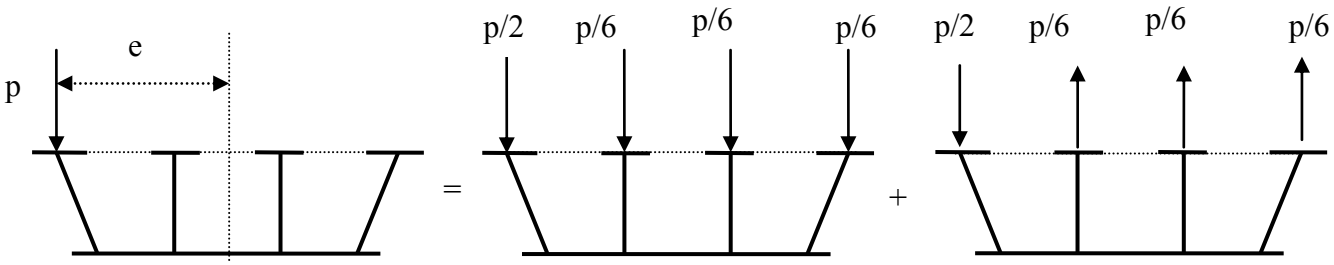

An arbitrary line load containing bending and torsion

A/ Loading component (A)

B/ Loading component (B)

Fig.3.3 Actions and reaction behavior of an open box girder

Alternative superposition formulations are also possible, for the fact that either all the panels (cells of the box) are supposed to rotate together or differently. Considering the rotation of the section as a unity, for instance, the following superposition can be made.

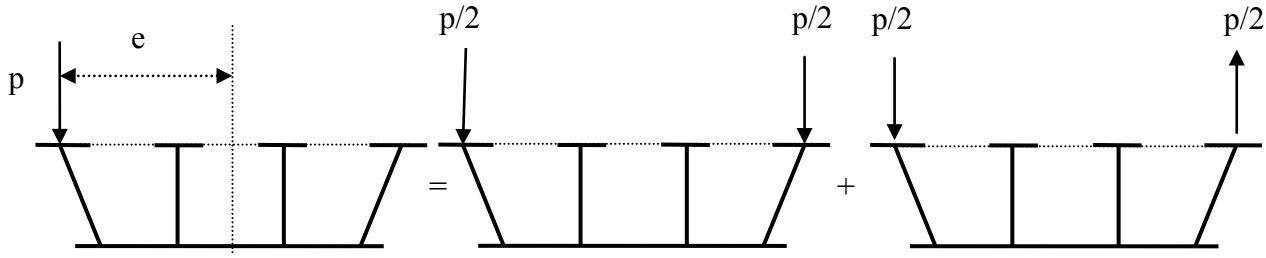

An arbitrary line load containing bending and torsion components

A/ Loading component (A)

B/ Loading component (B)

Fig.3.4 Actions and reaction behavior of an open box girder

Loading component A creates both **longitudinal bending stress** and **bending distortional stress** while loading component B creates both **mixed torsional stress** and **torsional distortion stresses**.

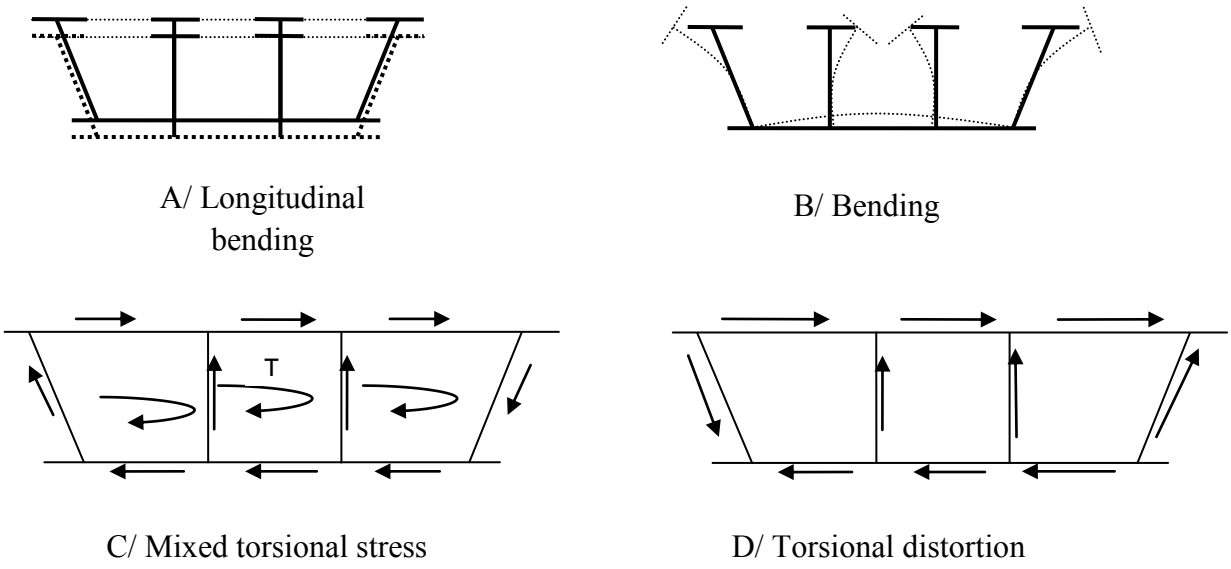

A/ Longitudinal bending

B/ Bending

C/ Mixed torsional stress

D/ Torsional distortion

Fig.3.5. Bending and torsional reaction behaviors of the section

3.3 Centrifugal Effect

The centrifugal force produces the same effect as the gravity direction load effect due bridge curvature. A counter acting flange force is produced. The centrifugal force is usually a function of speed of the vehicle, super elevation, radius of curvature of the bridge and traffic volume i.e lane width of the bridge.

The surface of the roadway has to be super elevated to prevent the outward slippage of the vehicles. The speed and weight of the vehicle, the friction coefficient of the surface and super elevation 'e' of the road are functional parameters to be considered. The design loads are then combined by superimposing all possible loading situations. The percent of the super elevation may be defined or designed either from the overall geometry or just above the composite slab or pavement layer.

The mechanics of the effect can be summarized as follows

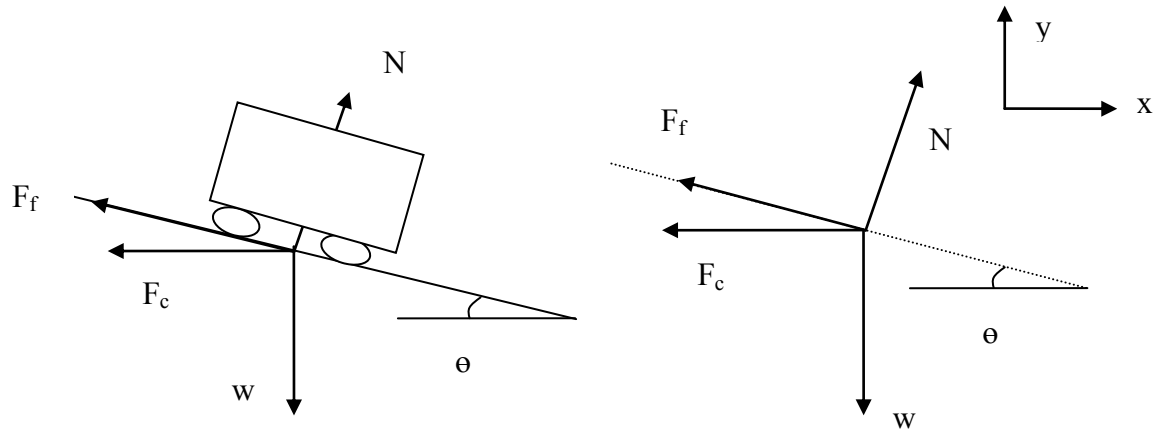

Fig.3.6 mechanics of the super elevation

From the equilibrium requirement

$$N_x - F_{fx} = f_c \quad (3.1a)$$

$$N_y - F_{fy} = W \quad (3.1b)$$

From simple mechanics, $F_f = \mu N$

The centrifugal force Fc, can also be given by

$$F_c = mv^2/R \quad (3.2)$$

Where μ= is friction coefficient of the surface and V is vehicular design speed. For the fact that the centrifugal force is a function of the vehicular load, traffic volume of the maximum possible occurrence, has also a distinctive influence over the general outward trust and hence girder torsion and distortion.

Up on simplification, the resultant action on the bridge due to vehicular speed and horizontal curvature of the bridge is as depicted below. Let the resultant centrifugal force of a single vehicle be, Frc.

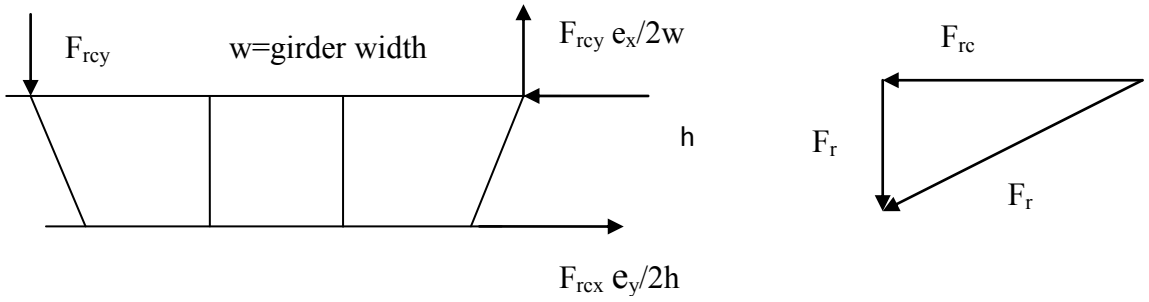

Fig.3.7a Coupled components of the resultant centrifugal force on the girder system

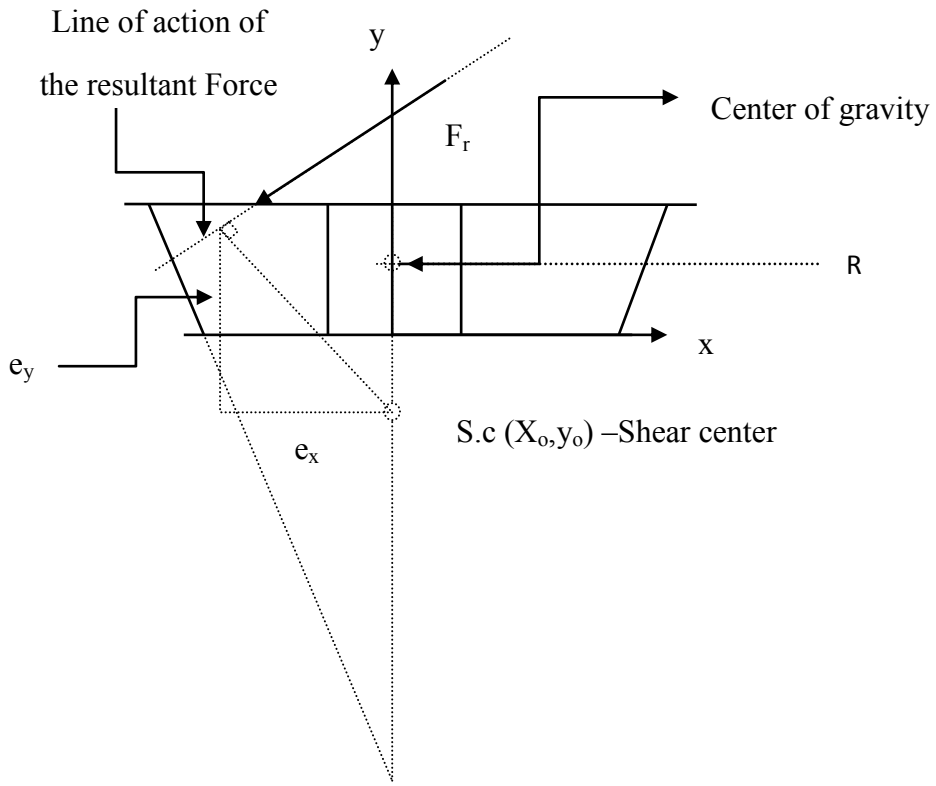

Fig.3.7b Line of Actions of the Centrifugal force and shear center

The counter acting components of the centrifugal force produces, therefore, the same torsional effect with different shear intensity.

3.4 Torsional Effects

The torsional load causes the section to,

1. Rotate rigidly (mixed torsion) and
2. Deform the section (torsional distortion).

3.4.1 Mixed Torsion

In curved box girder bridges, the transverse loads acting on the girder and centrifugal loads cause twisting about its longitudinal axis because of the bridge curvature. Uniform torsion occurs if the rate of change of the angle of twist is constant along the girder and warping is constant and unrestrained. St. Venant analyzed this problem and found that the St. Venant shear stresses occur in the cross section. If there is a variation of torque or if warping is prevented or altered along the girder, longitudinal torsional warping stresses develop.

In general, both St.Venant torsion and the warping torsion are developed when thin walled members are twisted. Box girders are usually dominated by St.Venant torsion because the closed cross section has a high torsional stiffness. Box girders have large St.Venant stiffness, which according to many other evidences, may 100-1000 times larger than that of a comparable I section.

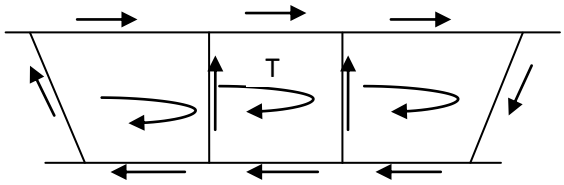

Fig.3.8 Shear flow pattern for a typical quasi- closed section

Torque and shear flow in each of the individual cells due to mixed torsion can theoretically be computed as follows.

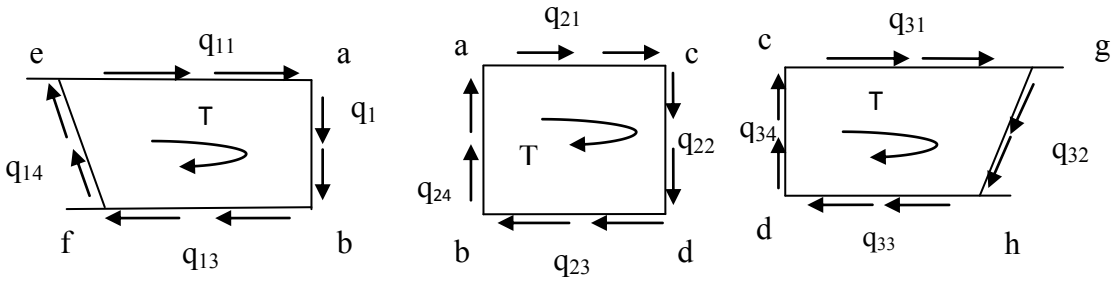

Fig.3.9 Shear flow inside the individual panel

Applying membrane analogy,

$$T=2q_iA_i \quad (3.3)$$

where A_i is area enclosed by the center line of the individual cells

$$q_i = t_it_i \quad (3.4a)$$

$$q_{ab} = q_{12}-q_{24} \quad (3.4b)$$

$$q_{cd} = q_{22}-q_{34} \quad (3.4c)$$

Shear flow into and out of junction is conserved.

$$q_{23} = q_{33}\pm q_{cd} \quad (3.5a)$$

$$q_{13} = q_{23}\pm q_{ab} \quad (3.5b)$$

$$q_{21} = q_{11}\pm q_{ab} \quad (3.5c)$$

$$q_{31} = q_{21}\pm q_{cd} \quad (3.5d)$$

Where t_i is individual segment thickness

A quasi closed section can be considered, just by applying an equivalent plate method i.e the top lateral and diagonal truss members are transformed into an equivalent plate. The intermediate panel and the exterior panel brace member configurations are different. Warren type horizontal top truss members are provided for the exterior panels and X- type horizontal top truss members are provided for the interior panel.

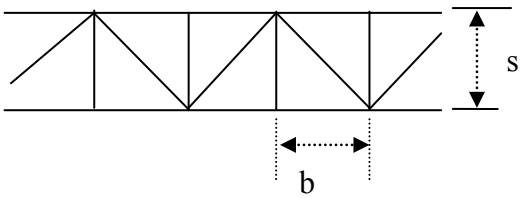

Warren type horizontal top truss between flange centerline (Straight lay out)

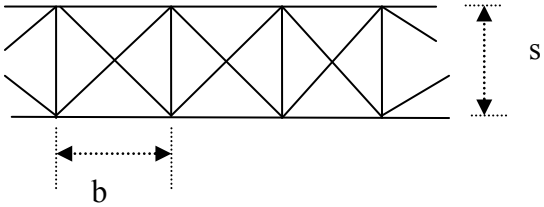

X- type horizontal top truss between flange centerline (Straight lay out)

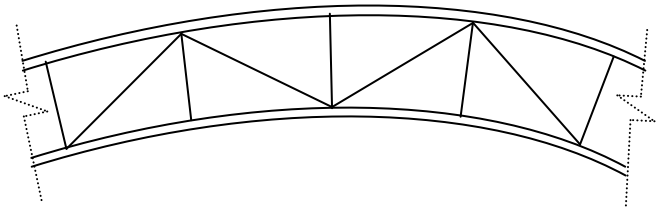

Warren type horizontal top truss between interior edges of the flange (curved lay out)

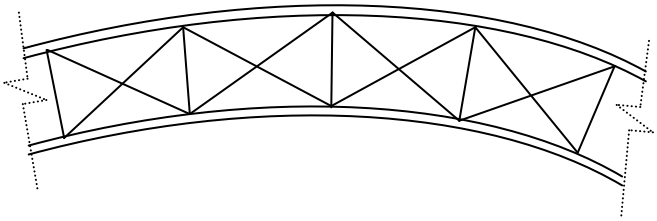

X-type horizontal top truss between interior edges of the flange (curved lay out)

Fig.3.10 Brace Layout (Configuration)

The equivalent plate thickness for the X- type and warren type bracing configurations can respectively be given as, (Chai H. Yoo, 2005),

$$t_{eqedxt} = \frac{E}{G}\frac{sb}{\frac{2d^3}{A_d}+\frac{b^3}{3A_s}+\frac{s^3}{12}\left(\frac{1}{A_u}+\frac{1}{A_l}\right)} \qquad (3.6a)$$

$$t_{eqedxt} = \frac{E}{G}\frac{sb}{\frac{d^3}{A_d} + \frac{s^3}{3}\left(\frac{1}{A_u} + \frac{1}{A_l}\right)} \qquad (3.6b)$$

Where s is distance between flange centerlines, b spacing between struts,

A_d =Area of diagonal, A_s =Area of struts, A_u and A_l =Area of girder top flanges (both sides)

Assuming the angle of twist as the same for the three cell box-girder,

$$\theta_1 = \theta_2 = \theta_3 = \theta \qquad (3.7)$$

The equations of consistent deformation or equilibrium equations are given by,

$$\sigma_{11}q_1 + \sigma_{12}q_2 - 2A_1\theta_1 = 0 \qquad (3.8A)$$

$$\sigma_{12}q_1 + \sigma_{22}q_2 - 2A_2\theta_2 = 0 \qquad (3.8B)$$

$$\sigma_{32}q_1 + \sigma_{33}q_2 - 2A_3\theta_3 = 0 \qquad (3.8C)$$

Where σ_{ij} are flexural warping coefficients and are given by

$$\sigma_{11} = \frac{1}{G}\oint_1 \frac{ds}{t} \qquad \sigma_{22} = \frac{1}{G}\oint_2 \frac{ds}{t} \qquad \sigma_{33} = \frac{1}{G}\oint_3 \frac{ds}{t}$$

$$\sigma_{12} = \sigma_{21} = \frac{1}{G}[ds/t]_{12} \qquad \sigma_{23} = \sigma_{32} = \frac{1}{G}[ds/t]_{23} \qquad (3.9)$$

Or it is simply the sum of the individual segment length to thickness ratio divided by G:

The torque is given by,

$$T = (2A_1q_1 + 2A_2q_2 + 2A_3q_3)\theta \qquad (3.10)$$

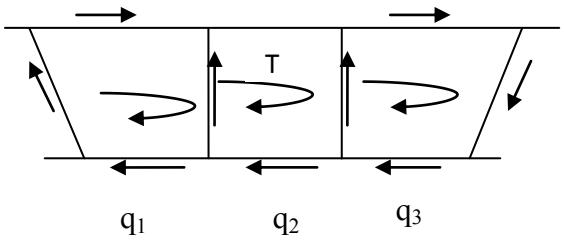

Fig.3.11 Shear flow within the closed section

Hence,
$$\begin{bmatrix} \sigma_{11} & \sigma_{12} & 0 \\ \sigma_{21} & \sigma_{22} & \sigma_{23} \\ 0 & \sigma_{32} & \sigma_{33} \end{bmatrix} = \begin{Bmatrix} q_1 \\ q_2 \\ q_3 \end{Bmatrix} = 2\theta * \begin{Bmatrix} A_1 \\ A_2 \\ A_3 \end{Bmatrix}$$

$$[\sigma]\ \{q\} = 2\theta\{A\} \qquad (3.11)$$

Hence the shear flow in each cell and the Torque are respectively given by,

$$\{q\}=[\sigma^{-}]\{A\}2\theta \quad (3.12a)$$

$$T = 2\theta\sum A_i q_i \quad (3.12b)$$

After some simplification,

$$q_1=2\theta\theta^{-1}A_1 \quad (3.13a)$$

$$q_2=2\theta\theta^{-1}A_2 \quad (3.13b)$$

$$q_3=2\theta\theta^{-1}A_3 \quad (3.13c)$$

Substituting into Eq3.9 and Eq3.11 and simplifying, θ can be obtained as;

$$\theta = \frac{1}{2}A_1.(\sigma_{11}q_1 + \sigma_{12}q_2) \quad (3.14)$$

3.5. Analysis of a Curved Girder

This section tries to address behavioral response of a general curved box girder bridge under different external action orientations. It elaborates the general idealized beam model (element) behavior of a curved bridge system (irrespective of its structural complexity) i.e only the bending and the twisting actions are idealized. It also elaborates the needs to consider additional moment reactions, even due to gravity loads only, when compared with a straight girder bridges.

3.5.1 Behavior of the girder under gravity point load

Let a general curved girder with a horizontal radius of curvature R be considered. The girder is assumed to have a fixed support at one end and a free support at the other end. This assumption for the boundary conditions does not hurt the generality of the problem. Also, it is assumed that the girder is under the uniform gravity load of w. The length of the girder is l and the angle subtended by the girder is θ. The origin of the coordinate axes is located at the fixed end of the girder. Figure 3.12 shows the general picture of the assumed girders.

From the equilibrium equations and boundary conditions, the following reaction behaviors can be obtained. To find the support reactions, the equilibrium equations about the axes X, Y and Z are written as,

$$Rx=R\ y= 0 \quad (3.15a)$$

$$Rz = wl \quad (3.15b)$$

$$M_x = \int_0^l dM_x \qquad (3.15c)$$

$$M_y = \int_0^l dM_y \qquad (3.15d)$$

$$Mz = 0 \qquad (3.15e)$$

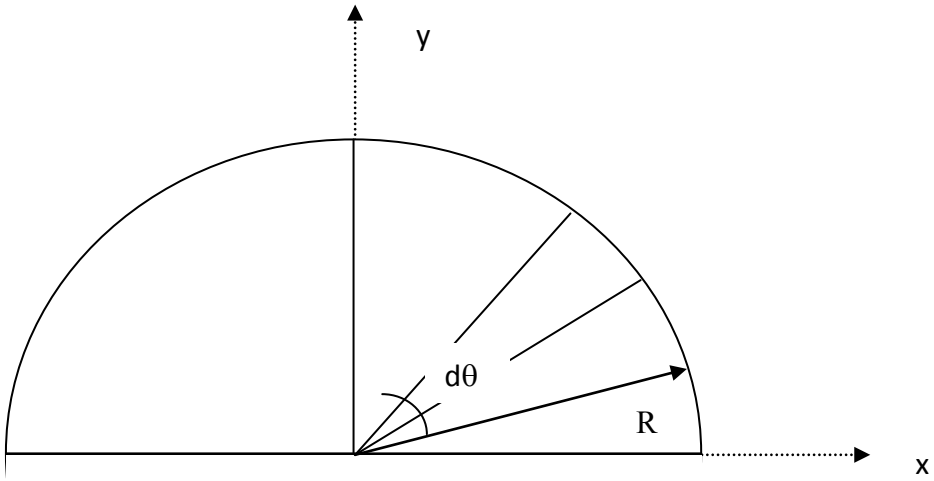

Fig.3.12 A typical curved bridge

As can be observed from the free body diagram, there is no reaction forces in the x and y directions, also no moment about z direction and the reaction along z direction is nothing other than the applied vertical load, which in this case is the weight of the girder. In order to calculate the moment reaction about x and y directions, an infinitesimal element of the girder with the length of dl and location coordinates of (a,b) is considered. The position of the element in the polar coordinates can be written as (Todd Helwig, April 2007),

$$a=-R(1-\cos\varphi) \quad \text{and} \quad b=R\sin\varphi \qquad (3.16)$$

Hence, from Eq.3.15c

$$M_x = \int_0^l dM_x$$

$$= \int_0^l (b)(wdl)$$

$$= \int_0^{\theta} (R\sin\phi)(wRd\phi)$$

$$\therefore M_x = R^2 w(1-\cos\theta)$$

$$M_y = \int_0^{l} dM_y = \int_0^{l} (a)(wdl)$$

$$= \int_0^{\theta} R(1-\cos\phi)(wRd\phi)$$

$$= R^2 w\int_0^{\theta} (1-\cos\phi)d\phi$$

$$\therefore M_y = R^2 w(\theta-\sin\theta)$$

Therefore,

$$M_x = R^2 w(1-\cos\theta) \qquad (3.17a)$$

$$M_y = R^2 w(\theta-\sin\theta) \qquad (3.17b)$$

The moment M_x is the bending moment of the curved girder at the support and the moment M_y is the torsional moment developed in the cross section of the girder at support. The noticeable fact is creation of torsional moment due to just gravity load, such as self weight, which cannot be noticed in the case of straight girders. To verify the above equations, let the values of M_x and M_y be evaluated for a special case of $R = \infty$ which is a straight girder;

$$\lim_{n\to\infty}(M_x) = w\lim R^2(1-\cos\theta) \qquad (3.18)$$

$$= w\lim_{n\to\infty}(\frac{1}{\theta})^2(1-\cos\theta)$$

$$= w\lim_{n\to 0}(\frac{1-\cos\theta}{\theta^2})$$

$$= wl^2 \lim_{n\to 0}\frac{\sin\theta}{2\theta}$$

$$= wl^2\lim_{n\to 0}\frac{\cos\theta}{2} = \frac{wl^2}{2} \qquad (3.19)$$

Similarly;

$$\lim_{n\to\infty}(M_y) = w\lim_{n\to\infty} R^2(\frac{\theta-\sin\theta}{\theta^2})$$

$$\lim_{n\to 0}(M_y) = wl^2 \lim_{n\to\infty}(\frac{1-\cos\theta}{2\theta})$$

$$\lim_{n\to 0}(M_y) = wl^2 \lim \frac{\sin\theta}{2} = 0 \qquad (3.20)$$

In the above calculations, the third and forth limits are evaluated using the L'Hopital's rule. The conclusions from this special case are in compliance with the common understanding of the behavior of straight girders. But, the major result of this part of study is for curved girders; development of torsional moment in the girder due to gravity loads in the absence of any external lateral or torsional loads.

3.5.2 Moment, torque, deflection and rotation behavioral relations

For curved girder under self-weight or gravity of concrete deck (distributed vertical load), the girder's deformation has an interaction of bending and twisting. Tung and Fountain (1970) described the deformation of curved girder with some basic differential equations, shown as Equation 3.21a ~ Equation 3.21c. For an infinitesimal segment at subtended angle β, the force equilibrium equation is shown as,

$$\frac{dv}{RdB} = \frac{dv}{dx} = -w \qquad (3.21a)$$

$$\frac{dM}{RdB} = \frac{dM}{dx} = \frac{-T}{R} + v \qquad (3.21b)$$

$$\frac{dT}{RdB} = \frac{dT}{dx} = \frac{M}{R} - t \qquad (3.21c)$$

Assumption,

T/R term is small and its effect can be neglect for moment. Then Moment can be approximated as straight girder

$$M = \frac{wx}{2}(1-x) \qquad (3.22)$$

For torque of vertical load w only, t=0

$$\frac{d^3T}{dx^3} = \frac{1}{R}\frac{d}{dx}(\frac{dm}{dx}) = \frac{1}{R}\frac{dv}{dx} = \frac{-w}{R} \qquad (3.23)$$

Integrating Eq 3.23 and evaluating for T(x), the general expression for T can be reduced as:

$$T(x) = \iiint \frac{-w}{R} dx = \frac{-w}{R}(x^3 + ax^2 + bx + c) \tag{3.25}$$

If support conditions are in such a way that the boundary condition is,

$$T(L/2)=0,\ T'(0)=T'(l)=0 \text{ and } T''(l/2)=0 \tag{3.26}$$

Similarly, the deformation equilibrium equations can be given as,

$$\frac{d\phi}{RdB} = \frac{d\phi}{dx} = \frac{-\phi}{R} + \frac{T}{GJ} \tag{3.27a}$$

$$\frac{d\theta}{RdB} = \frac{d\theta}{dx} = \frac{-\phi}{R} + \frac{M}{EI} \tag{3.27b}$$

Where, θ is rotation about the radial axis (R-axis) and φ is rotation longitudinally. Differentiating Equations Eq3.25 and substituting and simplifying, equations Eq. 3.26a through Eq. 3.26c, Eq3.27a and Eq3.27b will transform into Eq3.28a and Eq3.28b.

$$\frac{d^2\phi}{dx^2} = \frac{1}{R}\frac{d\theta}{dx} + \frac{1}{GJ}\frac{T}{dx} \tag{3.28a}$$

$$\frac{d^2\theta}{dx^2} = \frac{\phi}{R^2} + \frac{1}{EI}\left(\frac{dT}{dx} + t\right) + \frac{1}{GJ}\frac{dT}{dx} \tag{3.28b}$$

The term $\frac{\phi}{R^2}$ is usually has small value compared with other terms in the Eq3.28b. If no distributed torque T is applied, the equation is simplified as Eq3.29.

$$\frac{d^2\phi}{dx^2} = \left(\frac{1}{GJ} + \frac{1}{EI}\right)\frac{dT}{dx} \tag{3.29}$$

Thus, the longitudinal rotation of the curved girder is presented as

$$\phi(x) = \left(\frac{1}{GJ} + \frac{1}{EI}\right)\int_0^x T(s)ds \tag{3.30}$$

Up on substitution and simplification,

$$\phi_w(x) = \left(1 + \frac{EI}{GJ}\right)\int_0^x T(s)ds \tag{3.31a}$$

$$\Rightarrow \phi_w(x) = \frac{wl^2}{24R}\left(\frac{1}{GJ} + \frac{1}{EI}\right)\int_0^x \left(\frac{4s^3}{l2} - \frac{6s^2}{l} + l\right)ds$$

$$\therefore \phi_w(x) = \frac{wx}{24EIR}\left(1 + \frac{EI}{HJ}\right)(x^3 - 2Lx^2 + L) \tag{3.31b}$$

At mid-span, the maximum rotation is,

$$\phi_w(\frac{l}{2}) = \frac{5wl4}{384EIR}(1+\frac{EI}{GJ}) \quad (3.32)$$

The deflection of curved girder can be approximated by straight girder deflection and curved effect, such as,

$$\Delta_w(x) = \frac{wx}{24EI}(x^3 - 2lx^2 + l^3) + \varphi_w(x)d_o \quad (3.33)$$

Where $d_o = R(1-\cos(\frac{\beta_o}{2}))$

Substituting into Eq3.33,

$$\Delta_w(x) = \frac{wx}{24EI}(x^3 - 2lx^2 + l^3)[1+(1+\frac{EI}{GJ})(1-\cos(\frac{\beta_o}{2}))] \quad (3.34a)$$

$$\therefore \Delta_w(\frac{l}{2}) = \frac{5wl^4}{384EI}(1+(1+\frac{EI}{GJ})(1-\cos(\frac{\beta_o}{2}))] \quad (3.34b)$$

3.5.3 Behavior of the girder under point torque

Consider a simple span girder bridge supported at the extreme ends A and B. The torque at the support A and B is approximately in proportion to the distance of loading location to the other support,

$$T_A = \frac{b}{l}T = (1-\frac{a}{l})T \quad (3.35a)$$

$$T_B = \frac{a}{l}T = (1-\frac{b}{l})T \quad (3.35b)$$

$$\phi_T(x) = \frac{1}{GJ}\int_0^x T(s)ds \quad x \le a \quad (3.36a)$$

$$\phi T(x) = \frac{1}{GJ}[(1-\frac{a}{l})Ta + \int_0^x T(s)ds = \frac{Ta}{GJ}(1-\frac{x}{l}) \quad x \le a \quad (3.36b)$$

If the load is applied at mid-span,

$$\phi_T(x) = \frac{T_X}{2GJ} \quad (3.37a)$$

$$\phi_T(x) = \frac{T_x}{4GJ} \quad (3.37b)$$

3.5.4 Analysis of the Girder under Torsion

If the girder section is subjected to a general torsional loading, and if the total torsional moment of the section is T, the reaction would be in such a way that part of it develops warping shear forces in the flanges. The warping component is given by,

$$T_w = V'h \tag{3.38a}$$

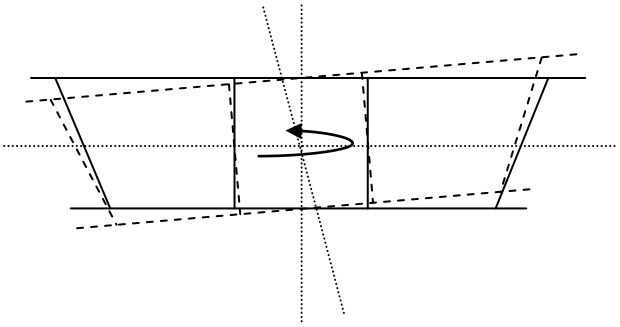

Fig3.13 Rotation geometry of the section under twisting moment
(About the axis perpendicular to plane of the section)

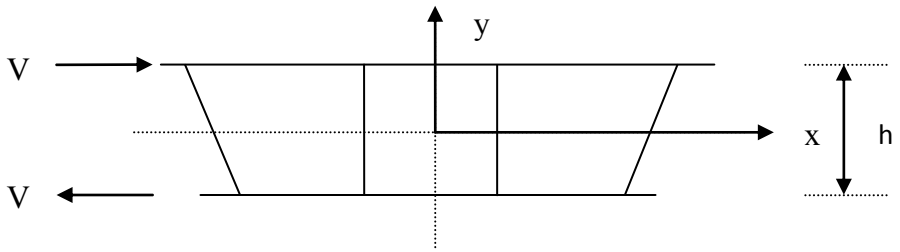

Fig3.14 Shear on the flanges

The other part of T is Ts which is the Saint-Venant torsion of the section.

$$Ts=JG\theta \tag{3.39}$$

In the above equations, the parameters h, the distance of the flange centroids, J, the torsional constant and G, the shear modulus of elasticity are known. The flange horizontal shearing force V and the angle of twist per unit length θ are unknown. To find these two unknowns, the first equation that can be written is static equilibrium of the section,

$$T=T_s+T_w \tag{3.40a}$$

$$T = JG\theta + V'h \tag{3.40b}$$

The other equation can be found from bending of the flange of girder:

$$Mf = \frac{EI}{2}\frac{d^2y}{dx^2} \tag{3.41}$$

in which M_f is the lateral bending moment of the flange, E is the modulus of elasticity and I is the moment of inertia of the section with respect to the vertical axis z, so that I_z is approximately equal to the moment of inertia of the flange about z axis. The above equation does not have any of the unknowns of the problem. The following geometric relation is used to introduce y into eq. 3.41,

$$y=h/2*B \tag{3.42}$$

This relates the lateral deflection of the flange p and the angle of torsion ρ. Two differentiations yields,

$$\frac{d^2y}{dx^2}=\frac{h}{2}\frac{d\beta}{dx}\text{and}\frac{d\beta}{dx}=\theta \tag{3.43}$$

Substituting and simplifying,

$$\frac{d^2y}{dx^2}=\frac{h}{2}\frac{d\theta}{dx} \tag{3.44}$$

$$\frac{EIh}{4}\frac{d\theta}{dx}=-M_f \quad \text{and} \quad \frac{dMf}{dx}=V' \tag{3.45}$$

$$\text{So,} \quad \frac{EIh}{4}\frac{d^2\theta}{dx^2}=-V^2 \tag{3.46}$$

Substituting Eq3.46 in to Eq3.40b,

$$\frac{EIh^2}{4GJ}\frac{d^2\theta}{dx^2}+\theta=\frac{T}{GJ} \tag{3.47a}$$

Let $a=\frac{h}{2}\sqrt{\frac{EI}{GJ}}$

$$a^2\frac{d^2\theta}{dx^2}+\theta=\frac{T}{GJ} \tag{3.48}$$

The solution for this second order differential equation is,

$$\theta=Ae^{\frac{x}{a}}+Be^{\frac{-x}{a}}+\frac{T}{GJ} \tag{3.49}$$

The value of A and B can be found by applying boundary conditions,

$$\frac{d\beta}{dx} = \theta = 0 @ x = 0 \tag{3.50a}$$

$$\frac{d\theta}{dx} = 0 @ x = 1 \tag{3.50b}$$

Finding the values of A and B, results the following values of θ and β,

$$\theta = \frac{T}{GJ}\left(1 - \frac{\cosh(\frac{l-x}{a})}{\cosh(\frac{l}{a})}\right) \tag{3.51}$$

Since, $\frac{d\beta}{dx} = \theta$ implies $\beta = \int_0^x \theta dx$

$$\beta = \frac{T}{GJ}\left(L - a\tanh\frac{l}{a}\right) \tag{3.52}$$

Substituting Eq3.51 into Eq3.40,

$$Ts = T\left(1 - \frac{\cosh(\frac{l-x}{a})}{\cosh(\frac{l}{a})}\right) \tag{3.53}$$

The maximum torsional shear τ_{max} can be calculated as,

$$\tau_{max} = \frac{2T_s h_{max}}{J} \tag{3.53}$$

And the lateral torsional moment of the flange is calculated as,

$$Mf = \frac{-T}{h} a \frac{\sinh(\frac{l-x}{a})}{\cosh(\frac{l}{a})} \tag{3.54}$$

So, the maximum lateral bending moment of the flange is equal to,

$$Mf = \frac{T}{h} a * \tanh\frac{l}{a} \tag{3.55a}$$

As the length of the girders are relatively large, the value of $\tanh\frac{l}{a}$ is approximately equal to a unity and the following values are obtained for β and $M_{f,}$

$$\beta = T(\frac{L-a}{GJ}) \quad \text{and} \quad M_f = \frac{T}{h}a \tag{3.55b}$$

3.5.5 Further on Uniform and non uniform torsion

For the same beam idealization above, the torsional behavior of the bridge is mainly described by twisting angles (θ_x) of its cross sections with respect to the longitudinal axis (x) passing through the torsional center C (y_c, z_c). The angle of twist per unit length at a particular position is calculated as a function of the torsional moment T resulting from the applied load T being the total external torque balancing torsional moment. When subjected to a torsional deformation, the cross section does not remain planar; it generally warps. This warping is measured by an axial displacement γ (Saadé, Année académique 2004-2005)
The torsion is so named as mixed when both T_s and T_w are different from zero,

3.5.5.1 Uniform torsion (Saint Venant torsion)

The warping (γ) is assumed to be constant along the longitudinal axis (x) of the beam. The axial displacement of any point q of the cross section under Saint Venant torsion can be given as,

$$\gamma = \omega(y,z)\theta_{x,x}(x) \tag{3.56}$$

Where $\theta_{x,x}$ is the rate of twist and $\omega(y,z)$ is the warping function of the cross section.

The expression of the displacement field can be simplified as,

$$\begin{aligned} U &= \omega\theta_x \\ V &= -(z-z_c)\theta_x \\ W &= (y-y_c)\theta_x \end{aligned} \tag{3.57}$$

where U, V and W are displacement fields along x, y and z directions respectively.

For a uniform warping along x, $\omega\theta_{x,x}$ is assumed to be a constant rate with respect to x. Thus, its derivative $\omega\theta_{x,xx}$ vanishes and the linear strain vector deduced from (3.57) is,

$$\begin{Bmatrix} \varepsilon x \\ 2\varepsilon xy \\ 2\varepsilon xz \end{Bmatrix} = \begin{bmatrix} 0 \\ -(\theta y + z - z_c)\theta_{x,x} \\ (-\omega z + y - y_c)\theta_{x,x} \end{bmatrix} \tag{3.58}$$

The torsional equation (Eq3.59) is usually deduced from equilibrium considerations. Alternatively, the principle of virtual work can be used with Hooke's law and strain

expressions (3.58). The differential equilibrium equation, relating the rate of twist $\theta_{x,x}$ to the torsional moment T and to the torsional stiffness GK , is obtained after integrating and isolating the virtual twisting angle θx*.

The torsional resultant is found to be,

$$T = [(y - y_c)\tau_{xz} - (z - z_c)\tau_{xy}]dA \tag{3.59}$$

Let the torsional constant K, be given by the expression (3.60),

$$K = \int [(-\omega_z(y - y_c) + \omega y(z - z_c) + (y - y_c)^2 + (z - z_c)^2]dA \tag{3.60}$$

Then,

$$\theta_{x,x} = \frac{T}{GK} \tag{3.61}$$

Equation (2.60) shows that the cross section warping influences the value of K. The warping function (ω) must first be computed in order to determine the torsional stiffness and to solve the Saint-Venant torsional problem. The evaluation of ω is different for each cross section and depends on the boundary conditions of the shear stresses and on the geometrical shape of the profile, especially whether the cross section is open or closed. Katty had also revised the formerly developed approximate expressions for the warping function (ω) of some thin-walled cross sections so that K can explicitly be evaluated.

It has to be noted however, that for open thin walled profiles, approximated values of (ω) lead to an incorrect value of K if directly substituted in (3.60). Therefore, deducing the torsional constant from explicit values of ω has to be detailed.

The Saint Venant theory is exact in the case of uniform torsional moment distribution without restrained warping of the cross sections. Similarly, for some particular profiles (symmetrical) which, due to their radial symmetry, do not warp, the Saint Venant theory of torsion is always exact, even if the torsional moment distribution is not uniform. For other particular geometries (none symmetrical) the contour warping vanishes and, if the thickness warping is neglected, the de Saint Venant theory is used. The distortional behavior of the box girder is briefly discussed in unite 4;

Chapter Four

4.0 The Stress Behavior of Steel Box Girders

4.1 Stress Preliminaries

According to the flow direction, with respect to plane of the section, stresses are named as normal and shear stresses. From the perspectives of the external actions through which they are induced from, stress can also be classified as bending stresses, torsional stresses, distorsional stress flexural stresses, direct compressive and tensile stress. The shear and normal stresses are induced in the bridge system due to either of the action and reaction mechanisms stated earlier.

4.1.1 Normal Stress Due to Curvature Effect of the Bridge

It has clearly been stated in chapter three that horizontally curved bridges will experience bending, twisting and distortional actions. The corresponding shear stresses are therefore, induced in the structural system.

The bending σ_b, distortional σ_d and torsional warping $\sigma_{t\omega}$ stresses are induced both on the bottom and top flange of the girder system.

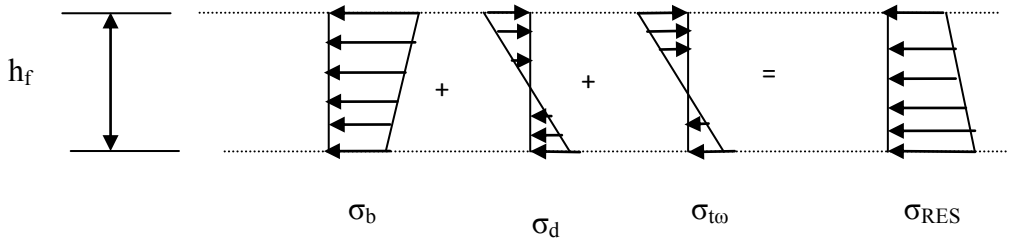

Fig.4.0 Normal stress component of top flange

Bending stress+ Distortional stress+ Tortional Warping Stress=Resultant stress

$$\sigma_{RES} = \sigma_b + \sigma_d + \sigma_{t\omega} \qquad (4.1)$$

The bottom and top flanges experience stresses differently (either tensile or compressive in an alternate sense). It is this resultant stress that produces either the tensile or compressive stresses in the respective sections. For the bending stress, for example, the top flange is usually under compression state while the bottom flange is under tension at mid span of the bridge.

As has been discussed under the general static behavior of a horizontally curved girder, the bending moment and torsional moment are always coupled with each other due to the

curvature of the girder axis. As a result, an externally applied vertical force is resisted internally by a combination of a bending component, a torsional component, and a distortional component. The internal bending component includes longitudinal normal stresses and flexural shear stresses in the cross section of the box girder. The torsional component includes pure torsion (usually called St.Venant torsion) and warping torsion (usually called non-uniform torsion). The St.Venant torsion induces torsional shear stresses and the warping torsion induces longitudinal normal stresses and shear stresses in the cross section of the box girder, which are referred to as torsional warping stresses (Chai H. You 2005). The distortional component induces distortional stresses that consist of longitudinal normal stress and shear stress.

Consider again the differential element (described in section 3.1.1) of a horizontally curved girder flange of width, db, length, ds, thickness, t, and radius, R, under bending normal stress (repeated for convenience).

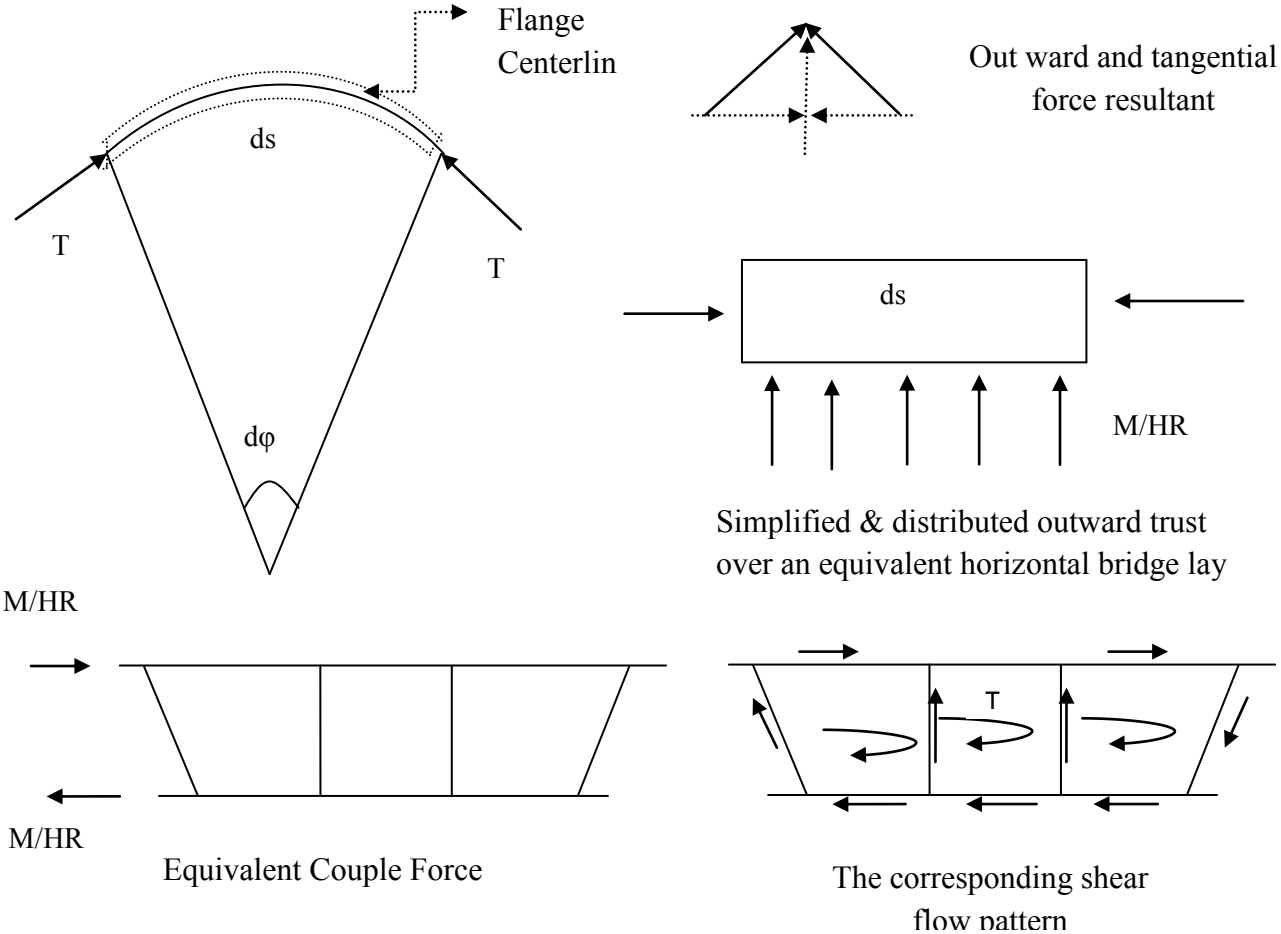

Fig.4.1a Shear Analysis of the Girder System

The force can then be resolved into radial and tangential components as shown in fig4.1a), producing an outward trust on the top flange (under compression). The counter balancing force is induced in the bottom flange and hence produces a horizontal couple.

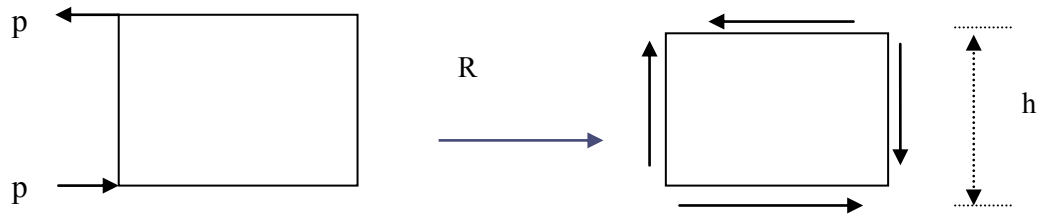

Fig.4.1b Negative moment region

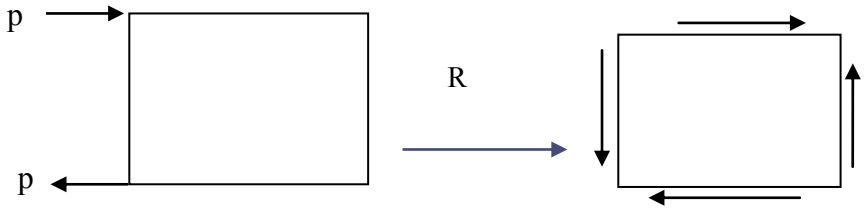

Fig.4.1c Positive moment region

The longitudinal stress in a box girder is therefore, composed of bending, distortional, and torsional warping stresses. It is well known that the distortion and the torsional warping induce a non-uniform normal stress distribution in the flanges as shown in Fig4.0. The torsional shear stress due to St.Venant torsion in a box girder is the main resisting mechanism against the applied torsion. Stresses induced by warping torsion are small compared to the St. Venant torsional shear stress. Therefore, stresses induced by warping torsion are usually less important in stiffened closed box type cross-sections. Since the stiffness of the box section against distortion is relatively weak compared with the bending stiffness or torsional stiffness, the distortional stresses may become fairly large if adequate distortional stiffeners are not provided to the box girder. Therefore, the distortional stresses must be examined closely in box girders that are subjected to torsional moment.

4.1.2 Distortional Stresses

The distortion of a box girder can be defined as the cross sectional deformation due to two pairs of coupled internal forces acting on the cross section which are equilibrated with each other. The distortional force occurs due to the horizontal induced forces in flanges as

described above (fig4.1). Distortional force acting on the cross-section, usually consisting of the two pairs of coupled forces, as shown in Fig. 4.1c and 4.2(b).

The distortional force can also occur when an eccentric loading is applied to a box girder of a symmetric cross-section. The applied force can be resolved into a vertical bending force, P, and a torsional force, Pb/2, as shown in Fig. 4.2(a). The torsional force is then divided into pure torsion and distortion as shown in Fig. 4.2(b). As can be noted from Fig. 4.2(b), the distortional force occurs in a box girder when a torsional force, represented by a pair of coupled forces, is not completely balanced with the St.Venant shear flow.

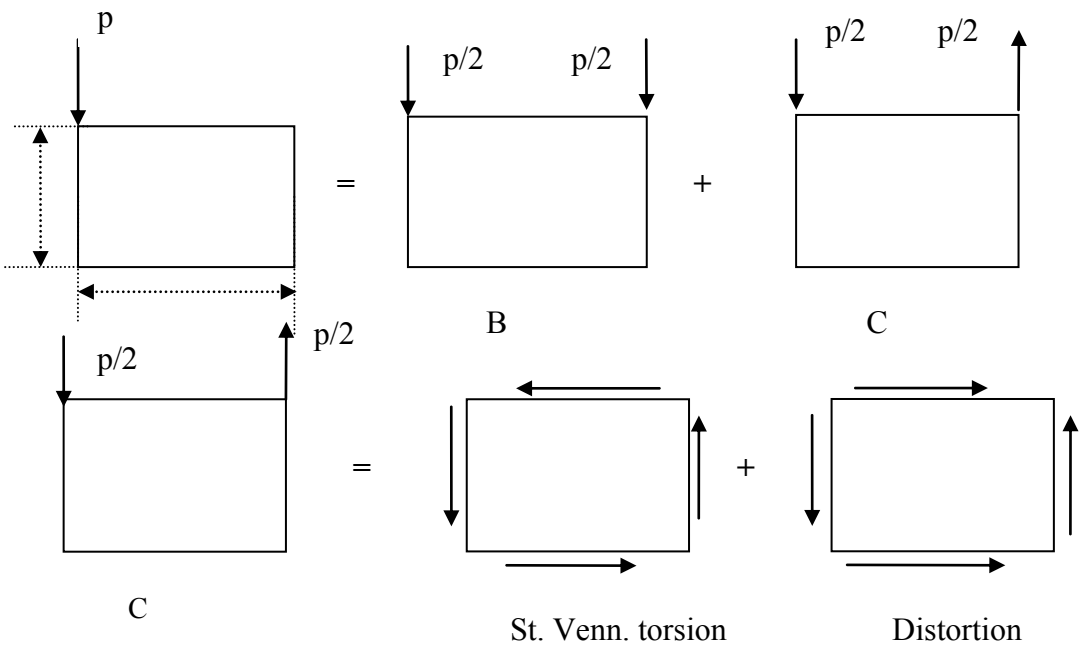

Fig.4.2 distortional stress in box section

The distortion of the box girder is expressed as the angular change of the cross section, as shown in fig. 4.3 and fig4.4. Let the rectangular coordinate axes (x, y, z) are taken at the distortional center, D and the curvilinear coordinate axis, s, be adopted along the perimeter of the cross-section. The angular change, ϕ , is defined as,

$$\phi = \frac{v_l - v_u}{h} + \frac{w_i - w_o}{h} \qquad (4.2)$$

where v and w are, the displacements in the direction of the *x* and *y* coordinate directions, respectively. They have their origin at the distortional center; *D*. Many literatures referred the first formal differential equation for distortion of a horizontally curved box girder which was proposed by Dabrowsky (1968) and is given by,

$$\phi^{iv} + 4\lambda\phi = \frac{1}{EI_{DW}}(\rho\frac{M_x}{R} + \frac{M_z}{2}) \qquad (4.3)$$

Where $\lambda = \sqrt[4]{\frac{k_{DW}}{4EI_{DW}}}$ (length -1 unit); K_{DW}, stiffness of the box section against distortion (force / angle unit); EI_{DW}, distortional warping rigidity (force x length^4 unit); I_{DW}, distortional warping constant (length^6 unit) $= \int \omega^2_D dA$, *R* = radius of curvature; *Mx,* bending moment; *Mz,* distortional force; ρ, dimensionless parameter consisting of cross-sectional geometric properties. ω_D , distortional warping function, is expressed as,

$$\omega_D(s) = \int_0^s r(s)ds + C_1 \qquad (4.3)$$

where C_1 is an integration constant and r(s*)* represents the vertical distance parallel to the *y* axis along the perimeter of cross section, s. It is noted that the unit of ω_D is length square. The derivative of the angular distortion, ϕ', yields the displacement, *γ*, in the direction of the longitudinal *z*-axis.

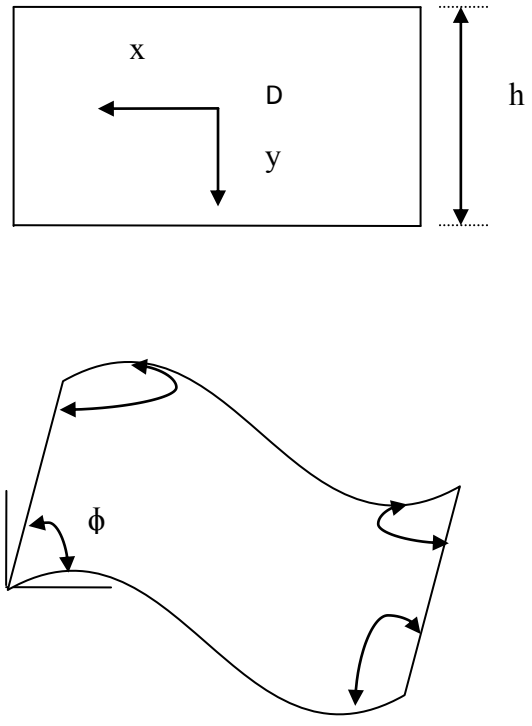

Fig4.3 Angular change ϕ in box sections due to Distortion

The distribution of distortional normal stress can then be developed by applying hook's law and equilibrium equations.

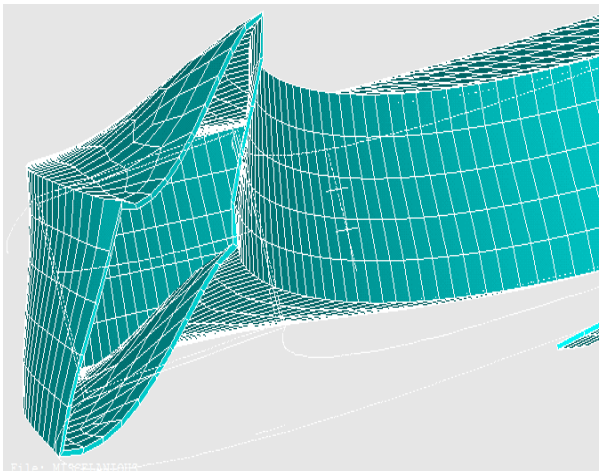

Fig.4.4 a Atypical distorted rectangular unite cell section,
Subjected to a counter acting actions

4.1.3 Center of twist

Each individual panel can separately be considered to compute its respective center of twist. Then, the overall twist center of the section can be calculated. Let the translational displacements in the X and Z directions respectively be u and w, and rotational displacement about Y be θ.

Assuming a general closed section and v_t as the tangential component of the overall stress in the section, the expression for v_t will be,

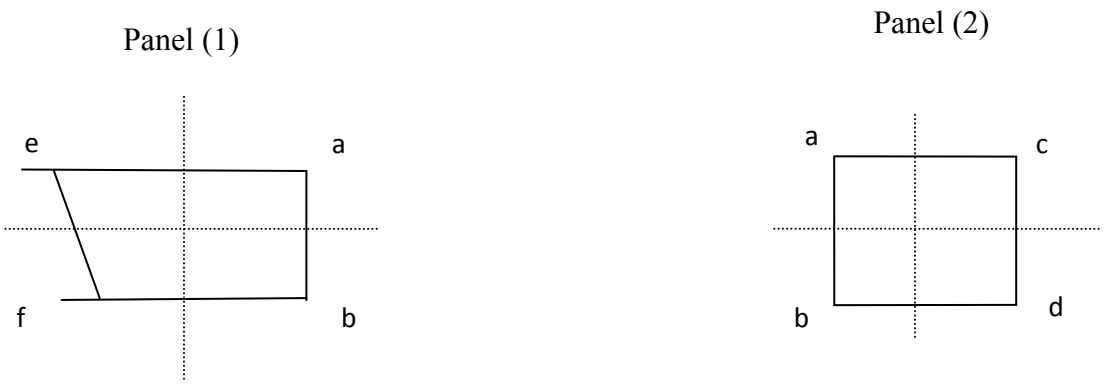

Fig.4.5 Center of twist

Where ψ is the angle between the local x- axis and the direction of the shear flow, and ρ is the perpendicular distance from the origin to the shear, under consideration,

$$v_t = \rho\theta + u\cos\psi + w\sin\psi \qquad (4.4)$$

Differentiating eq4.4 with y gives;

$$\frac{\partial v_t}{\partial y} = \rho\frac{d\theta}{dy} + \frac{du}{dy}\cos\psi + \frac{dw}{dy}\sin\psi \qquad (4.5)$$

The displacements u, w and θ is equivalent to pure rotation about the R (Center of twist)

$q=\rho R\,\theta$

Differentiating,

$$\frac{\partial v_t}{\partial y} = \rho\frac{d\theta}{dy} - X_R\sin\psi\frac{d\theta}{dy} + Z_R\cos\psi\frac{d\theta}{dy} \qquad (4.6)$$

Comparing the coefficients in 3 and 4,

$$X_R = \frac{dw/dy}{d\theta/dy} \qquad Z_R = \frac{du/dy}{d\theta/dy} \qquad (4.7)$$

4.1.4 Shear in the Section

The Shear q in the section along the path S can analytically be computed, in the z-x coordinate axis as,

$$\frac{\partial q}{\partial s} = \frac{S_x I_{xx} - S_z I_{xz}}{I_{xx}I_{xz} - I_{xz}^2}tx - \frac{S_z I_{zz} - S_x I_{xz}}{I_{xx}I_{zz} - I_{xz}^2}tz \qquad (4.8)$$

$$\text{Let } A = \frac{S_x I_{xx} - S_z I_{xz}}{I_{xx}I_{xz} - I_{xz}^2} \quad \text{and} \quad B = \frac{S_z I_{zz} - S_x I_{xz}}{I_{xx}I_{zz} - I_{xz}^2}$$

$$\frac{\partial q}{\partial s} = Atx + Btz \qquad (4.9)$$

If an origin is chosen for S where shear flow is $q_{s,0}$

$$q_s = A\oint_0 txds - B\oint_0 tzds + q_{s,o} \qquad (4.10)$$

The term $A\oint_0 txds - B\oint_0 tzds$, is open section shear,

Rewriting the shear, $q_s = q_b + q_{s,0}$

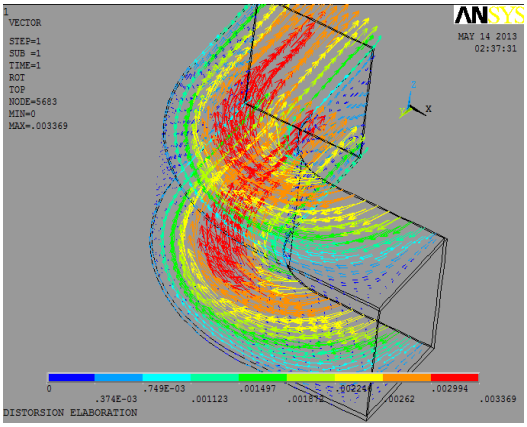

(a)

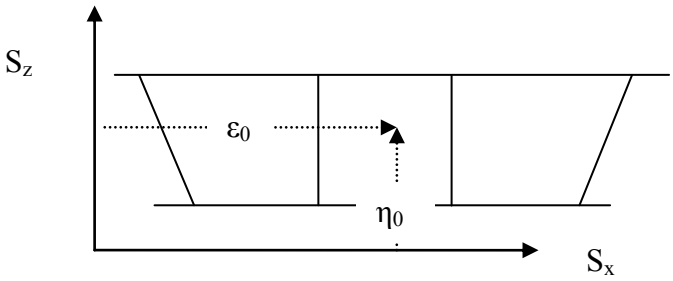

(b)

Fig.4.6 (a) Load vector on a warped section for a random loading and (b) shear flow origin

$$S_x\eta_o - S_z\varepsilon_o = \oint \rho q_b ds + 2Aq_{s,o} \qquad (4.11)$$

if moment center is chosen to coincide with lines of actions S_x and S_z,

$$0 = \oint \rho q_b ds + 2Aq_{s,o} \qquad (4.12)$$

4.1.5 Shear center

The location of the shear center and the warping constant was determined using a finite difference approach presented by Heins (1975) and was derived for use with open sections. For pseudo-closed cross sections, the shear center is nearly coincident with that of the open section. The endpoints of the flanges and intersection points where the webs and flanges meet correspond to the centerline of the flanges. The arrows next to each element define the element's orientation and flow direction, which should not be confused with the actual shear flow. These flow directions are used to maintain proper signs during calculations.

For sections that have one axis of symmetry, I_{xy} is equal to zero. As a result, the shear center coordinates for the trapezoidal section simplify to,

$$X_o = \frac{I_{xy}I_{wz} - I_yI_{wz}}{I_{xy}^{\ 2} - I_xI_y} \qquad (4.13a)$$

$$Y_o = \frac{I_{xy}I_{wz} - I_yI_{wz}}{I_{xy}^{\ 2} - I_xI_y} \qquad (4.13b)$$

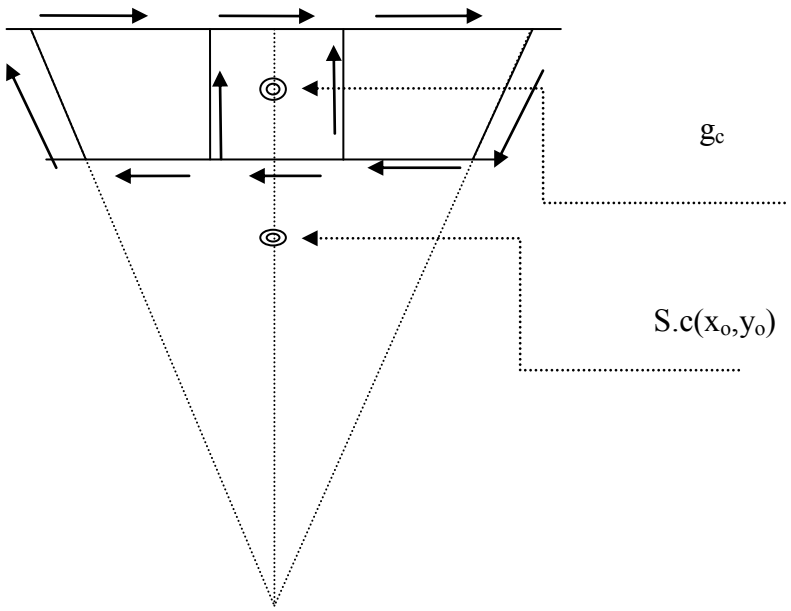

Fig.4.7 Shear center

More common hand methods can be used to determine the moment of inertia, and a tabular format for a finite difference approach implementation can be formalized to calculate center of twist.

4.1.6 Eccentricity between Shear Center and Centroid

The eccentricity between the centroid and shear center is relatively small for closed cross sections except the partially closed (quasi-closed) sections, during construction. The above stiffness matrix computation is based on the assumption that the centroid and the shear center of the cross section coincide. Although the shear center and centroid of a section are coincident in many engineering shapes, the (quasi-closed) sections during construction violate the coincidence.

During construction, prior to the full composite action of the concrete and the flange, the shear center often falls below the bottom flange while the centroid is usually within the plates (flanges and webs). Hence, a large eccentricity is created. It would be an inaccurate modeling if in centricity is not accounted. Therefore, the derived stiffness matrix is treated by a special transformation for that purpose.

If a general cross section for which the shear center and the centroid doesn't coincide is considered, the eccentricity between the shear center and centroid leads to a coupling between torsion and bending DOFs. If it is supposed that the local coordinate system *x* passes through the centroid line and that the *y* and *z* represent the weak and strong bending axes, respectively,

a shear force acting at the centroid of the cross section, but not the shear center, generates extra torsion because of the eccentricity.

The effect of the eccentricity (0, dy, dz) is accounted by using the following transformation equation, (Dubigeon and Kim 1982). The transformation matrix size is equivalent to the total size of the stiffness matrix.

$$Ksc=Tsc*K*Tsc^{T} \quad (4.14)$$

4.1.7 Warping stress ratio

One of the main goals of this research is to determine the effect of warping on both shear and normal stresses. This is achieved by investigating the ratio between approximate stresses calculated using classical beam theory (i.e. ignoring warping) and exact stresses which include the effect of warping.
The Technical Report Performed by Center for Transportation research, University of Texas at Austin, 2005, Titled with bracing systems for trapezoidal steel box girder bridges, formalizes an investigative procedure and briefly states the significance of warping effects.

For each bridge, ratios pertaining to both normal and shear stresses are calculated at selected key points in critical sections with the highest exact stresses. The key points to be considered in each cross-section shall be selected based on the best of technical scenarion.
The warping stress ratios for both normal stresses, ($WSR-N$) and shear stresses ($WSR-S$) are then calculated as follows,

$$WSR-N=\frac{\sigma_{exact}-\sigma_{approx}}{\sigma_{approx}} \quad (4.12)$$

$$WSR-N=\frac{\tau_{exact}-\tau_{approx}}{\tau_{approx}} \quad (4.13)$$

Where N is normal stress and S is shearing stress.

Chapter Five

5.0 Formulation of the stiffness matrix

A number of approaches can be applied to formulate stiffness matrix. The structural unite is considered as general shell element, the rotational degrees of freedoms being the central concern. The local coordinate axis has to be carefully selected in a manner that the z axis is directed into the shorter dimension of the shell. The local coordinate system has to be transformed into global coordinate system.

From this general perspective, the structural element can be constructed by separately considering and dividing the six nodal shell elements into an equivalent **membrane element** and plate **bending element.**

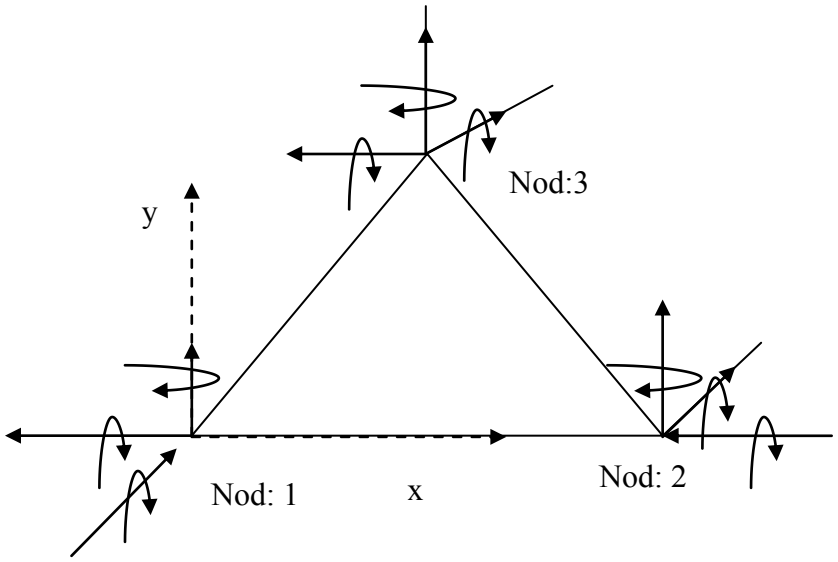

Fig.5.1a six plus one nodal DOF shell element

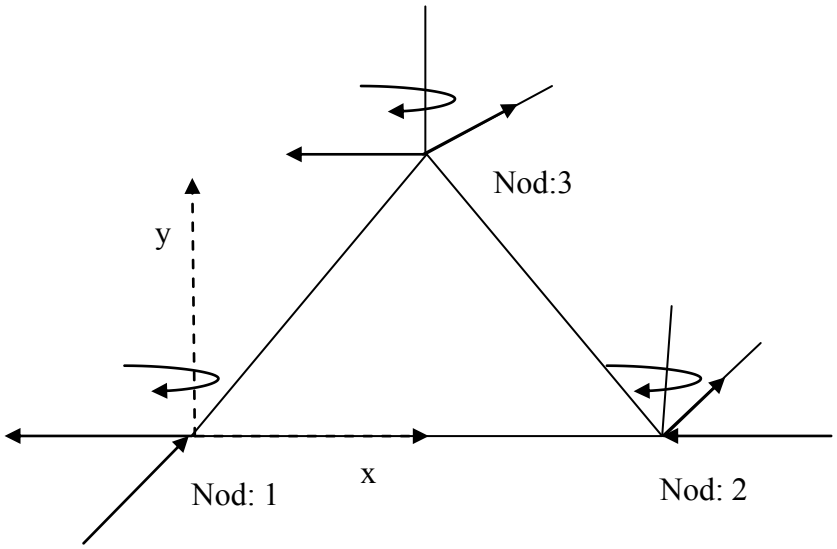

Fig.5.1b membrane element

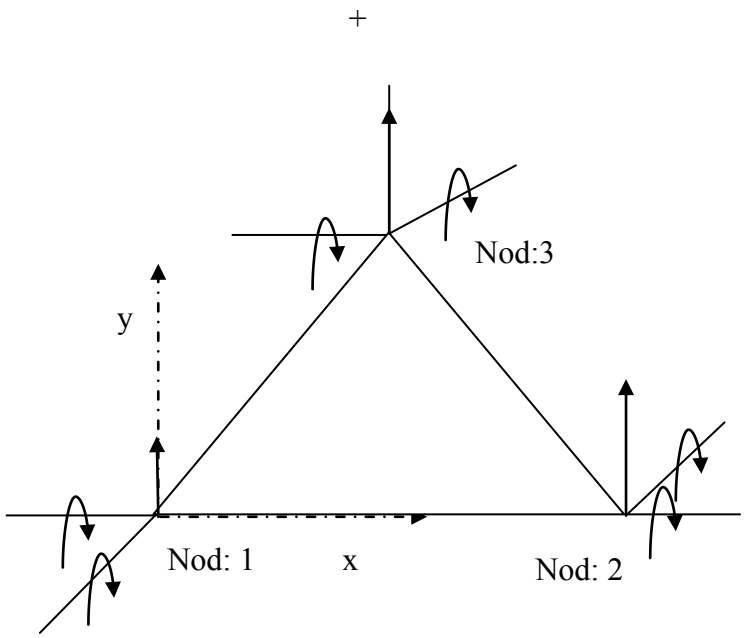

Fig.5.1c plate bending element

5.1 Plate Bending Element

5.1.1 Introduction

The element shown in fig5.1c with one translational and tow rotational DOFs is usually called the plate bending element. The plate stiffness, kp and membrane stiffness, k_{mem}, can be combined after sepatetly formalized.

$$k = \begin{bmatrix} k_{mem} & 0 \\ 0 & k_p \end{bmatrix}$$

The general procedures adopted in the stiffness matrix formulation of the element are,

- Identification of the appropriate nodal degrees of freedom say {q},
- Assume an appropriate solution for the displacement field over the element w(x,y) Obtain the corresponding shape functions {N(x,y) for {q} so that, $w(x,y)=\{N(x,y)^T\{q\}$
- The element stiffness matrix will then take the usual form of

$$[k] = \int_v [B]^T [D][B] dV$$

Where $\{\sigma\}=[D]\{\varepsilon\}$

[D] is the matrix of elastic properties in the stress-strain relation

5.1.2. Plate Degrees of Freedom and Displacement Function

Let a rectangular plate bending element be taken to show the general procedure in this section, and degrees of freedoms at the ends of each edge which are analogous to that of beam theory, be chosen i.e., a transverse displacement and normal rotation about each axis. Figure 5.2 shows a rectangular plate with the following degrees of freedom at each of the four comer nodes: w_i, θ_{xi}, θ_{yi} where $\theta_{xi}=dw_i/dy$ and $\theta_{yi}=dw_i/dx$ where are the transverse displacement and rotations about the x and y axis, respectively, at node i.

Note that θ_{yi} is a vector in the negative y direction and node "1" is located at the lower left comer of the plate (x=-a, y=-b) and that the nodes are numbered 1,2,3,4 in a CW direction around the plate. We assume that the plate dimensions are given by 2a and 2b as shown in

Figure 5.2 and that the x-y coordinate system is located at the center of plate. The 12 degrees of freedom are arranged in the {q} matrix as;

$$\{q\}^T=\{w_1\ \theta_{x1}\ \theta_{y1}\ w_2\ \theta_{x2}\ \theta_{y2}\ w_3\ \theta_{x3}\ \theta_{y3}\ w_4\ \theta_{x4}\ \theta_{y4}\} \quad (5.2)$$

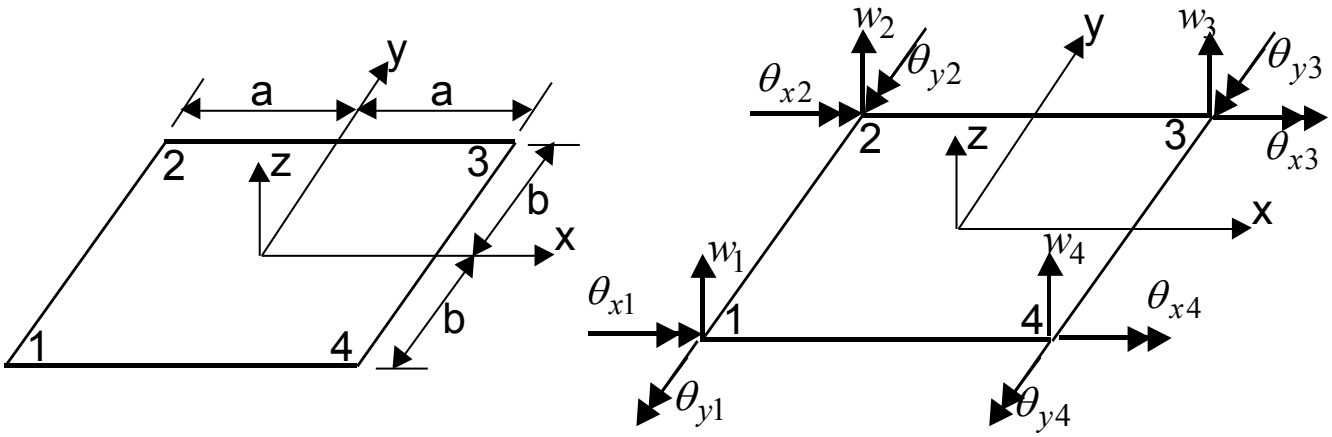

Fig.5.2 Rectangular Plate Geometry and Nodal Degrees of Freedom

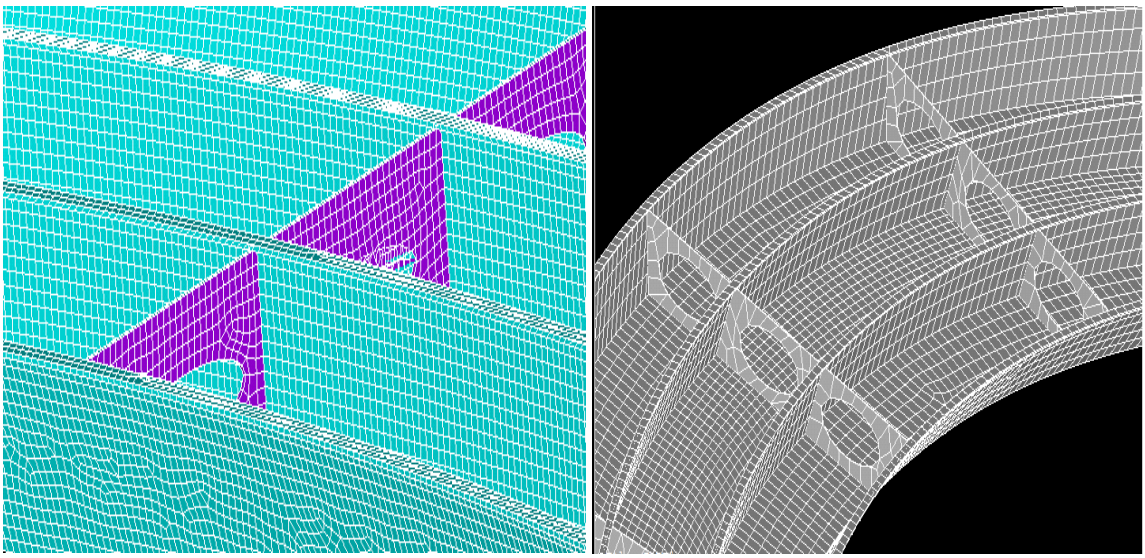

Fig.5.3 A rectangular mesh element for the girder and diaghram component of the bridge

We assume that w(x,y) is some function over the plate geometry. A general quartic polynomial expression for w(x,y) can be written as 15 terms

$$W(x,y)=a_1+a_2x+a_3y+a_4x^2+a_5xy+a_6y^2+a_7x^3+a_8x^2y+$$
$$a_9xy^2+a_{10}y^3+a_{11}x^4+a_{12}x^3y+a_{13}x^2y^2+a_{14}xy^3+a_{15}y^4 \quad (5.3)$$

The expression for w(x,y) is referred to as a complete fourth-order polynomial since it contains all fourth-order products of x and y. However, consistent with the assumption of 12 degrees of freedom for the rectangular plate element, it is necessary to choose only the most appropriate 12 terms for w(x,y).

Consequently, we will choose the complete set of cubic terms (10 terms) and the two quartic terms x^3y and xy^3,

$$W(x,y)=a_1+a_2x+a_3y+a_4x^2+a_5xy+a_6y^2+a_7x^3+a_8x^2y$$
$$+a_9xy^2+a_{10}y^3+a_{11}x^3y+ a_{12}xy^3 \quad (5.4)$$

It is generally adjusted in such a way that an attempt is made to satisfy stress continuity conditions along the edges and improve the convergence characteristics of the element for stresses.

In defining the geometry, as well as the displacement functions, it is expedient to define normalized coordinates ξ and η such that $\xi = x/a$ and $\eta = y/b$. In the normalized (ξ ,η) coordinate system, the plate coordinates are given by-$1 \le \xi \le 1$ and $-1 \le \eta \le 1$.

In order to obtain the shape functions in the x,y coordinate system, we follow the standard procedure and write one equation for each of the 12 degrees of freedom as follows,

$$w_1=q_1 = f(x=-a,y=-b)$$

$$\theta_{x1}= q_2 =dw/dy=f(x=-a,y=-b)$$

and so forth through the 12th equation;

$$\theta_{y4}= q_{12} =dw/dx=f(x=a,y=b)$$

These 12 equations may be solved for the 12 unknown coefficients a_1, a_2, and $a_3 \ldots a_{12}$ (which will be in terms of the 12 nodal degrees of freedom q_i). Substituting the solution for the coefficients into w(x,y), and rearranging into the form of

$$w(x,y)=\{N(x,y)\}^T\{q\} \qquad (5.5)$$

Gives the following for some of the shape functions,

$$N_1(x,y)=1/8(1-x/a)(1-y/b)(2-x/a-y/b-(x/a)^2-(y/b)^2) \qquad (5.6)$$

or, in terms of non-dimensional coordinates (ξ,η) using the transformation ξ=x/2 and η=b/2,

$$N_1(\xi,\eta)=1/8(1-\xi)(1-\eta)(2-\xi-\eta-\xi^2-\eta^2)$$

Similarly,

$$N_2(\xi,\eta)=(b/8)(1-\xi)(1-\eta)^2(1+\eta)$$

$$N_3(\xi,\eta) =(a/8)(1-\xi)^2(1-\xi)2(1-\eta) \qquad (5.7)$$

And so forth through $N_{12}(\xi,\eta)$. Note that {N} is a (12x1) column matrix (since we have 12 degrees of freedom).

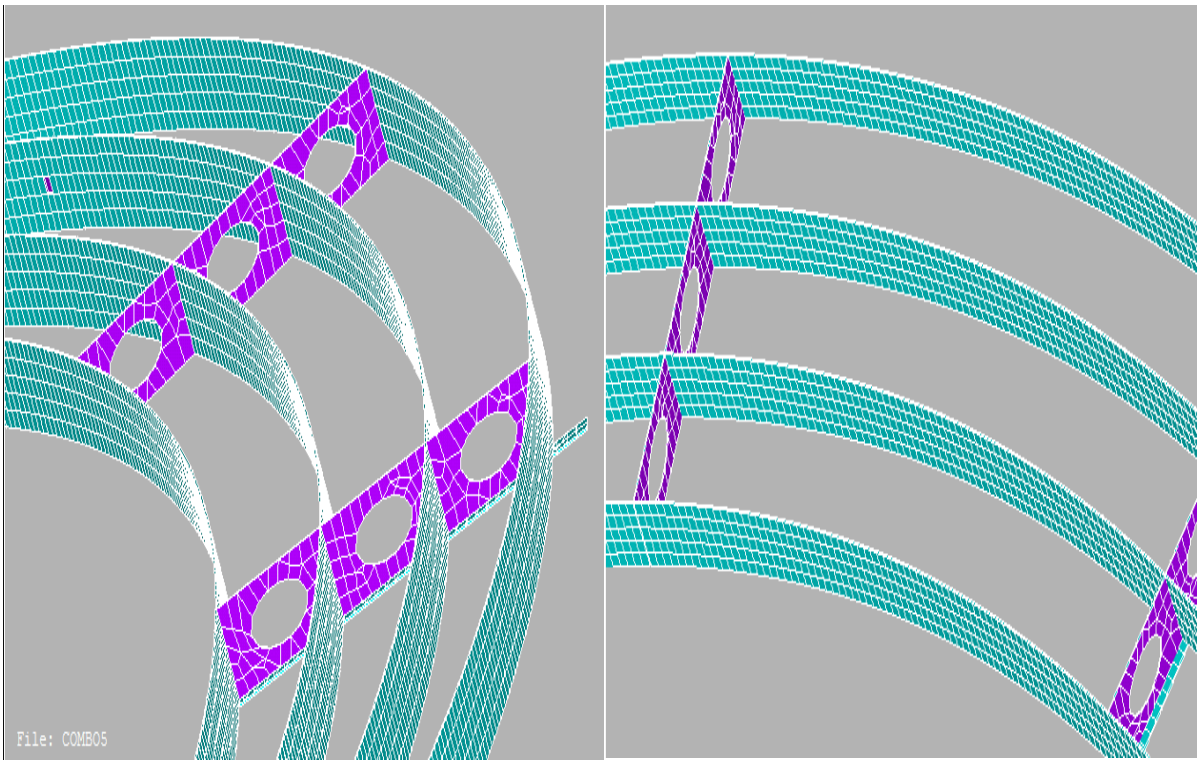

Fig.5.4 web- diaghram system

5.1.3 Stress and Strain Relations

The stress-strain relations (for plane stress) and strain-displacement relations can be written as

$$\{\sigma\}=[D]\,-\{\varepsilon^{T}\} \tag{5.8}$$

Where

$$[D]=\frac{E}{1-\nu^{2}}\begin{bmatrix}1 & \nu & 0\\ \nu & 1 & 0\\ 0 & 0 & (1-\nu)/2\end{bmatrix} \quad \text{and} \quad \{\varepsilon^{T}\}=\text{thermal strain}=\frac{E\alpha\Delta T}{1-\nu}\begin{Bmatrix}1\\1\\0\end{Bmatrix}$$

and the strain-displacement relations are given by (only have the bending part)

$$\{\varepsilon\}=\begin{Bmatrix}\varepsilon_{xx}\\ \varepsilon_{yy}\\ \varepsilon_{xy}\end{Bmatrix}=\begin{Bmatrix}-z\,\partial^{2}w/\partial x^{2}\\ -z\,\partial^{2}w/\partial y^{2}\\ -2z\,\partial^{2}w/\partial x\partial y\end{Bmatrix} \tag{5.10}$$

The assumed displacement function for w(x,y) may be substituted into the strain expressions to obtain,

$$\{\varepsilon\}=[B]\{q\} \tag{5.11}$$

where

$$[B]=\begin{bmatrix}-z\,\partial^{2}N_{1}/\partial x^{2} & -z\,\partial^{2}N_{2}/\partial x^{2} & \ldots & -z\,\partial^{2}N_{12}/\partial x^{2}\\ -z\,\partial^{2}N_{1}/\partial y^{2} & -z\,\partial^{2}N_{2}/\partial y^{2} & \ldots & -z\,\partial^{2}N_{12}/\partial y^{2}\\ -2z\,\partial^{2}N_{1}/\partial x\partial y & -2z\,\partial^{2}N_{1}/\partial x\partial y & \ldots & -2z\,\partial^{2}N_{1}/\partial x\partial y\end{bmatrix} \tag{5.12}$$

It should be noted that $N_i=N_i(x,y)$ and that [B] is a (3x12) matrix whose elements are functions of (x, y and z). For example,

$$\begin{aligned}B_{11}&=-\frac{3}{4a^{2}}z(x/a)(1-y/b)\\ B_{12}&=0\\ B_{21}&=-\frac{3}{4b^{2}}z(y/b)(1-x/a)\end{aligned} \tag{5.13}$$

It should be clear that we need to transform these to non-dimensional coordinates (ξ,η). For example, we obtain:

$$B_{11} = -\frac{3}{4a^2} z\xi(1-\eta)$$
$$B_{12} = 0$$
$$B_{21} = -\frac{3}{4b^2} z\eta(1-\xi) \qquad (5.14)$$

5.1.4 Element Stiffness Matrix

We are now ready to construct the stiffness matrix using the general relation

$$K=\int_v [B]^T[D][B]dV \qquad (5.15)$$

In this case, the differential volume element dV = tdxdy and the integral is over the range x=-a to +a and y=-b to +b. However, since [B] is written in terms of the non-dimensional coordinates, we need to transform the volume integral from (x,y) to (ξ,η) coordinates. Hence, in non-dimensional coordinates, dV=abtdξdη and integration is over the range ξ = -1 to+1 and η = -1to +1. The stiffness matrix then becomes,

$$[k] = abt\int_{-1}^{1}\int_{-1}^{1}[B]^T[D][B]d\xi d\eta \qquad (5.16)$$

Note that the element stiffness matrix, [k], is a (12x12) matrix (recall that [B] is (3x12) and [D] is (3x3)). It should be noted that the purpose of transforming from dimensional (x,y) to non-dimensional (ξ,η), Cartesian coordinates was two-fold: 1) the form of the displacement function w(x,y) and resulting [N] matrix is simpler in form, and 2) the integration is simpler because of non-dimensional limits. In addition, because the limits are -1 to +1, Gaussian quadrature may easily be used to perform the integration numerically.

5.1.5 Element Force Matrix

The element force matrix {F} is obtained for the plate element in the same manner as can be done for elements like the CST. It has to strongly be noted that this formulation procedure is not to lay down manual calculation frameworks but to highlight the general applicability of

the approach before directly going to the software program. One of the major difficulties in handling a structural thin walled curved box girder bridges is the loading situation or orientation over the integral system.

Let the applied load is a distributed pressure acting normal to the surface (in +z direction), for now. Recall the external potential expression,

$$V = -\int_A p_z w dA \tag{5.17}$$

where the integral is over the area, A, which the normal load P_z acts (normally 2a x 2b). Substituting the displacement function, into V gives

$$V = -\int_A p_z w dA = -\int_{-b}^{+b}\int_{-a}^{+a} p_z \{N\}^T \{q\} dx dy \tag{5.18}$$

Transforming to (ξ,η) and noting that the element DOF {q} may be taken outside the integral gives,

$$V = -\left(ab\int_{-1}^{+1}\int_{-1}^{+1} p_z \{N\}^T d\xi d\eta \right)\{q\} = -\{F\}^T \{q\} \tag{5.19}$$

The quantity in the parenthesis can be identified as the generalized nodal force matrix {F}. Hence, we have,

$$\{F\} = ab\int_{-1}^{+1}\int_{-1}^{+1} p_z \{N\} d\xi d\eta \tag{5.20}$$

Note that {F} is a (12x1) column matrix (recall that {N} was also a 12x1 matrix, and contains both forces and moments, i.e., F_1 is a force in the z direction at node 1, F_2 is a moment about the x-axis at node 1, F_3 is a moment about the y-axis at node 1 and so on. If thermal effects are being considered, this will add another term to the element force matrix.

5.1.6. Strain and Stress for each Element

The assembly of element stiffness and force matrices to form global equations of equilibrium is exactly the same as any other element type. The boundary conditions for a structure

consisting of plate elements are similar to beam elements; i.e., we may specify that transverse displacement w_i, rotation about the x-axis θ_{xi} and rotation about the y-axis θ_{yi} are known at global nodes. As with any finite element analysis, care must be exercised that sufficient boundary conditions are given to prevent rigid body motion. Physically, this means that when the load is applied, the plate is prevented from translating the x, y and directions; and from rotating about the x and y-axis as a rigid body. If rigid body motion is not suppressed, the stiffness matrix will be singular and solution is not possible. Rigid body modes are permissible only when a dynamic analysis is conducted (mass matrices are included).

Once the global equations of equilibrium have been solved for the global nodal displacements and rotations, the strain and stress for each element may be obtained. We simply use for each element $\{\varepsilon\}=[B]\{q\}$ and $\{\sigma\}=[D]\text{-}\{\varepsilon\}^T$ where $\{q\}$ are displacements (and rotations) for the element in question and are obtained for the global displacement vector.

5.2 Seventh DOF Approach

5.2.1 A 21 degree of freedom triangle

This is a more realistic approach for those thin walled, and integrated structural unites, where the general geometry is continuously changing. The global coordinate system is directly used without coordinate transformation, (Bletzinger(prof.Doc-Ing), 2002)

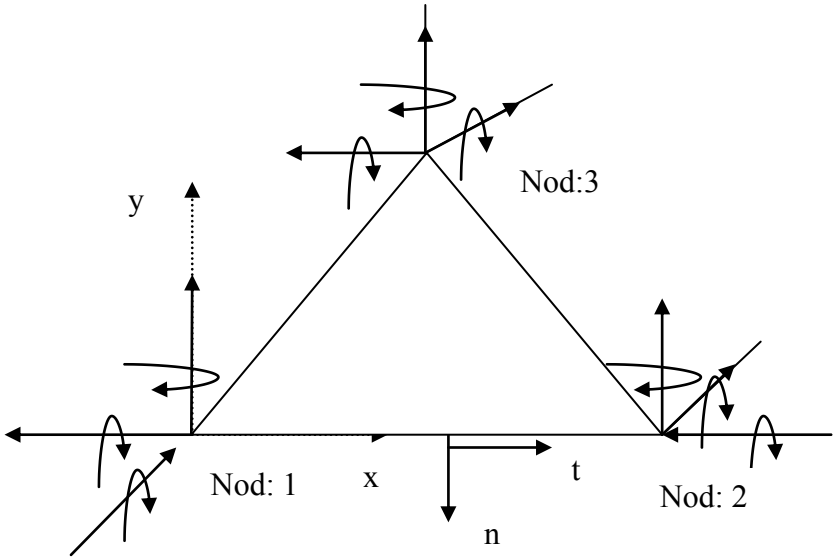

Fig.5.5 C_1-Continuity at edge 1-2

The displacements, both the first derivatives, in (x,y) direction, and the second mixed derivatives, indicating the twist of the displacements. With respect to an arbitrarily oriented edge, now, the first and second derivatives have to be prescribed normal and tangential to the edge. The first and second mixed derivatives at edge 1-2 are evaluated by the chain rule differentiation:

$$\frac{d\omega}{dn} = \frac{d\omega}{dx}\frac{dx}{dn} + \frac{dw}{dy}\frac{dy}{dn}$$

$$\frac{d\omega}{dt} = \frac{d\omega}{dx}\frac{dx}{dt} + \frac{d\omega}{dy}\frac{dy}{dt}$$

$$\frac{\partial^2 w}{\partial n \partial x} = \frac{\partial^2 \omega}{\partial x^2}\left(\frac{dx}{dn}\frac{dx}{dt}\right) + \frac{\partial^2 \omega}{\partial x \partial y}\left(\frac{dx}{dn}\frac{dy}{dt} + \frac{dx}{dt}\frac{dy}{dn}\right) + \frac{\partial^2 \omega}{dx^2}\left(\frac{dy}{dn}\frac{dy}{dt}\right)$$

It follows that all second derivatives with respect to the global coordinate (x,y) have to be supplied at the nodes. At any node, the displacement field is $\{w\ w_x\ w_y\ w_{xx}\ w_{yy}\ w_{zz}\ w_{xy}\}$. These corresponds to [u v w θ_x θ_y θ_z θ_x']. Together at all corners of the triangle, the total DOFs are 3x6=18 plus 3x1=3 (distortional displacements) at each corner.

1

x y

x^2 xy y^2

x^3 x^2y xy^2 y^3

x^4 x^3y x^2y^2 xy^3 y^4

x^5 x^4y x^3y^2 xy^4 xy^4 y^5

Fig5.7 Pascal's triangle

5.2.2 Degrees of Freedom and Displacement Function

The displacement field is given by

$$\{q\}^T = \{u_1\ v_1\ w_1\ \theta_{x1}\ \theta_{y1}\ \theta_{z1}\ \theta_{x1}' \ldots\ \theta_{x3}'\} \qquad (5.21)$$

To maintain geometric isotropy and continuity a 21 term polynomial has to be selected. Let w(x,y) be some assumed function over the plate geometry. A general fifth order polynomial expression for w(x,y) can be written as 21 terms. The distortional displacement is usually taken as the derivative of θ_x

$$W(x,y)=a_1+a_2x+a_3y+a_4x^2+a_5xy+a_6y^2+a_7x^3+a_8x^2y+a_9xy^2+a_{10}y^3+a_{11}x^4+a_{12}x^3y+a_{13}x^2y^2+$$

$$a_{14}xy_3+a_{15}y^4+a_{16}x^5+a_{17}x^4y+a_{18}x^3y^2+a_{19}x^2y^3+a_{20}xy^4+a_{21}y^5 \qquad (5.22)$$

It is impossible to devise a simple polynomial function with only three nodal degrees of freedom that will be able to satisfy slop continuity requirement at all locations along element boundaries. The alternative is to impose curvature parameters at nodes although has disadvantages such as:

- Difficulties to impose boundary conditions for higher order derivatives
- Nodes with different numbers and type of parameters
- Imposing excessive conditions of continuity. The latter involves inconsistency when discontinuous variation of material properties occurs. Then moments are continuous and curvatures are discontinuous.

One may still feel a justifiable preference for the more intuitive formulation involving displacements and slops only, despite the fact that very good accuracy is demonstrated for higher order quartic and quintic elements. It is generally adjusted in an attempt to satisfy stress continuity conditions along the edges and improve the convergence characteristics of the element for stresses.

The remaining displacement functions can kinematic ally be derived from the following expressions.

$$U=-z\,\theta_x(x,y), \quad v=-z\,\theta_y(x,y), \qquad w=w_o(x,y) \qquad (5.23)$$

$$\theta_x = \frac{\partial u}{\partial z} \quad , \quad \theta_y = \frac{\partial v}{\partial z}$$ **(**not "physical" rotation**)**

In defining the geometry, as well as the displacement functions, it is expedient to define normalized coordinates ξ and η.

In order to obtain the shape functions in the x,y coordinate system, we follow the standard procedure and write one equation for each of the 21 degrees of freedom, but is usually difficult to handle due to the above constrictive factores.

Those 21 equations may be solved for the 21 unknown coefficients $a_1.a_2,\ldots a_{21}$ (which will be in terms of the 21 nodal degrees of freedom q_i). The solution is substituted into w(x,y), for the coefficients and rearranged into the form of,

$$w(x,y)=\{N(x,y)\}^T\{q\} \quad (5.24)$$

Gives the following for some of the shape functions,

$$N_i(x,y)=\text{some } f(x,y) \quad (5.25)$$

or, in terms of non-dimensional coordinates (ε, η) using the appropriate transformation,

$$N_i(\varepsilon, \eta)=\text{some } f(\varepsilon,\eta) \quad (5.26)$$

i is for nodal number =[1,21] and so forth through N_{21} (ε, η). Note that {N} is a (21x1) column matrix (since we have 21 degrees of freedom).

5.2.3. Stress and Strain Relations

The stress strain relations are similar to the expressions in section one, with some size adjustments.

The assumed displacement function for w(x,y) may be substituted into the strain expressions to obtain,

$$\{\varepsilon\}=[B]\{q\} \quad (5.27)$$

The size of the B matrix will be equal to N_i , and is (3x21), whose elements are functions of (x,y,z) and the corresponding (ε,η,z)

5.2.4. Element Stiffness Matrix

We are now ready to construct the stiffness matrix using the general relation

$$K=\int_v [B]^T[D][B]dV \quad (5.28)$$

In this case, the differential volume element dV=tdxdy and the integral range has to be defined. However, since [B] is written in terms of the non-dimensional coordinates, we need

to transform the volume integral from (x,y) to (ξ,η) coordinates. Hence, in non-dimensional coordinates, dV=abtdξdη and integration range will correspondingly be changed. Note that the element stiffness matrix, [k], is a (21x21) matrix (recall that [B] is (3x21) and [D] is (3x6)).

5.2.5 Element Force Matrix

The element force matrix {F} is obtained for the plate element in the same manner as can be done for elements like a CST element. For the integral system consists of a curved girder geometry with a configured bracing and stiffening members in accordance with the deformation characteristics, it, in the theoretical basis, is usually difficult to justify the general loading orientation for the separate mesh elements, under study. It is because, in the first instance the loading direction has to separately be studied with all possible combinations, and second the loaded part is usually the top flange systems. For the purpose of elaboration, let the applied load be taken as a distributed pressure acting normal to the surface (in +z direction). Recall the external potential expression,

$$V = -\int_A p_z w dA \tag{5.29}$$

where the integral is over the area, A,

5.3. Torsion related degree of freedoms only

Stiffness relations for the element can also be derived using the direct method or the virtual work principle. In the direct method, each DOF is released while other DOFs are restrained; one at a time. A unit deformation is then imposed on the released DOF resulting in reactions at the restrained DOFs. The reactions constitute the stiffness terms of the column elements corresponding to the released DOF. This straight forward method is suitable for simple elements where the reactions due to the imposed unit deformation can be easily quantified.

The virtual work principle is based on the concept of energy conservation. It is a well known approach, but its essential features will be outlined here for completeness. A virtual displacement, $\delta\Delta$, is imposed on the structure – in this case the plate. The external work done to impose this virtual displacement has to be equal to the internal strain energy,

$$\delta W = \delta W_{ext} - \delta W_{int} = 0 \qquad (5.30)$$

The virtual displacement field imposed on the element follows an assumed displacement field characterized by shape functions, [N]. The relationship between the displacement, Δ, at any point and nodal displacements for a general element with n DOFs is given by

$$\Delta = N_1\Delta_1 + N_2\Delta_2 + \ldots + N_n\Delta_n = \Delta \Sigma N\, i\, \Delta i = [N\,][\,\Delta] \qquad (5.31)$$

where N_i is the shape function corresponding to the i^{th} DOF. The strain energy is calculated with the help of the strain displacement matrix, [B], which contains derivatives of the shape functions and relates generalized strains to nodal displacements. For example, the generalized axial strain is obtained using the first derivative of [N axial], where [N axial] contains the shape functions pertaining to the axial degrees of freedom.

$$\varepsilon_{axial} = [N'_{axial}]\{\Delta\} \qquad (5.32)$$

It establishes the fact that the strain-displacement matrix for axial deformation DOFs is,

$$[B_{axial]} = [N_{axial}] \qquad (5.33)$$

A relationship involving the second derivative of [N] yields [B] matrix for flexural terms. In general, the strain energy due to the imposed virtual displacement field is given as;

$$\delta W_{int} = \int [\delta\varepsilon][D]\,[\varepsilon]d(vol) \qquad (5.34)$$

where [D] is the constitutive matrix, which differs based on the DOF under considerations. For example, [D] for axial deformations is simply the modulus of elasticity. The external work done to impose the virtual displacement field, $\{\delta\Delta\}$and when simplified to the general stiffness relations, provides the following expression;

$$[k\,] = \int_{vol} [B^T\,]\,[D\,][B\,]d(vol\,) \qquad (3.35)$$

The accuracy of the derived stiffness matrix depends on the quality of the assumed shape functions representing various displacement fields.

Warping is accounted for through an added seventh DOF. The additional DOF is the first derivative of the twisting angle, θ_x'. At each node, the DOFs for this element become

$$\{ u\ v\ w\ \theta_x\ \theta_y\ \theta_z\ \theta'_x \}^T, \tag{3.36}$$

in the local coordinate system (CS) of the element. Other implementations of warping are possible; however, the formulation presented next captures the essential aspects of the behavior (Sherif El-Tawil, October 2002). It has been discussed in the previous chapters that St. Venant torsion, T_s , which is often referred to as uniform torsion, is a function of the torsion constant, J , the Shear Modulus, G , and the twisting angle, θ_x. Similarly, the biomoment, m_ω, which accompanies torsion and causes out of plane deformations is a function of warping constant, I_ω, modulus of elasticity, E, and the second derivative of the twisting angle,

$$m\omega = EI_\omega\theta'' \tag{3.37}$$

Thus, the total applied torsion can be expressed as,

$$T = GJ\theta' - EI_\omega\theta'' \tag{3.38}$$

Suppose a triangular mesh element is assumed. Considering one of the edges of the triangle, the four DOFs related to torsion are,

$$[\theta_{1x}\ \ \theta_{2x}\ \ \theta'_{1x}\ \theta'_{2x}]^T \tag{3.39}$$

Assuming an appropriate displacement field, the element stiffness matrix can now be derived from,

$$[K] = \int_0^l [N']G\{N'\}Jdx + \int_0^l [N'']G\{N''\}Edx \tag{3.40}$$

If for instance a four term polynomial is assumed as,

$$\theta_x = a_1 + a_2x + a_3x^2 + a_4x^3 \text{ then}$$

$$\theta'_x = a_2 + 2a_3x + 3a_4x^2 \tag{3.41}$$

The coefficients, a_i, can then be found using the appropriate boundary conditions. Hence, all torsion related DOFs can be solved.

Upon substitutions and simplifications, the element stiffness matrix is,

$$[K]=\begin{bmatrix} (\frac{6}{5}+12a) & (-\frac{6}{5}+12a) & (\frac{1}{10}+6a)L & (\frac{1}{10}+6a)L \\ & \frac{6}{5}+12a & -(\frac{1}{10}+6a)L & -(\frac{1}{10}+6a)L \\ & & (\frac{2}{15}+4a)L^2 & (-\frac{1}{30}+2a) \\ & & & (\frac{2}{15}+4a)L^2 \end{bmatrix}$$

$$\text{Where} \qquad a=\frac{EI_{\omega}}{GJL^2}$$

The size of each individual sub matrix is therefore [7X7]. The overall size of the line element matrix would then be [14X14].

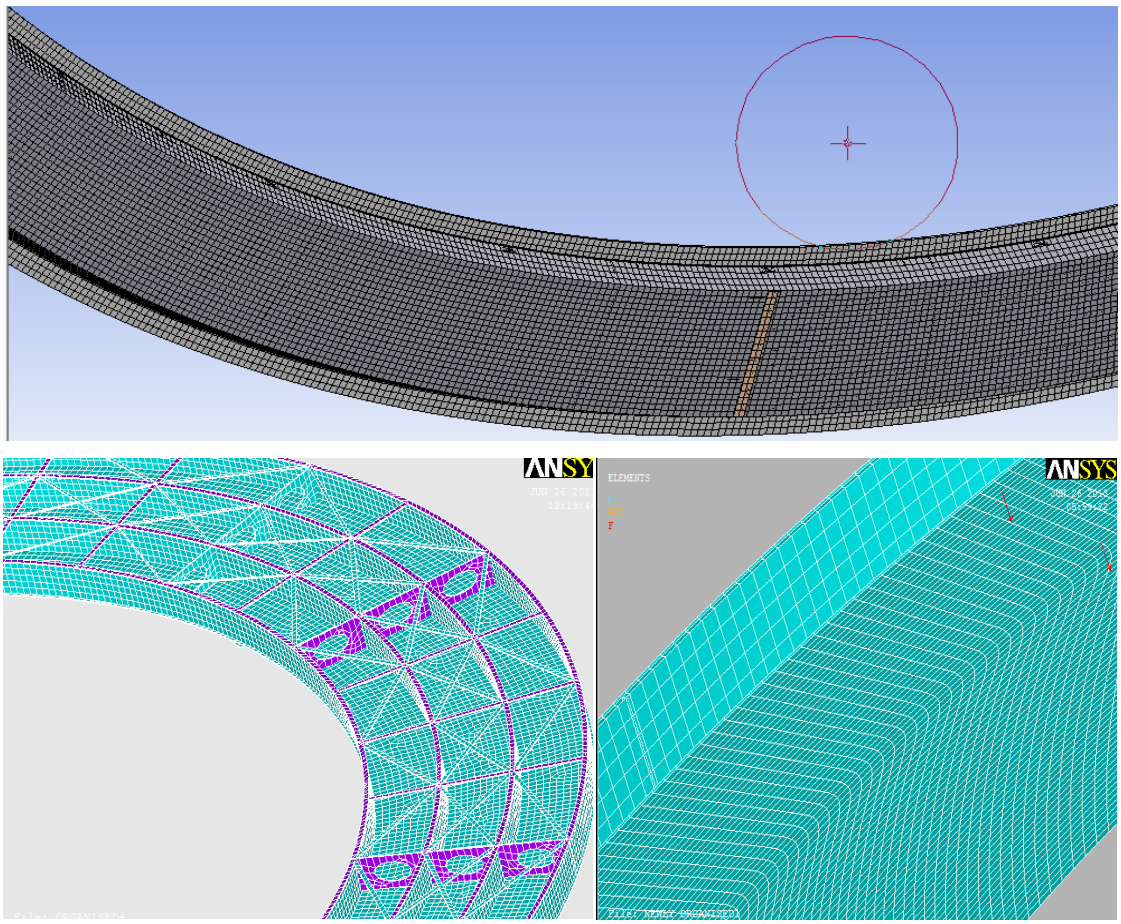

Fig.5.6 Rectangular mesh elements of the superstructure

Chapter six

6.0 Stiffening Mechanisms

Current design guides provide little or no guidance for the design of top-lateral bracing systems. This lack of guidance has led many engineers to develop either overly conservative or, in some instances, inadequate bracing designs. According to many literatures most failures testify the need for a comprehensive and rational design methodology.

The forces in top-lateral bracing systems due to torsion are related to the torsional shear flow within the psuedo-closed cross section. The shear flow in a single panel element of a closed section is given by (B. S. Chen, 2005)

$$q=T/2A_0 \qquad (6.1)$$

Where A_0 is the area enclosed by the centerline of the walls
The total shear force in the brace panel is

$$V=Tb/2A_0 \qquad (6.2)$$

where b is the brace panel width defined. For truss bracing, the transverse shear can be resolved into a diagonal brace force

$$p_d=Td/2A_0 \qquad (6.3)$$

The diagonal force, P_d, is independent of the brace member size and depends only the vertical placement (A_o) and geometry (d) of the bracing. For X-type systems, the brace forces are one-half the magnitude of those with single-diagonals and are equal and opposite in magnitude.

6.1 Bracing Requirement for TOP-Flange Lateral Buckling

For a lateral brace to be effective it must have both sufficient strength and stiffness. Top lateral truss and metal-deck bracing for box-girders can be classified as relative bracing systems because they prevent the relative lateral movement of adjacent brace points along the length of a compression member.

6.2 Brace Strength Requirements

Brace forces in top-lateral bracing systems of steel box-girders originate from four primary sources:

1.) Girder torsional moments

2.) Girder bending moments

3.) Vertical flange loads on inclined webs

4.) Lateral-buckling forces of the top flanges

6.2.1 Girder Torsional Moments

Torsional moments on the girder create shear flow in the quasi-closed cross section, which generate forces in top-lateral bracing systems. Researchers proved that results obtained from the laboratory test program have demonstrated that application of the equivalent plate approximation produces reasonably accurate brace force predictions. The magnitude of the brace forces can be determined by calculating the shear force on the brace panel. For truss systems, individual member forces can be determined by resolving the panel shear force and applying basic truss analysis techniques. These truss forces are independent of the member sizes and depend only on the truss-configuration and brace panel geometry.

6.2.2 Girder Bending Moments

The brace forces introduced by box-girder bending are the direct result of compatibility between the bracing and the top flanges. Top-lateral bracing attached to or near the top flanges attracts compressive forces under positive bending moments. These forces increase with both increasing member size and brace panel length (angle between diagonals and top flange decreases).

These forces can be quite significant and are often times equal to or greater than the forces generated by torsion. (Chai H. Yoo, 2005) have revised all the formerly made researches, on top horizontal both lateral and diagonal braces and inclined interior brace characteristics on a two single box girder bridges. They have noted that these bending induced brace forces can be calculated using expressions developed by Fan and Helwig (1999).

Metal-deck bracing systems, on the other hand, if proposed, have advantage for it doesn't develop the bending induced forces that occur in truss systems. This is because the in-plane stiffness of the deck panel transverse to the corrugation ribs is extremely small. Therefore,

strength design of metal- deck top-lateral bracing systems need not consider forces induced by vertical bending of the box-girder.

6.2.3 Horizontal Force Components from Vertical Flange Loads

The vertical construction loads acting on the top flanges create lateral force components due to the inclined webs as shown in Figure 7.6. Bracing is necessary to resist these forces and control distortional and lateral flange stresses. Both top laterals and internal diaphragms can carry these force components. If the designer has chosen to have the top-lateral bracing system carry these force components, then their contribution should be included in the strength design.

For truss systems, the member forces will vary depending on truss arrangement. Fan and Helwig (1999) conducted analytical studies on both single diagonal and X-type truss systems and found that the brace forces due to the horizontal components tended to be small compared to those generated by bending and torsion. Therefore, it was recommended that the struts be designed to carry the entire lateral force component with the diagonal forces remaining unchanged.

6.2.4 Lateral Stability Requirements for Top Flanges

Lateral instability of the top flanges in compression regions can be handled using top-lateral systems and/or internal diaphragms. Both systems are effective at preventing the lateral movement of the top flanges. Like the horizontal force components, if the designer has elected to use the top-lateral bracing to provide the lateral stability for the top flanges then the force requirements should be accounted for in the strength design. Brace forces can either be tensile or compressive, depending on the direction the flange goes to buckle. Unlike the brace forces generated by bending and torsion, which can be additive or subtractive with one another, the brace forces from lateral stability will always increase the magnitude of the design brace force.

6.2.5 Brace Forces Superposition

The comprehensive strength design for top-lateral bracing systems must account for the four potential force components previously described. Care should be taken to maintain proper sign conventions when using superposition of the individual components to obtain the design brace forces. For example, for warren single-diagonal brace geometry, torsional moments on

the girder cause adjacent diagonals to alternate between tension and compression. Vertical bending of the girder, however, causes compression in all the diagonals in positive moment regions. Brace forces from lateral stability requirements will always increase the magnitude of the resultant brace force from torsion and bending effects. The design forces for straight girders differ from curved girders only in the fact that the torsional force components are not present.

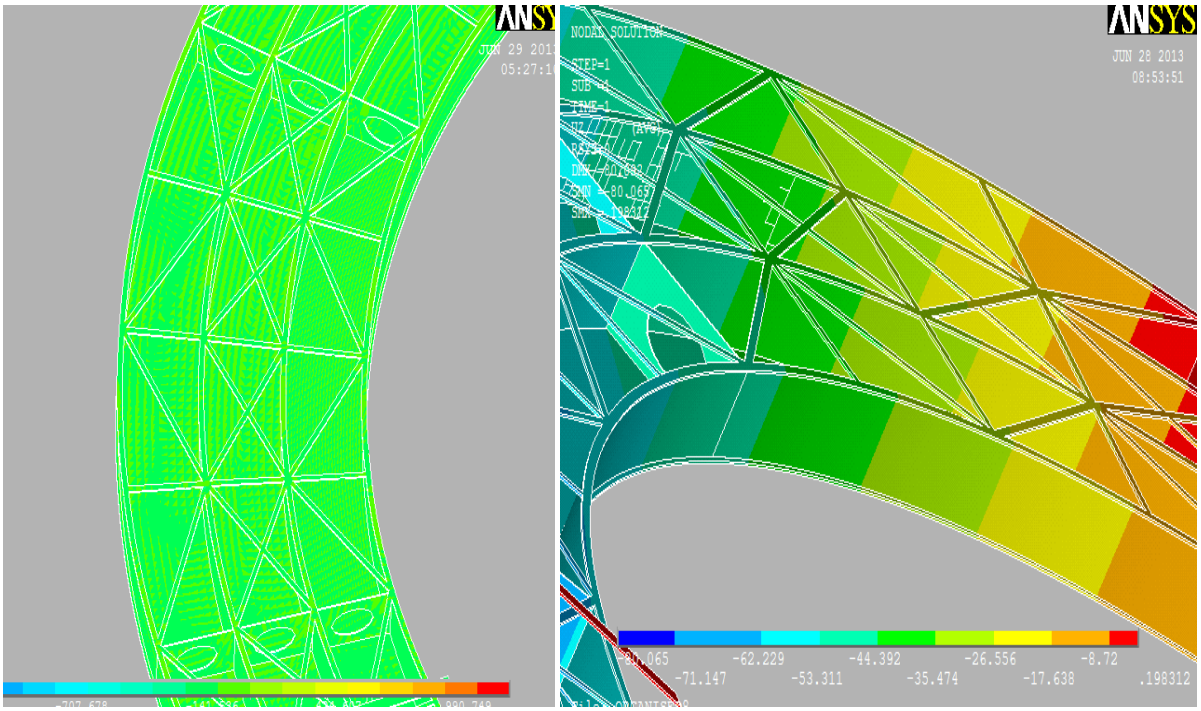

Fig.6.1 Brace and diagrams configurations

6.3 Brace Stiffeners Requirements

The following governing scenario has to be satisfied for the brace stiffness requirements of top-lateral bracing systems.

1.) Controlling girder rotations

2.) Controlling warping stresses

3.) Preventing lateral buckling of the top flanges

Adequate bracing design must satisfy the criterion with the greatest lateral-brace stiffness requirement.

6.3.1 Controlling Girder Rotations

In curved steel box-girder bridge systems, the large torsional moments observed during casting of the bridge deck can cause bridge girders to undergo significant rotations. In multi-girder bridges, this results in differential rotations between adjacent girders.

These misalignments in the super elevation pose both construction difficulties and roadway ride ability problems. Controlling these rotations can be accomplished by either providing external diaphragms to maintain alignment between adjacent girders or increasing the torsional stiffness of the girders themselves.

To design the top-lateral system, there must be a criterion for the allowable differential rotations between girders. Unfortunately, no uniform criterion exists. One suggestion has been applied to limit the vertical displacement at the outer tips of the top flanges to a specific number based on the engineering judgment and experience of senior bridge designers. Since the girder section is a closed box with a continuous bottom flange, the extent of the differential rotation of the girder sections is insignificant. The buckling and deformation limit of the bottom flange needs; however, a care full investigation. The interior diaghrams also contributes for the global rotational rigidity of the girder.

For quasi-closed box-girders, the thickness of the equivalent plate representing the top-lateral bracing is the dominant factor in controlling the torsional stiffness. In design, the bridge span, curvature, and cross sectional dimensions will generally be established before the bracing system is designed. Thus, the primary property affecting the torsional stiffness is the pure torsion constant, K_T, which almost is directly proportional to the equivalent plate thickness representing the top-lateral bracing. Determination of the required equivalent plate thickness can be obtained by substituting the plate dimensions of a quasi-closed trapezoidal box girder Eq.6.4a and Eq.6.4b.

6.3.2 Controlling Warping Stresses

Top-lateral brace systems increase not only the torsional stiffness of the girder, but can also be used to control warping stresses. Since the determination of all the stresses in a curved box-girder bridge under torsion and bending is difficult, it is advantageous to determine when it is necessary to calculate both the pure and warping tortional stresses. Heins (1978) has conducted stress ratio parameter determinations on various curved box girder geometries (Chai H. Yoo, 2005). Results indicated that for box-sections with width-to-depth ratios

between 1 and 3, the ratio of the normal bending and warping normal stresses was less than 10% if the top-lateral equivalent plate thickness was greater than 1.27mm. Therefore, if this stiffness criterion is satisfied, secondary warping stresses calculation will be less important.

6.4 Lateral Stability Requirements for Top Flanges

Top lateral and diagonal bracing systems are provided to stabilize the top flanges in this research. Interior diagrams with elliptic holes designed to allow an interior passage are also provided to meet the required structural integrity.

6.4.1 Conceptualization on Design Brace Stiffness

Adequate design of top-lateral systems for stiffness should satisfy all of those criteria that the designer deems applicable. For example, a designer may elect to use external diaphragms to control differential rotations and use internal diaphragms to stabilize the top flanges. In this case, the stiffness requirement may only be based on satisfying the warping stress criterion. In cases where multiple criteria are applicable, the bracing design should satisfy the one with the greatest stiffness requirement.

For a quasi-closed box girder, the torsion analysis can be performed using the equivalent plate method (EPM) in which the truss system is transformed into a fictitious plate with a uniform thickness. Equivalent thickness of several types of bracing systems has been developed prior to the works of (Chai H. Yoo, 2005) to evaluate strain energy stored in the system. One type of a abracing configuration can be as shown in figure 6.4. Accordingly opposite sides of the top interior flange are supposed to experience structural strains independently. A X-type interior and a warren type exterior and both X-type brace configurations at both panels are considered separately in this research.

It could be totally difficult, to apply and formalize an equivalent thickness method if the members on opposite sides of the flange are considered to join at a point i.e a five member joint.

Had it been applied so, a more rational and acceptable out put would have been obtained on all the earliest analytical approaches. The reason is that the bracing lay out is structurally indeterminate. Remember, one of the aims of this research is to interactively investigate the general mechanics and features of typically the entire stiffening mechanisms. An equivalent

plate thickness for the warren type and X-type configurations have theoretically been given respectively as follows, (Chai H. Yoo, 2005),

$$t_{eqedxt} = \frac{E}{G}\frac{sb}{\frac{2d^3}{A_d} + \frac{b^3}{3A_s} + \frac{s^3}{12}\left(\frac{1}{A_u} + \frac{1}{A1}\right)} \qquad (6.4a)$$

$$t_{eqedxt} = \frac{E}{G}\frac{sb}{\frac{d^3}{A_d} + \frac{s^3}{3}\left(\frac{1}{A_u} + \frac{1}{A_l}\right)} \qquad (6.4b)$$

Where d= diagonal length = sqrt(s^2+b^2), b=spacing between struts and s=spacing between flange-strut bond centerlines.

A_d =Area of diagonal, A_s =Area of struts

A_u and A_l =Area of girder top flanges (both sides)

This equation represents, both the interior and exterior panels brace configurations and corresponding equations for equivalent thickness, figure6.4. The quasi-closed box theory or EPM allows the torsional properties of the box girder to be approximated. The value of the equivalent plate thickness is dependent on the bracing configuration and cross-sectional areas of bracing members.

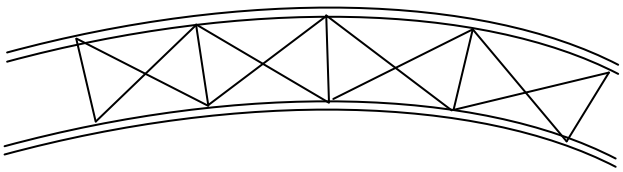

X- type (SD) horizontal top truss (Interior panel)

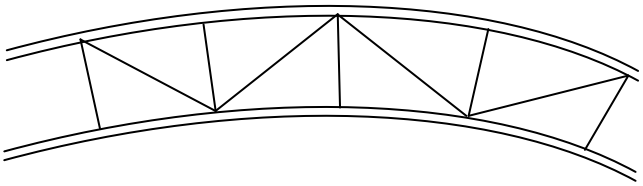

Warren type (SD) horizontal top truss (Exterior panels)

Fig.6.2 (a, b) horizontal brace lay out

The resulting shear flow in individual panels of the closed section, q, has been formulated in section 3.4. Here is repeated for convenience,

$$q_1=2\theta^{-1}A_1$$

$$q_2=2\theta^{-1}A_2$$

$$q_3=2\theta^{-1}A_3$$

where θ is angle of twist of the whole section(assumed to rotate rigidly) and A_i is individual panel areas.

The shear flow acting on the fictitious plate is then transformed to axial forces of diagonal members in the lateral bracing system as, (Chai H. Yoo, 2005).

$$D_{tor,sd} = \pm\frac{qb}{\sin\alpha} = \pm\frac{b}{2A_o\sin\alpha} \qquad (6.5a)$$

$$D_{tor,xd} = \pm\frac{qb}{2\sin\alpha} = \pm\frac{b}{4A_o\sin\alpha} \qquad (6.5b)$$

Where $D_{tor,SD}$, $D_{tor,XD}$ = forces in SD type and XD type diagonals due to applied torque, respectively; b = top flange width between webs; α = angle between the diagonal and the top flange.

It should be noted, however, that both torsion and vertical bending induce forces in the lateral bracing members. Diagonals in the lateral bracing systems are subjected to the same total longitudinal deformation as the top flanges. In addition, the lateral force component resulting from the sloping webs can also affects member forces in the lateral bracing system as discussed in the preceding sections. The magnitude of lateral force component is evaluated from the equivalent moment induced by the applied load on the top flange as shown in Fig. 6.5. Fan and Helwig (1999) developed equations to predict brace forces in SD types and XD types and proposed the following expressions for design purposes:

$$S_{tot}=S_{bend}+S_{lat} \qquad (6.6a)$$

$$D_{tot}=D_{EPM}+D_{bend}+D_{lat} \qquad (6.6b)$$

Where S_{tot} and $D_{tot,}$ total force in the strut and diagonal, respectively; S_{bend} and D_{bend}, force in the strut and diagonal due to bending of box girder, respectively; S_{lat} and D_{lat}, force in the strut and diagonal due to lateral force components, respectively; diagonal force from the torsional moment determined using the EPM suggested by equations (6.4a) and (6.4b).

For simplicity, Fan and Helwig (1999) recommended designing the strut to carry the entire lateral load component, i.e. S_{lat} = s times w_{lat} and D_{lat} = 0 where S = spacing between struts; w_{lat} = lateral load component. This is essentially tantamount to state that the entire lateral force components are carried by the struts only. Chen has set up to 30% discrepancies between the values predicted in equations (6.5a) and (6.5b), in some box girder bridges. This is the impetus of undertaking the effort to derive improved predictor equations that yield a better correlation. Please also note that these formulations are equivalent to the trapezoidal separate unite box girder unites.

Consider a box girder with double span of total length of 89.44 m and 18 panels. Cross-frames are installed under every 10^o.

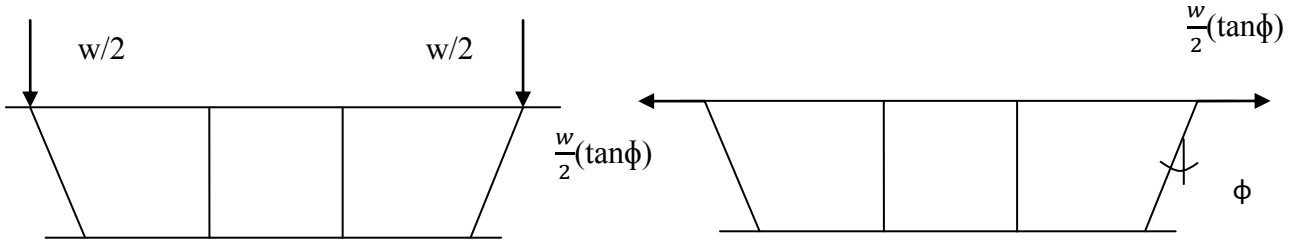

Fig.6.3 horizontal force component of top flanges due to vertical load

6.4.2 Bracing Member Forces due to Torsional Loads

Forces in lateral bracing members are affected by longitudinal deformations of top flanges and differential lateral displacements between top flanges. Lateral displacements of top flanges are a major cause of the development of top truss member forces in box girders subjected to torsional loads as longitudinal deformations of the box flanges are comparatively small. Lateral force components shown in Fig. 6.6, DH, which are identified from a vector sum of two adjacent diagonal forces at diagonal-strut junctions, are expressed as:

$$D=(D^{-}+D^{+})\sin\alpha \qquad (6.7)$$

where D^{-}, D^{+} = torsion induced axial forces in two consecutive diagonals. It should be noted that D^{-} and D^{+} are functions of the torsional moment along the box girder and in opposite signs in two adjacent bays in the case of a SD type top truss. It can be seen that the maximum differential lateral displacements occur at both ends of the box girder. This phenomenon is attributable to the fact that there is no adjacent diagonal as shown in Fig. 6.7. For simplicity, consider top flanges and struts as a separate two-dimensional structure in the horizontal plane

as illustrated in Fig. 6.7(a). Parallel top flanges may be considered as beams connected to each other with struts along the span and solid diaphragms at ends. The net lateral load induced from top diagonals acting on this simplified structure may be divided into two sets of force components as shown in Fig. 6.7(b) and Fig. 6.7(c). The forces shown in Fig. 6.7(b) are carried entirely by two top flanges. Forces shown in Fig. 6.7(c) are carried in parts by two top flanges and struts. Net forces applied in the adjacent repeating panels and corresponding deformation configurations are illustrated in Fig 6.7(d).

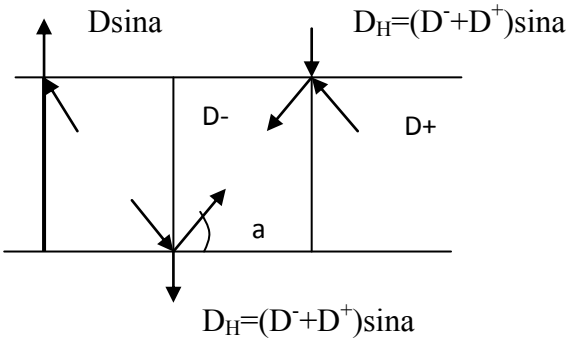

Fig.6.4 Lateral force resultants balanced from diagonal forces

Although DH is a function of torsional moment that varies along the girder length, strut forces are approximated from lateral forces that are assumed to be the same in magnitude within two adjacent panels, a reasonable approximation as any difference will be small.

$$S_{tor} = \frac{(2s)^3 / 192I_f}{b/2As + (2s)^3/192I_f} D_H \qquad (6.8)$$

where S_{tor} = strut force due to pure torsional component; I_f, second moment of inertia of one top flange with respect to the vertical centroidal axis; A_S, cross-sectional area of a strut; and s, spacing between struts.

A

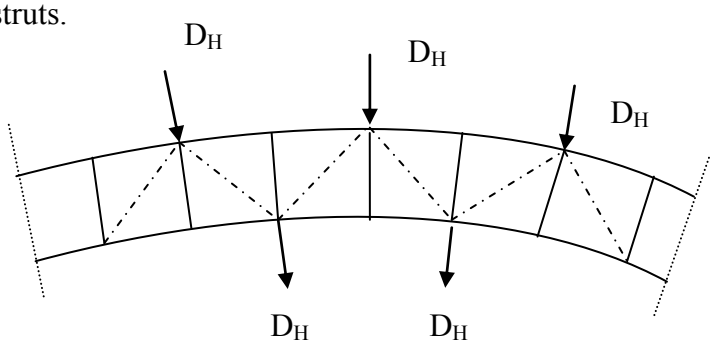

Fig.6.5 Lateral forces from diagonals over the SD type brace layout

These force diagrams can equivalently be decomposed as follows,

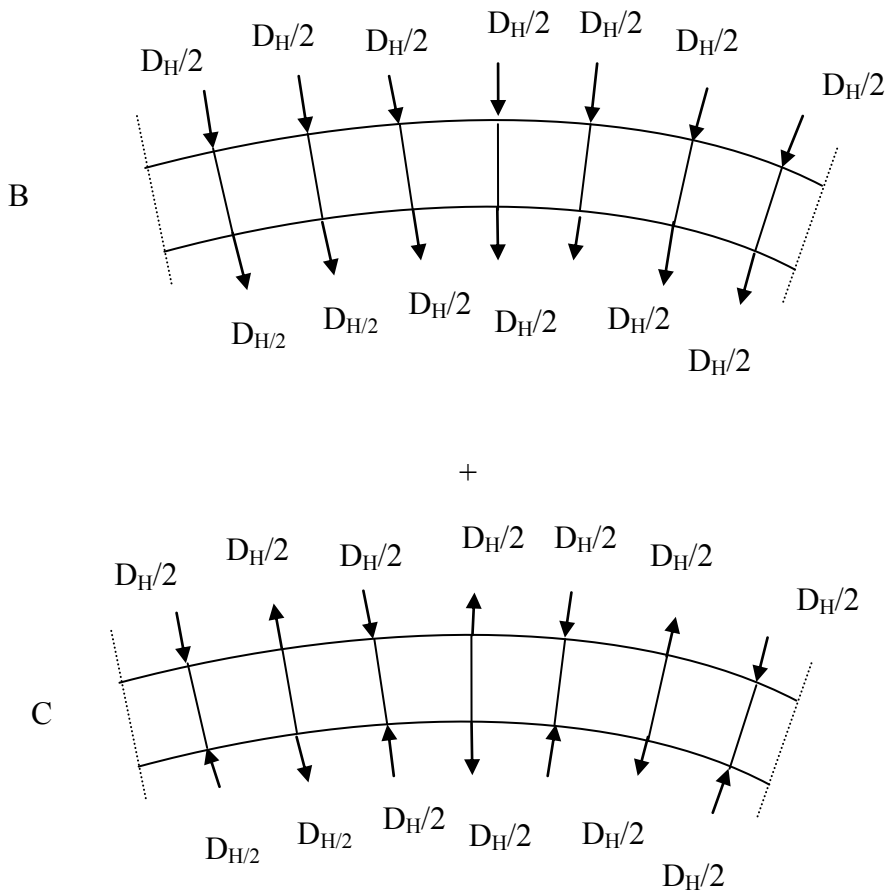

Fig.6.6(a) Lateral forces from diagonals; (b) Lateral force affecting lateral bending; (c) Lateral force affecting struts

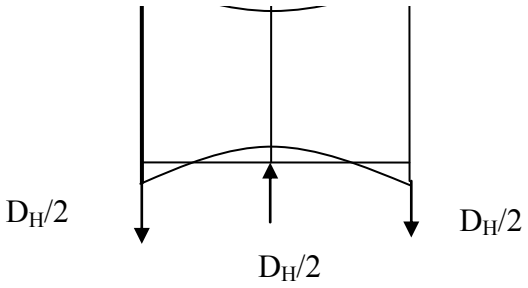

Fig.6.6 (d) Deformation of two repeating adjacent panels

Axial forces are also developed in struts due to distortional components. Diagonal members of cross-frames resist distortional deformations of the box cross section and consequently the resulting member forces are transferred to the top horizontal truss. The magnitude of horizontal force components, K_H, is determined using the force component associated with distortion referenced by (Chai H. Yoo, 2005). Horizontal force component, K_H, acting on the

top truss can be evaluated approximately by multiplying the horizontal force from distortional components.

$$KH = 2Sq_{H,dis} = \frac{S}{a+b}\left(\frac{M}{R} - \frac{a}{b}ew\right) \qquad (6.9)$$

Duplicating the procedure used in the development of forces in struts due to pure torsional components in Fig. 6.7, net forces applied in the adjacent repeating panels and corresponding deformation configurations are illustrated in fig6.8. It illustrates the summary of strut force resolution and the integral interface.

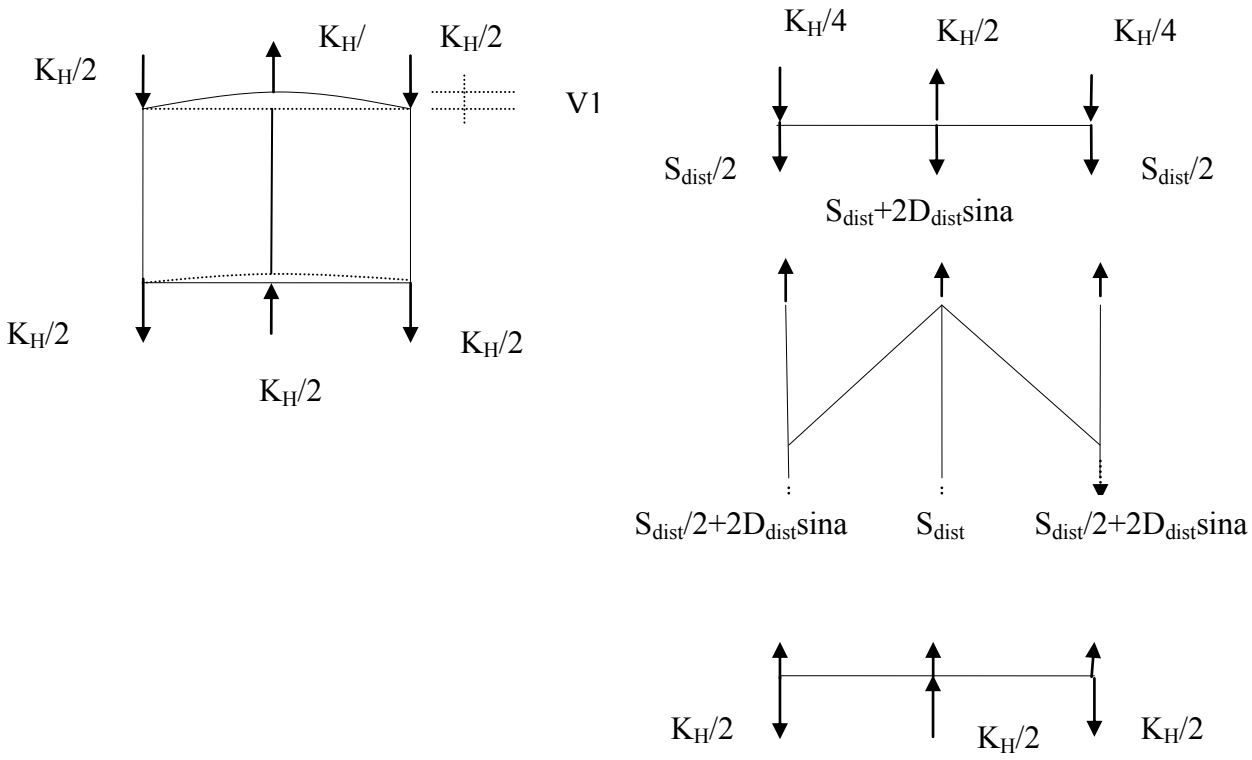

Fig.6.7 Deformation of two repeating adjacent panels and Interface forces

Although K_H is a function of bending and torsional moment that varies along the girder length, bracing member forces can also be approximated from lateral forces that are assumed to be the same in magnitude within two adjacent panels. Since the lateral stiffness of the web is negligible, individual top flange should be in lateral equilibrium (Fig. 6.8 (b)), which yields:

$$S_{dist}=D_{dist}\ Sina \qquad (6.10)$$

where S_{dist}, D_{dist} = forces in struts and diagonals due to distortion, respectively. Forces in lateral diagonal members can be determined by their elongations and force-deformation relationships represented by Hooke's law. The elongation of the lateral diagonal, δD, shown in Fig. 6.9 is given by,

$$\sigma D=(v_1+v_2)\sin a \qquad (6.11)$$

where v_1= relative displacement of the strut as shown in Fig. 6.8 in the lateral v_1 direction; v2, axial elongation of the strut.

Interactive forces between the interface of the top flange and bracing assemblies are shown in Fig. 6.8. The relative lateral deflection between two adjacent panel points, v_1, is computed to be v_2, axial elongation of the strut. Each top flange is assumed to bend like a continuous beam between two adjacent strut locations, as shown in Fig. 6.8.

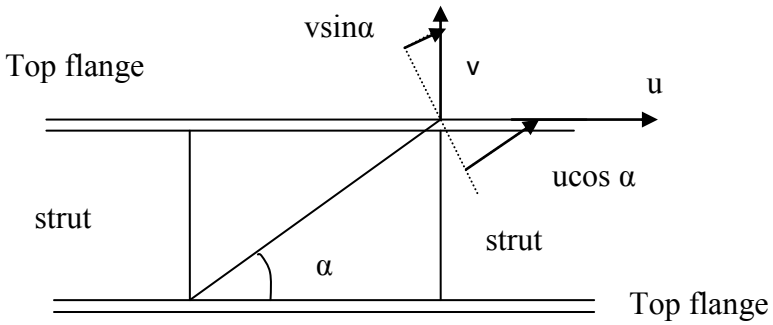

Fig.6.8.Elongation components of a diagonal member

$$V_1 = \frac{(2s)^3}{192EI_f}\left(\frac{K_H}{2} + S_{dist}\right) \qquad (6.12)$$

Similarly, elongations of the strut, v_2, and the diagonal, δD, can be given by

$$V_2 = \frac{bSd_{ist}}{EA_s} \quad \text{and} \quad \sigma_D = \frac{L_D D_{dist}}{EA_D} \qquad (6.13)$$

where A_S, A_D = cross-sectional areas of strut and diagonal, respectively; L_D, length of diagonal. Substituting and simultaneously solving the above equations, D_{dist}, yields

$$D_{dist} = \frac{A_D A_s S^3 \sin\alpha}{48A_s L_D I_f + 2A_s A_D \sin^2\alpha + 48A_D b I_f \sin^2\alpha} K_H \qquad (6.14)$$

Care must be taken at sections where solid diaphragms are installed. It is to be recommended that forces in the lateral diagonal due to distortion be neglected at the panels immediately

adjacent to interior solid diaphragms in order to avoid the disturbing effect caused by the solid diaphragm.

6.4.3 Bracing Member Forces due to Vertical Bending

Equations for forces in SD type lateral bracing members due to vertical bending in a tub girder may be derived based on the following assumptions: (B. S. Chen, 2005), (Todd Helwig, April 2007), (Chai H. Yoo, 2005)

(1) Cross-frames are assumed installed at every other strut location.

(2) Vertical bending affects the longitudinal deformation and lateral buckling of the flanges due to inclined webs

(3) The webs have negligible lateral resistance against lateral bending of the top flanges. This assumption has been verified by analyzing a number of examples of hypothetical box girders (the web contributes approximately 2% of the top flange bending resistance).
The first assumption has an important implication for the behavior of box girders with SD type lateral bracing systems. If cross-frames are installed at every strut location, the lateral bracing system and cross-frames interact substantially differently from those described heretofore.

Concerning the second assumption, (Chai H. Yoo, 2005) reviewed the works of Fan and Helwig (1999) that they could able to successfully derive equations to predict brace forces induced by longitudinal stresses of the top flanges. Although they had assumed, for simplicity, the struts to carry the entire lateral load, a logical redistribution of lateral force components to struts and diagonals leads to a better estimation of brace forces.

Considering the warren type lateral bracing system subjected to lateral loads, w_{lat}, the interactive forces between top flanges and lateral bracing members, interactive forces, QA and QB, figure,6.10 are determined from the simple equilibrium considerations,

$$Q_A+Q_B=2Sw_{lat} \quad (6.15a)$$

$$Q_A=2D_{lat}\sin a+S_{lat} \quad (6.15b)$$

$$Q_B=S_{lat} \quad (6.15c)$$

where S = spacing between struts; D_{lat}, S_{lat} = forces in diagonal and strut, respectively. Substituting and rearranging yields,

$$S_{lat} = S_{wlat} - D_{lat}\sin a \qquad (6.16)$$

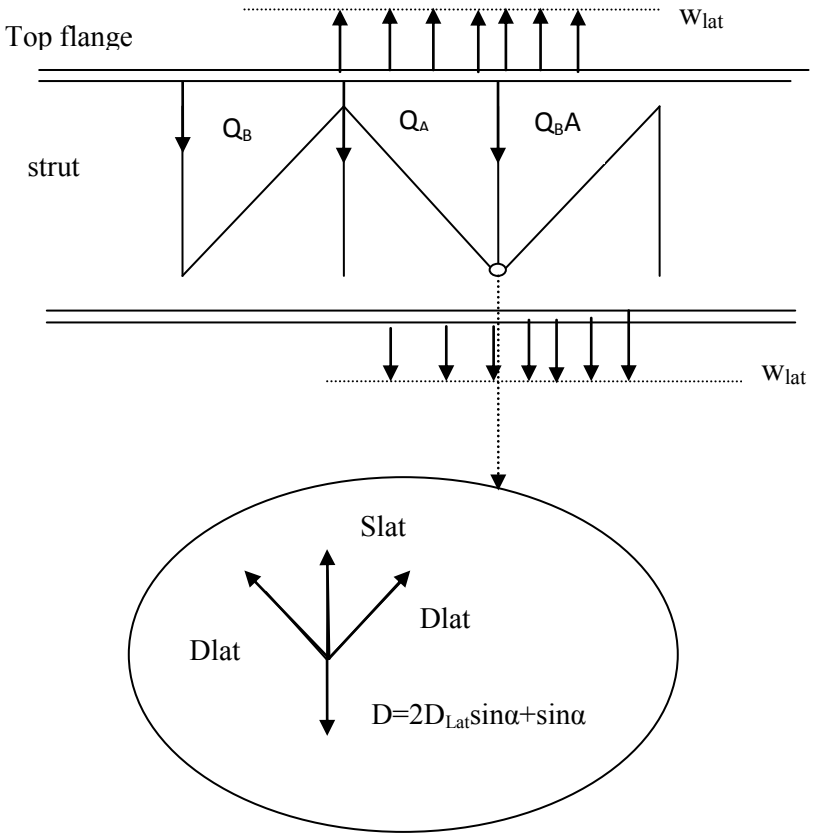

Fig.6.9 Interface forces between the top flange and lateral bracing members due to lateral force components

The induced lateral load component due to inclined webs causes the top flange to bend in a manner similar to a continuous beam between panel points. The relative lateral deflection between two adjacent panel points can be determined from the superposition of deflections due to distributed lateral load, w_{lat}, and concentrated load, Q_A,V_1

$$V_1 = \frac{w_{lat}(2S)^4}{384EI_f} - \frac{Q_A(2S)^3}{192EI_f} \qquad (6.17a)$$

The elongations of the strut,, and diagonal, δD, is V_2

$$V_2 = \frac{S_{lat} b}{EA_s} \quad \text{and} \quad \sigma_D = \frac{D_{lat} L_D}{EA_D} \tag{6.17b}$$

Up on substitution and simplification, D_{lat} yields the following expression for the diagonal member force induced by lateral loading,

$$D_{lat} = \frac{24A_d bsI_f \sin\alpha}{24A_s L_D I_f + A_D \sin^2\alpha (A_s S^3 + 24bI_f)} W_{lat} \tag{6.18}$$

3.6 Equations for Brace Forces

Forces in diagonals, *D*, and struts, *S*, in the SD type lateral bracing system due to vertical bending and torsional loading are summarized as followings,

$$D = D_{bend} + D_{lat} + D_{tor} + D_{dist} \tag{6.19}$$

$$S = S_{bend} + S_{lat} + S_{tor} + S_{dist} \tag{6.19b}$$

$$D_{bend} = \frac{f_{xtop} S \cos\alpha}{\frac{L_D}{A_D} + \frac{b\sin^2\alpha}{A_s} + \frac{s^3}{24I_f}} \tag{6.19c}$$

$$F_{xtop} = \frac{24A_D bsI_f \sin\alpha}{24A_s L_D I_f + A_D (A_s S^3 + 24bI_f)\sin^2\alpha} W_{lat} \tag{6.19d}$$

$$D_{tor} = \pm \frac{b}{24A_o \sin\alpha} T \tag{6.19f}$$

$$D_{dist} = \frac{A_D A_S S^3 \sin\alpha}{48A_s L_D I_f + (2A_S S^3 + 48A_D bI_f)\sin^2 a} K_H \tag{6.19g}$$

$$S_{bend} = \frac{(2s)^3 \big/ 192I_f}{\frac{b}{2A_s} + \frac{(2S)^2}{192I_f}} D_H \tag{6.19h}$$

$$S_{bend} = -D_{bend} \sin\alpha \,,\; S_{lat} = S_{wlat} - D_{lat}\sin\alpha \quad \text{and} \quad S_{dist} = -D_{dist} \sin\alpha \tag{6.19i}$$

Most of these equations were developed before the introduction and interactive applications of the Finite Element Approaches. For these same reason, academic staffs and organized staffs in US including those involved in published references such as (B. S. Chen, 2005),

(Chai H. Yoo, 2005), (Todd Helwig, April 2007) have carried a technical report on a number of previously made steel composite box girder bridges. Almost all these structural preliminaries were developed based on analytical approaches and none complete design codes. It should be noted that all force components are functions of bending and tortional moments. It is acceptable for diagonal forces to be computed by superimposing only D_{bend} and D_{tor} because the magnitudes of D_{lat} and D_{dist} are relatively small for a relatively stiff box girder bridges. For strut forces, however, at least three components, S_{bend}, S_{lat}, and S_{tor} are needed. In the case of nonprismatic flanges, the average of the flange moment of inertia with respect to the centroidal vertical axis should be used.

6.5 Interior diaghrams

Interior diaghrams are required to keep the local and global stability of the webs. Since internal diaphragms resist the coupled forces on a box girder that cause an internal distortional force, placing adequate internal diaphragms to a box girder greatly increases the stiffness against distortion and facilitates to retain the original shape of the cross-section.

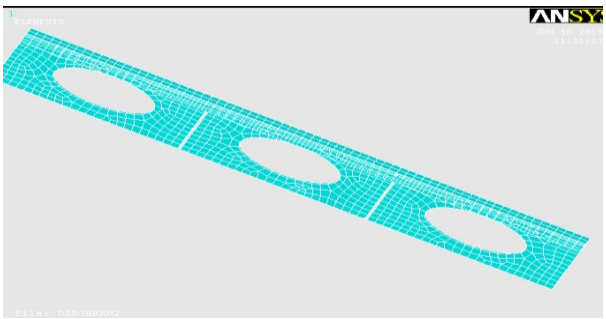

Fig.6.10 an elliptical openings on the diaphragm plate to allow an interior passage

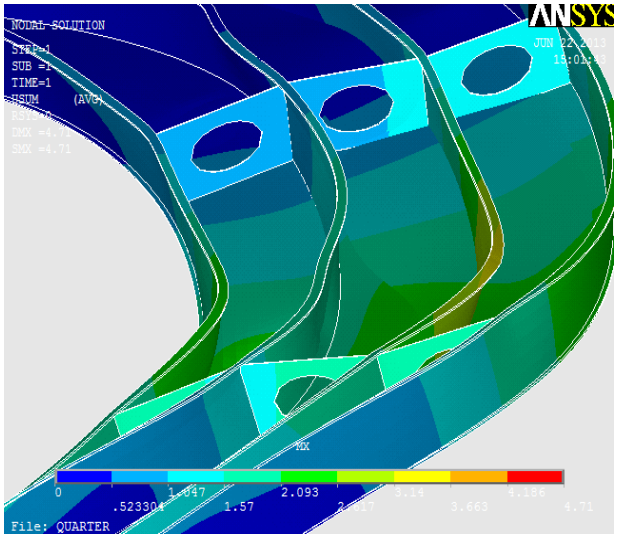

Fig.6.11 Displacement Behavior of the Girder versus diagrams (without bracing systems)

One of the principal advantages of closed sections, as has been discussed earlier, is to allow an interior passage when required during maintenance and retrofitting works. For the same advantage therefore, the interior solid diaphragms are designed with openings.

6.5.1 Effects of Internal Diaphragm on Distortional Stresses

The diaphragm member usually keeps the structural integrity and safety against buckling. Inclined interior cross frames can also be recommended in place of solid diaphragms. The analysis analogy is also different. Interactive studies on the mutual integration behaviors of solid diaphragms haven't so far been studied, except that some analytical stiffness contributions of none generalized literatures are available. An academic research cataloged as (ping, 2010), titled as a Grillage Analyses of Bridges Based on Euro code, tries to classify stiffness categories and their structural relations (generalized i.e irrespective of material type).

Total torsion rigidity, H

From the stiffness requirements, the bridge system can be characterized by the following rigidity categories, relations,

Longitudinal rigidity, D_1

Transverse coupling rigidity, D_2

Longitudinal torsional rigidity, D_{xy}

Transverse torsional rigidity, D_{yx}

Longitudinal flexural rigidity, D_x

Transverse flexural rigidity, D_y

$$H=(D_{xy}+D_{yx}+D_1+D_2)/2 \qquad (6.20)$$

Yee Ping (2010), formulated some of the rigidity relations interns of material and cross sectional parameters. For multi cell box beam bridge

$D_x=EI_x$ I_x=second moment of area about x

$D_y=EI_y$ I_y=second moment of area about y

$$GJ=\frac{GA^2t}{b}\left(\frac{1-2\rho a(a^n-1)}{n(a-1)(a-1)(a^2-1)+(a^2+a)}\right) \qquad (6.21)$$

$$r=\frac{2btx}{ndt^3}$$

$$a=1+r+\sqrt{2r+r^2}$$

$$\rho=\frac{tx}{t^3}$$

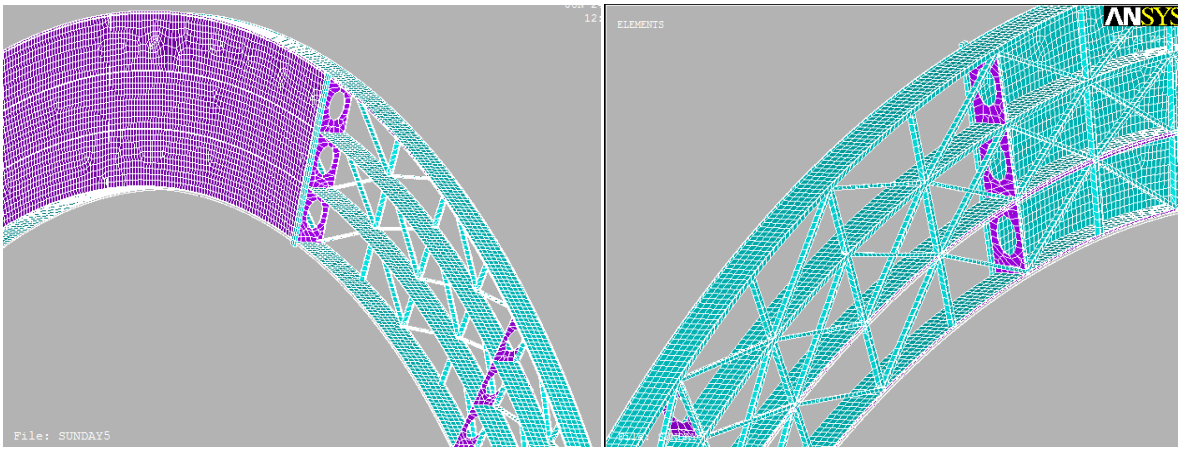

Fig.6.12 structural integrity of the bridge

Chapter Seven

7.0 Program Output

7.1 ANSYS Introductory Notes for Structural Shell

SHELL93 is particularly well suited to model curved shells. The element has six fundamental degrees of freedom at each node: translations in the nodal x, y, and z directions and rotations about the nodal x, y, and z axes. The deformation shapes are quadratic in both in-plane directions. The element has plasticity, stress stiffening, large deflection, and large strain capabilities.

Input Data

The element is defined by eight nodes, four thicknesses, and the orthotropic material properties. Mid side nodes may not be removed from this element. A triangular-shaped element may be formed by defining the same node number for nodes K, L and O.

Orthotropic material directions correspond to the element coordinate directions. The element x and y axes are in the plane of the element. The x axis may be rotated an angle THETA (in degrees) toward the y axis.

The element may have variable thickness. The thickness is assumed to vary smoothly over the area of the element, with the thickness input at the corner nodes. The thickness at the mid side nodes is taken as the average of the corresponding corner nodes. If the element has a constant thickness, only TK(I) need be input. If the thickness is not constant, all four thicknesses must be input. The total thickness of each shell element must be less than twice the radius of curvature, and should be less than one-fifth the radius of curvature.

Pressures may be input as surface loads on the element faces. Positive pressures act into the element. Edge pressures are input as force per unit length. Temperatures may be input as element body loads at the "corner" locations. The first corner temperature T_1 defaults to TUNIF. Only the lumped mass matrix is available.

Output Data

The solution output associated with the element is in two forms:

- nodal displacements included in the overall nodal solution
- additional element output

Printout includes the moments about the x face (M_X), the moments about the y face (M_Y), and the twisting moment (M_{XY}). The moments are calculated per unit length in the element coordinate system. The element stress directions and force resultants (N_X,M_X,T_X,etc.) are parallel to the element coordinate system. The basic element printout is given at the center of the top of face IJKL, the element centroid, and at the center of the bottom of face IJKL

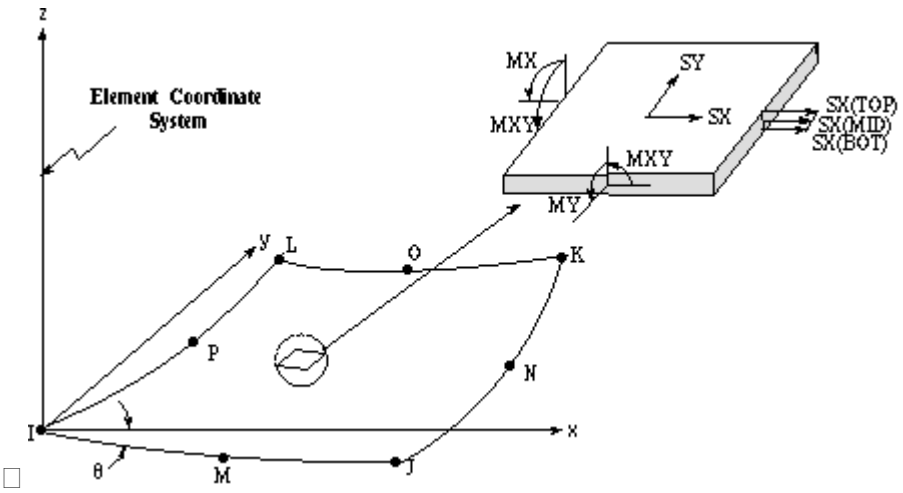

Fig.7.1 SHELL93 action orientations

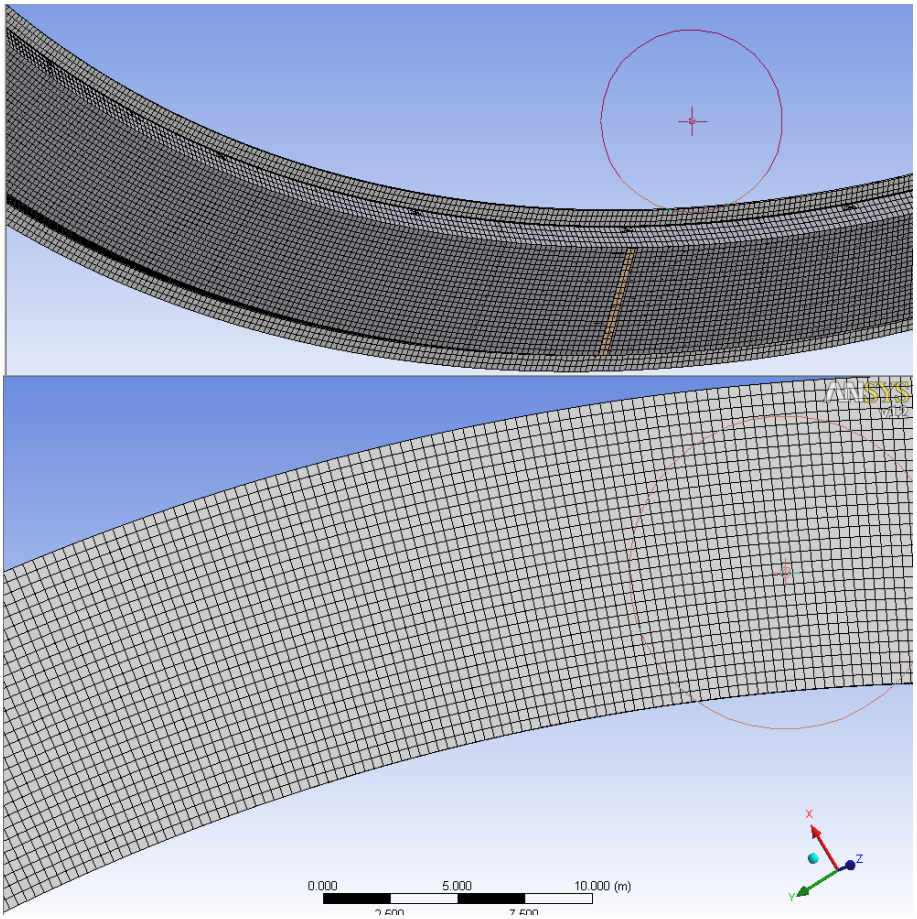

Fig.7.2rectangular mesh elements

7.2 Structural loading

All loading conditions and possible combinations haven't been discovered in this research. Wind load, seismic and temperature (vital in steel bridges) effects haven't also been addressed. All the fundamental bridge loads, and the required combinations have, however, been addressed.

Simple but very interesting bridge load distribution and combination analysis software, a QconBridge software, is used to preprocess the fundamental ANSYS input load format.

Only the governing values of the moment and shear envelops are required for this research work. It has to strongly be noted, however, that this software provides the standard load reaction results such as those used and standardized in concrete structures, based on ASHTTO Bridge design specification. Only flexural bending and shear (straight bridge correspondent) results are obtained. Shear and moment governing envelops are shown in fig. 7.3 below.

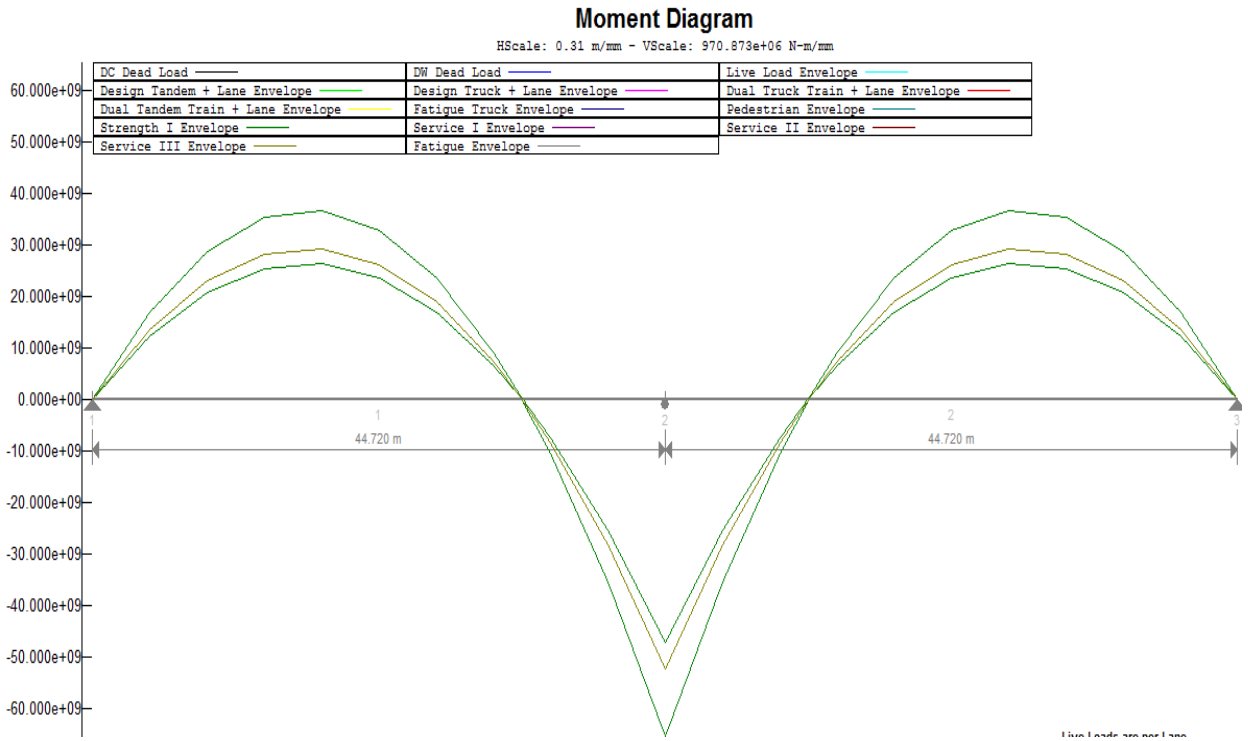

Fig7.3 Moment diagram on the double span bridge

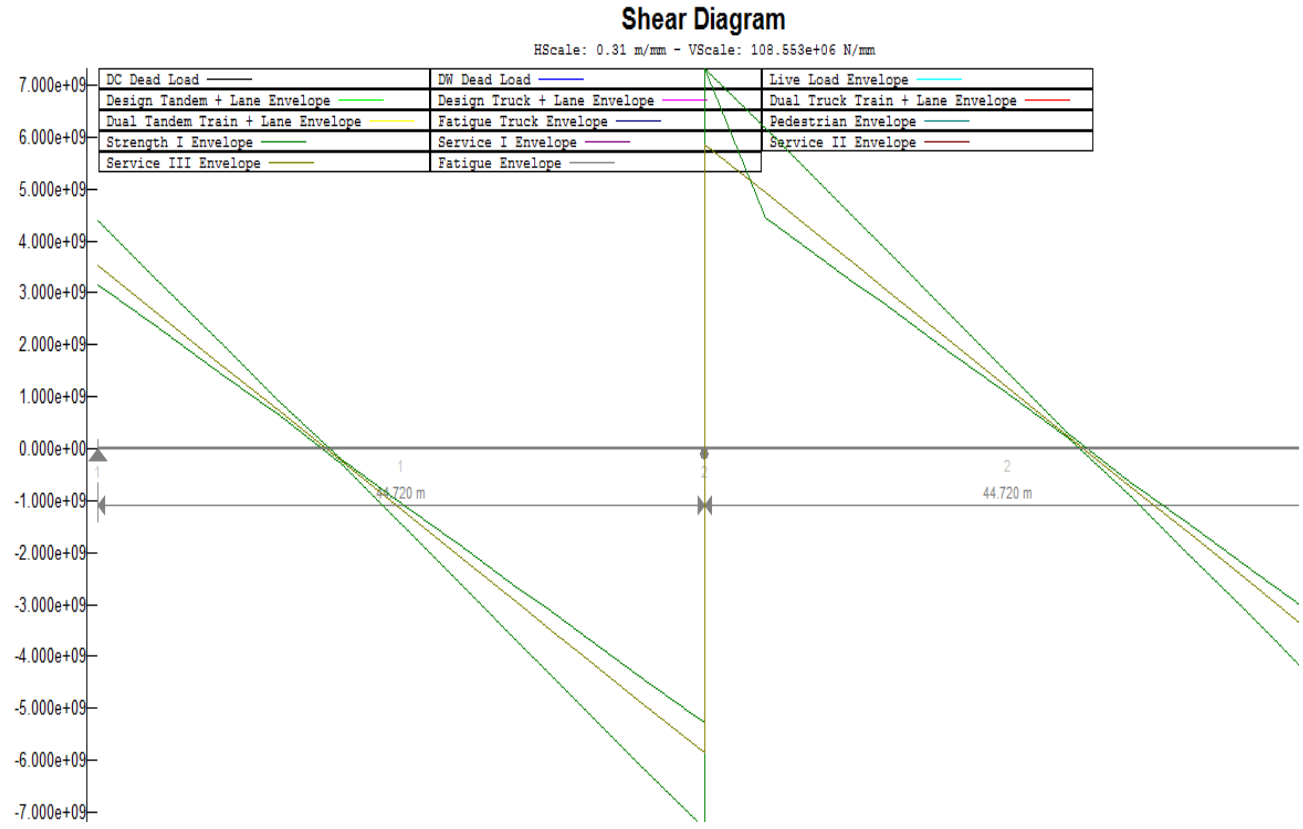

Fig.7.3 Shear Force diagram on the double span bridge

7.3 Analysis the Model

7.3.1 Double span 30m radius

A curved triple celled trapezoidal and rectangular steel box girder is modeled to extend the integral concept of torsional behaviors of box sections. The bridge girder is a double span 47.1239m each with pin and roller supports at the ends and the center respectively. The whole features of the integral structural system can after all be considered as a shell structure due to its reaction behavior. The bottom flange of the girder is continues forming a closed and stiffened section. It cumulatively provides the bridge stability against global buckling. All the displacement and reaction results are obtained from the model analysis results, using the most interactive and general purpose software, the ANSYS. Displacement results at typical critical sections are presented for convenience in table 7.1.

Table 7.1 Displacement Results for nodes at some typical critical sections for degree of freedoms in global coordinate system with ansys v.12

NODE	U_X	U_Y	U_Z	R_{OTX}	R_{OTY}	R_{OTZ}	W_{ARP}
2221	-4.5535	2.7419	-0.3323	-1.6399	-2.8009	-0. 2538	0.0000
2222	-4.5380	2.7442	-0.2470	-1.6368	-2.8019	-0.1142	0.0000
2223	-4.5125	2.7377	-0.1642	-1.6393	-2.8066	-0.2008	0.0000
2224	-4.4773	2.7229	-0.0836	-1.6288	-2.7970	-0.2847	0.0000
2225	-4.4327	2.7002	-0.0066	-1.6200	-2.7875	-0.3657	0.0000
2226	-4.3786	2.6697	0.0685	-1.6012	-2.7673	-0.4443	0.0000
2227	-4.3155	2.6320	0.1412	-1.5820	-2.7454	-0.5197	0.0000
2228	-4.2436	2.5873	0.2115	-1.5553	-2.7146	-0.5918	0.0000
2229	-4.1632	2.5361	0.2793	-1.5273	-2.6807	-0.6603	0.0000
2230	-4.0749	2.4789	0.3446	-1.4935	-2.6398	-0.7253	0.0000
2231	-3.9789	2.4160	0.4076	-1.4580	-2.5953	-0.7860	0.0000
2232	-3.8757	2.3479	0.4682	-1.4180	-2.5448	-0.8429	0.0000
2233	-3.7658	2.2751	0.5266	-1.3761	-2.4907	-0.8949	0.11E-05
2234	-3.6496	2.1980	0.5827	-1.3310	-2.4317	-0.9427	0.0000
2235	-3.5278	2.1171	0.6365	-1.2841	-2.3691	-0.9852	0.0000
2236	-3.4009	2.0329	0.6882	-1.2350	-2.3027	-1.0229	0.0000
2237	-3.2696	1.9459	0.7378	-1.1844	-2.2331	-1.0546	0.000
2238	-3.1345	1.8566	0.7853	-1.1326	-2.1606	-1.0807	0.000
2239	-2.9964	1.7656	0.8309	-1.0797	-2.0855	-1.1003	0.000
2240	-2.8562	1.6734	0.8744	-1.0264	-2.0085	-1.1132	0.00001
2241	-2.7146	1.5805	0.9161	-0.9723	-1.9293	-1.1193	0.31E-05
2242	-2.5727	1.4877	0.9560	-0.9189	-1.8496	-1.1169	0.000

2243	-2.4314	1.3955	0.9940	-0.8649	-1.7681	-1.1076	0.000
2244	-2.2920	1.3044	1.0304	-0.8126	-1.6873	-1.0875	0.000
2245	-2.1555	1.2153	1.0652	-0.7596	-1.6042	-1.0608	0.000
2246	-2.0235	1.1289	1.0982	-0.7096	-1.5250	-1.0179	0.000
2247	-1.8974	1.0459	1.1297	-0.6577	-1.4446	-0.9708	0.000
2248	-1.7786	0.9671	1.1599	-0.6117	-1.3658	-0.9046	0.000
2249	-1.6685	0.8933	1.1886	-0.5657	-1.2783	-0.8395	0.000
2250	-1.5706	0.8248	1.2152	-0.5175	-1.1999	-0.7206	0.000
2251	-1.4893	0.7648	1.2410	-0.4593	-1.1412	-0.6077	0.000
2252	-1.4222	0.7147	1.2638	-0.4417	-1.0789	-0.4808	0.000
2253	-1.3709	0.6763	1.2839	-0.4402	-1.0395	-0.3709	0.000
2254	-1.3246	0.6460	1.3030	-0.4336	-1.0102	-0.3549	0.000

7.3.2 Multi span 30m radius with 20m intermediate tangent

Continuity of the span and support conditions of the bridge also influences the overall reaction behavior of the super structure. A ‘s’ shaped super structure with tow curved each with 188.4956m center line length and with opposite radius of curvature separated with a 20m span intermediate tangent, is modeled to investigate the reaction behavior of a multi-span bridge structure fig7.4.

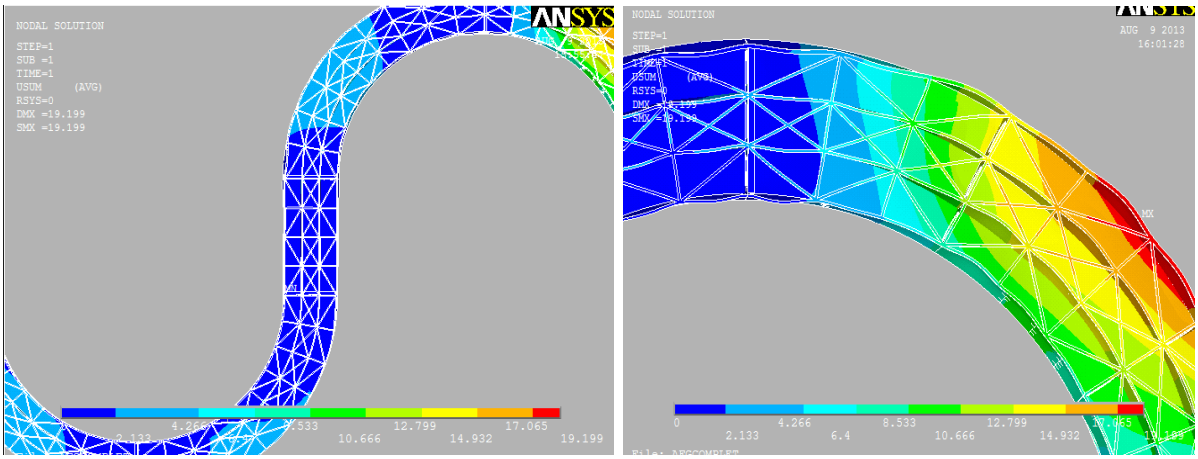

Fig.7.4 Displacement Structure of the super structure when viewed on the top

7.3.2.1 With X-braced top diagonals (exterior panels)

This final best structural model is supposed to clearly state the ongoing research. In this model, the spacing and layout of the bracing unites is revised in such a way that both the outer

and the middle panel diagonal brace is arranged in the X-pattern. This makes the integral system much stiffer and the corresponding stress intensities result a more practical value.

If the governing design value of each structural element is predefined in the ANSYS program, an indicative alert confirming the acceptance and or none acceptance of the structural integrity (structural failure), will be displayed when run. This alert can also lead the designer to revise the brace configurations being the other parameters constant. In this model, the span is also made to be continuous and for this reason an idealized loading is used (pre load analysis is not made by Qcon Bridge Software).

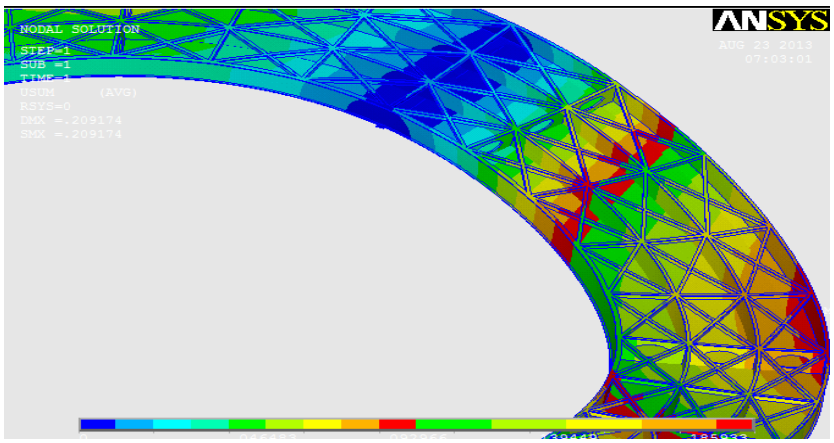

Fig.7.5a Displacement Vector Sum contour for a typical section.

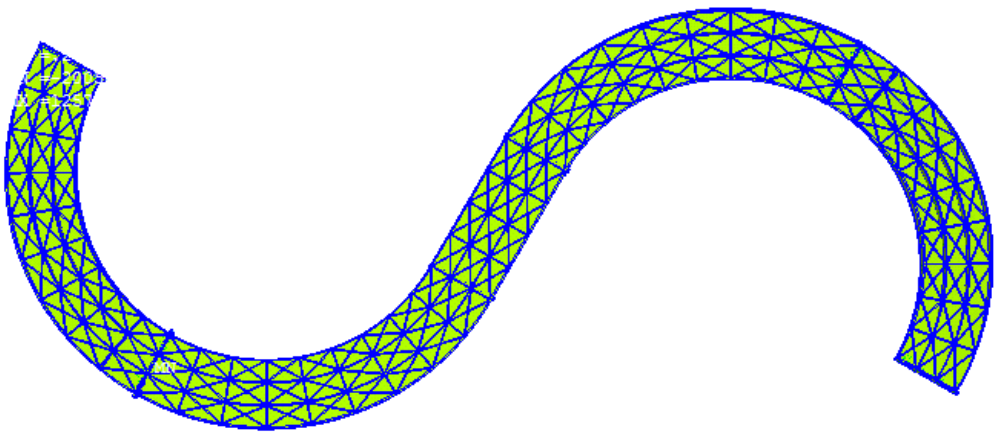

Fig.7.5b Top view of the a typical X-braced structural complex

7.4 Miscellaneous Model to Further Investigate Warping

Distortional effects of the exclusive actions on a closed section stiffened with internal diagrams (for webs), lateral bracings (for top flanges), and longitudinal stiffeners for the

bottom flange, and webs, couldn't be clearly observed, if, for an academic elaboration is required. Consider a rectangular unite cell curved box, cantilevered section, subjected to actions in a manner that angular distortion is high.

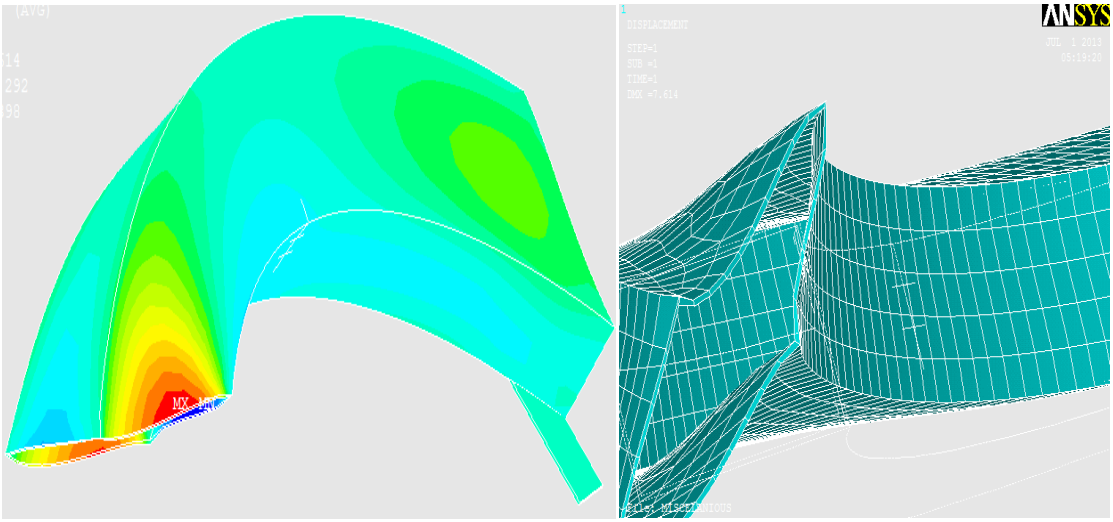

Fig.7.6 Distorted Section due to a coupled moment on a unite cell rectangular section

The most interactive and general purpose software, the ANSYS, provides all the displacement values of the defined seven Degrees of Freedoms, such as, displacements Ux, Vy, Wz, and Rotational DOFs R_{otx}, R_{oty}, R_{otz} and W_{arp}.

The obvious fact is that the top and most important requirement in the box section is to satisfy the stiffness, not necessarily the material, the section and geometrical needs. Provisions of the required stiffening mechanisms imply just exercising a magical game through which the fatal flexural actions are converted in to a freely circulating shear inside the walls of the sections out of which cancel each other.

7.4 Conclusions and Recommendations

The most important parameters considered in steel box girder bridges are, generally,

- Top lateral and diagonal bracing units, geometrical and connection types and their respective behaviors. The theoretical techniques of transforming bracing unite into an equivalent plate system and back conversion of plate reaction loads into the required brace correspondences.
- Section verifications of the flange web and bracing systems for the respective elasto-plasitic resistance. Additional section resistance parameters are required, in this regard, to be inputted under 'Failure criterion' in the ANSYS command, when design is needed.
- Spacing, configurations and structural integrity of the bracing systems with the respective web, flange and diaghram systems
- All the reaction forces and stresses are the cumulative results of the combined and separate actions of the external loads such as dead load, live load(vehicular and pedestrian) loads out of which (tandem ,lane and vehicular) loads can be derived and most important of all centrifugal load.

All the associated conceptual and theoretical preliminaries have all been exclusively dealt, although an idealized loading is adopted for the model in section 7.3.2.1.

It has been noted in section 7.3.2.1 that if the governing design value of each structural element is predefined in the ANSYS program, an indicative alert confirming the failures of the system in accordance with the failure criterion set, will be displayed, when run. The other important alert is when the warping of the section is out of limit. It has been noted earlier that for this typical model for which the number of cells is three and with crosswise solid diaghrams , warping and distortional effects are found to be insignificant.

For the fact that sophisticated structural units, like steel box girder bridges, can after all be solved with the aid of program applications and hence it makes the analysis prospect easier, it has to be strongly be noted that a new construction culture of steel box girder bridges have to be introduced in the country. This endover may with the same reason create an alternative construction habit. In line with this, it off course requires a manufacturing mill to manufacture steel plate elements in accordance with the upcoming construction needs. A design guidelines and design codes have also to be formalized in a national sense.

Reference

B. S. Chen, J. A. (2005). Top-Lateral Bracing Systems for Trapezoidal Steel Box-Girder Bridges. Austin: The University of Texas.

Bletzinger(prof.Doc-Ing), K. u. (2002, winter). theory of plates. lecture notes . technische universitat munchen.

Chai H. Yoo, K. K. (2005). RESEARCH ON HORIZONTALLY CURVED STEEL BOX GIRDERS. Alabama: Highway Research Center, Auburn University.

Doust, S. E. (November, 2011). Extending Integral Concepts to Curved Bridge Systems. Lincoln, Nebraska: University of Nebraska - Lincoln.

ping, k. y. (2010). grillage analysis and bridge loading based on eurocode. universty teknologi mayisia.

Saadé, K. (Année académique 2004-2005). Finite Element Modeling of Shear in Thin Walled Beams with a Single Warping Function. Brussels: UNIVERSITE LIBRE DE BRUXELLES Faculté des Sciences.

Shama, M. (2010). Torsion and Shear Stresses in Ships. Berlin: Springer-Verlag Berlin Heidelberg.

Sherif El-Tawil, p. a. (October 2002). Behaviour and design of curved composite box girder bridges. Orlando: University of Central Florida.

Todd Helwig, J. Y. (April 2007). Design Guidelines For Steel Trapezoidal Box Girder Systems. Austin: The University of Texas.